

## Are there higher electron densities in narrow emission line regions of Type-1 AGN than Type-2 AGN?

XUEGUANG ZHANG<sup>\*1</sup>

<sup>1</sup>Guangxi Key Laboratory for Relativistic Astrophysics, School of Physical Science and Technology, GuangXi University, No. 100, Daxue Road, Nanning, 530004, P. R. China

Submitted to ApJ

### ABSTRACT

In the manuscript, we check properties of electron densities  $n_e$  traced by flux ratio  $R_{sii}$  of [S II] $\lambda$ 6716Å to [S II] $\lambda$ 6731Å in narrow emission line regions (NLRs) between Type-1 AGN and Type-2 AGN in SDSS DR12. Under the framework of Unified Model considering kpc-scale structures, similar  $n_e$  in NLRs should be expected between Type-1 AGN and Type-2 AGN. Based on reliable measurements of [S II] doublet with measured parameters at least five times larger than corresponding uncertainties, there are 6039 Type-1 AGN and 8725 Type-2 AGN (excluding the Type-2 LINERs and the composite galaxies) collected from SDSS DR12. Then, lower  $R_{sii}$  (higher  $n_e$ ) in NLRs can be well confirmed in Type-1 AGN than in Type-2 AGN, with confidence level higher than  $5\sigma$ , even after considering necessary effects including effects of electron temperatures traced by [O III] $\lambda$ 4364, 4959, 5007Å on estimating  $n_e$  in NLRs. Two probable methods are proposed to explain the higher  $n_e$  in NLRs in Type-1 AGN. First, the higher  $n_e$  in NLRs of Type-1 AGN could indicate longer time durations of AGN activities in Type-1 AGN than in Type-2 AGN, if AGN activities triggering galactic-scale outflows leading to more electrons injecting into NLRs were accepted to explain the higher  $n_e$  in NLRs of Type-2 AGN than HII galaxies. Second, the lower  $n_e$  in NLRs of Type-2 AGN could be explained by stronger star-forming contributions in Type-2 AGN, considering lower  $n_e$  in HII regions. The results provide interesting challenges to the commonly and widely accepted Unified Model of AGN.

*Keywords:* galaxies:active - galaxies:nuclei - galaxies:emission lines - galaxies:Seyfert

### 1. INTRODUCTION

Different observed phenomena between broad line AGN (Active Galactic Nuclei) (Type-1 AGN) and narrow line AGN (Type-2 AGN) can be well explained by the known Unified Model (UM) of AGN, considering expected different orientation angles of central accretion disk Antonucci (1993), combining with different properties of central activities and inner dust torus etc., as well discussed in Marinucci et al. (2012); Oh et al. (2015); Mateos et al. (2016); Balokovic et al. (2018); Brown et al. (2019); Kuraszkiwicz et al. (2021); Zhang (2022a). More recent reviews on the UM can be found in Netzer (2015). The elegant UM has been strongly supported by clearly detected polarized broad emission lines and/or clearly detected broad infrared emission lines in some Type-2 AGN (Miller & Goodrich 1990; Heisler, Lumsden & Bailey 1997;

Tran 2003; Nagao et al. 2004; Onori et al. 2017; Savic et al. 2018; Moran et al. 2020) and strong resonance of silicate dust at  $10\mu\text{m}$  is seen in absorption towards many Type-2 AGN but in emission in Type-1 AGN reported in Siebenmorgen et al. (2005). Under the current framework of the UM, Type-1 AGN are intrinsically like Type-2 AGN of which central regions including central accretion power source around black hole (BH) and broad line regions (BLRs) are hidden by central dust torus.

However, even after considerations of different properties of central dust torus and central activities related to central black hole (BH) accreting power source, there are some other challenges to the being constantly revised UM. Franceschini et al. (2002) have discussed the probably different evolutionary patterns in Type-1 and Type-2 AGN. Hiner et al. (2009) have shown that host galaxies of Type-2 AGN have higher average star formation rates than Type-1 AGN. Villarroel & Korn (2014) have shown different environment characteristics with different neighbours around Type-1 AGN and Type-2 AGN. More recently, Zou et al.

Corresponding author: XueGuang Zhang  
xgzhang@gxu.edu.cn

(2019) have shown lower stellar masses of host galaxies in Type-1 AGN than Type-2 AGN, through X-ray selected AGN. Bornancini et al. (2020) have shown significantly different properties of UV/optical and mid-infrared colour distribution of the different AGN types. More recently, we Zhang (2022b) have shown statistically larger stellar velocity dispersion in Type-1 AGN than in Type-2 AGN. As the detailed discussions on the UM in Netzer (2015), the UM has been successfully applied to explain different observed features between Type-1 and Type-2 AGN in many different ways, however, the AGN family with many other features considering the reported challenges to the UM are far from homogeneous.

The UM has been well accepted that Type-1 AGN are intrinsically like Type-2 AGN, there are not only similar properties of central region on scale of sub-pcs including central BLRs but also similar properties of NLRs (narrow emission line regions) on scale of kpcs. Therefore, considering NLRs on scale of kpcs under the framework of the UM, there should be similar properties of electron densities in NLRs between Type-1 AGN and Type-2 AGN, which is the starting point of the manuscript. Moreover, not similar as properties of central power source and BLRs which can be affected by physical properties of dust torus on scale of pcs, there are few structures on scale of kpcs having effects on physical properties of NLRs on scale of kpcs. In other words, physical properties of NLRs are pure, leading to more robust final results without additional contaminations. Furthermore, flux ratios of [S II] doublet are mainly considered in the manuscript, indicating that moving dust clouds and orientation effects have no effects on our final results on flux ratios of [S II] doublet.

Properties of electron densities  $n_e$  in NLRs are mainly considered and discussed between the Type-1 AGN and the Type-2 AGN, which will provide further clues to support the UM or will provide further clues leading a challenge to the UM. Electron densities  $n_e$  in emission line regions can be well and conveniently determined by narrow forbidden emission line ratios. In 1950s, Seaton (1954) has shown that the electron densities in planetary nebulae can be well estimated by relative intensities of the forbidden lines, and then followed and improved by Osterbrock (1955); Osterbrock & Flather (1959); Osterbrock (1955a, 1960); Saraph & Seaton (1970); Aller & Epps (1976). In 1980s, Canto (1980) have shown that forbidden [S II] $\lambda\lambda 6716, 6731\text{\AA}$  line ratios can be effectively applied to determine electron densities based on solutions of collision strengths and transition probabilities, and then followed by Stanghellinir & Kale (1989). Then, in the classic book of 'Astrophysics of Gaseous Nebulae and Active Galactic Nuclei' (Osterbrock 1989; Osterbrock & Ferland 2006), there are detailed review on the theoretical method to determine electron densities in emission line regions by line ratios of forbidden doublets. More recently, Zhang et al. (2013); Dors et al. (2014); Proxauf et al.

(2014); Sanders et al. (2016); Kawasaki et al. (2017); Kakkad et al. (2018); Kewley et al. (2019); Flury & Moran (2020); Kazuma et al. (2021); Riffel et al. (2021); Dors et al. (2022) have shown the methods and/or corresponding discussions to determine electron densities in emission regions by forbidden line ratios. Among line flux ratios of forbidden doublets, the ratio of [S II] $\lambda\lambda 6716, 6731\text{\AA}$  doublet is preferred in the manuscript to trace properties of  $n_e$  in NLRs, because the collected low redshift emission line objects are from SDSS DR12 (Sloan Digital Sky Survey, Data Release 12, Alam et al. (2015)), with apparent [S II] $\lambda\lambda 6716, 6731\text{\AA}$  doublets in their SDSS spectra.

Based on the parameter  $R_{sii}$ , flux ratio of [S II] $\lambda\lambda 6716\text{\AA}$  to [S II] $\lambda\lambda 6731\text{\AA}$ , properties of  $n_e$  in NLRs can be well conveniently checked between Type-1 AGN and Type-2 AGN collected from Sloan Digital Sky Survey (SDSS) data release 12 (DR12). Section 2 presents data samples of Type-1 AGN and Type-2 AGN, methods to measure [S II] doublets. Section 3 shows main results and necessary discussions on properties of electron densities in NLRs of different kinds of AGN. Section 4 gives a further implication. Section 5 gives final summaries and conclusions. And in the manuscript, the cosmological parameters of  $H_0 = 70\text{km} \cdot \text{s}^{-1}\text{Mpc}^{-1}$ ,  $\Omega_\Lambda = 0.7$  and  $\Omega_m = 0.3$  have been adopted.

## 2. DATA SAMPLES

### 2.1. Parent samples of Type-1 AGN and Type-2 AGN

The work is based on large samples of low redshift Type-1 AGN and Type-2 AGN which have apparent [S II] $\lambda\lambda 6716, 6731\text{\AA}$  doublets. Therefore, low redshift AGN with  $z < 0.3$  in SDSS DR12 are mainly considered.

Criterion of redshift smaller than 0.3,  $z < 0.3$ , is applied to collect 12342 low redshift Type-1 AGN from SDSS pipeline classified QSOs (Richards et al. 2002; Ross et al. 2012; Peters et al. 2015; Lyke et al. 2020) in DR12, through the SDSS provided SQL (Structured Query Language) Search tool (<http://skyserver.sdss.org/dr12/en/tools/search/sql.aspx>) by the following query

```
SELECT plate , fiberid , mjd
FROM SpecObjall
WHERE class='QSO' and z<0.30 and zwarning=0
```

where 'SpecObjall' is SDSS pipeline provided database including basic properties of emission line galaxies in SDSS DR12. More detailed information of the database 'SpecObjall' can be found in <http://skyserver.sdss.org/dr12/en/help/docs/tabledesc.aspx>. The collected information of plate, fiberid and mjd can be conveniently applied to download SDSS spectra of the 12342 Type-1 AGN.

The same criteria  $z < 0.3$  combining with criterion 'subclass='AGN'' are applied to collect all the 16269 low redshift

Type-2 AGN from SDSS pipeline classified main galaxies in DR12, by the following query

```
SELECT plate , fiberid , mjd
FROM SpecObjall
WHERE class='GALAXY' and zwarning=0
      and subclass = 'AGN' and z<0.30
```

More detailed information of SDSS spectroscopic catalogs (subclass, class, etc.) can be found in <https://www.sdss.org/dr12/spectro/catalogs/>.

### 2.2. Parent samples of HII galaxies

Besides Type-1 AGN and Type-2 AGN collected from SDSS DR12, HII galaxies are also simply discussed in the manuscript, which will provide clues on AGN activity contributions to properties of  $n_e$  in NLRs by comparing HII galaxies and Type-2 AGN.

The criterion  $z < 0.3$  combining with criterion of 'subclass='starforming'' are applied to collect all the 245590 low redshift HII galaxies from SDSS pipeline classified main galaxies in DR12, by the following query

```
SELECT plate , fiberid , mjd
FROM SpecObjall
WHERE class='GALAXY' and z<0.30 and zwarning=0
      and subclass = 'starforming'
```

### 2.3. Method to measure the line parameters of [S II] doublet

In order to well measure line intensities of [S II] $\lambda$ 6716, 6731Å, host galaxy contributions included in SDSS spectra should be firstly subtracted.

The common SSP method (Simple Stellar Population) (Bruzual & Charlot 2003; Kauffmann et al. 2003; Cid Fernandes et al. 2005; Cappellari 2017) has been applied to determine the host galaxy contributions, similar as what we have done in Zhang (2014); Zhang et al. (2016); Rakshit et al. (2017); Zhang et al. (2019, 2021); Zhang (2021a,b, 2022b, 2023). We have exploited the 39 simple stellar population templates in Bruzual & Charlot (2003), which can be used to well describe the characteristics of almost all the SDSS galaxies as discussed in Bruzual & Charlot (2003). Meanwhile, an additional power law component is applied to describe intrinsic AGN continuum emissions, especially in Type-1 AGN. Meanwhile, when the SSP method is running, narrow emission lines in spectrum are masked out, by full width at zero intensity about  $450\text{km s}^{-1}$ . And the wavelength ranges from 4450 to 5600Å and from 6250 to 6750Å are also masked out for the broad H $\beta$  and the broad H $\alpha$  and optical Fe II emission lines. Then, through the Levenberg-Marquardt least-squares minimization technique (the known MPFIT package), the best descriptions can be well determined to the SDSS spectra with emission lines being masked out. Moreover, when the SSP method is running, only one restriction is accepted that the

strengthened factor of each stellar population template is not smaller than zero. Left panels of Fig. 1 shows two examples on the SSP method determined host galaxy contributions in one Type-1 AGN and one Type-2 AGN.

After subtractions of the host galaxy contributions (if there are), emission lines around H $\alpha$ , within rest wavelength from 6250 to 6850Å, can be well described by multiple Gaussian functions. Simple descriptions on the measurements of emission lines are as follows, similar as what we have recently done in Zhang (2021a,b,c). Three broad Gaussian functions plus one narrow Gaussian function are applied to describe the broad and narrow H $\alpha$ , six narrow Gaussian components are applied to describe the [O II], [N II] and [S II] doublets, a power law component is applied to describe the continuum emissions underneath the broad H $\alpha$ . Then, through the Levenberg-Marquardt least-squares minimization technique, emission lines can be well described by multiple Gaussian functions, and uncertainties (formal  $1\sigma$  errors) of the model parameters can be determined by the covariance matrix. When the model functions above are applied, the following restrictions are accepted. First, the components of each forbidden narrow emission line doublet ([S II], [N II], [O II]) have the same redshift and the same line width in velocity space. Second, each emission component has intensity not smaller than zero. Third, each narrow Gaussian component has line width (second moment) smaller than  $500\text{km/s}^2$ . Fourth, each broad Gaussian component in broad H $\alpha$  has line width larger than the line width of narrow H $\alpha$ . Fifth, the flux ratio of [N II] doublet is fixed to the theoretical value 3. And when the fitting procedure is running, the starting values of the parameters are as follows. For each narrow emission line, theoretical central wavelength,  $2\text{Å}$  and 0 are accepted the starting values of central wavelength, second moment and line intensity. For the three broad Gaussian components in broad H $\alpha$ , the starting values of [central wavelength, second moment, intensity] are [6540, 20, 0], [6564, 25, 0] and [6580, 20, 0], respectively. Right panels of Fig. 1 shows two examples on the best descriptions to the emission lines around H $\alpha$ , after subtractions of host galaxy contributions.

Moreover, because line intensities of [O III] $\lambda$ 4959, 5007Å and narrow H $\beta$  will be discussed in the following section, simple descriptions are as follows on the fitting procedure applied to describe the emission lines around H $\beta$  within rest wavelength range from 4400 to 5600Å after subtractions of the host galaxy contributions. Similar as what we have recently done in Zhang (2021a,b,c), three broad Gaussian functions plus one narrow Gaussian function are applied to describe the

<sup>1</sup> The maximum full width at half maximum of narrow H $\alpha$  of SDSS quasars in Shen et al. (2011) is around  $1200\text{km/s}$  (second moment about  $509\text{km/s}$ ). Therefore,  $500\text{km/s}$  is accepted as the upper limit of second moment of narrow emission lines.

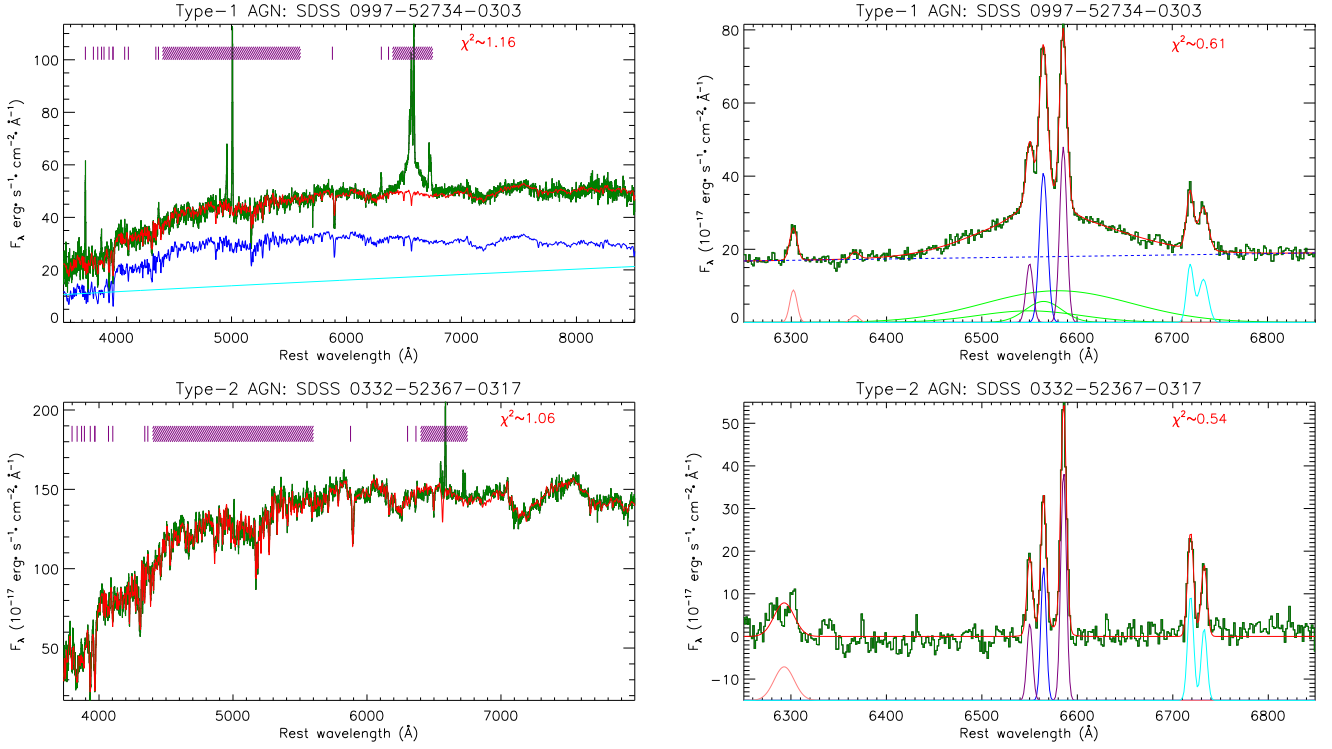


**Figure 1.** Left panels show the SSP method determined best descriptions (solid red line) to the SDSS spectra (solid dark green line) of Type-1 AGN 0997-52734-0303 (PLATE-MJD-FIBERID) and Type-2 AGN 0332-52367-0317. In each left panel, from left to right, the vertical purple lines point out the emission lines being masked out when the SSP method is running, including  $[\text{O II}]\lambda 3727\text{\AA}$ ,  $\text{H}\theta$ ,  $\text{H}\eta$ ,  $[\text{Ne III}]\lambda 3869\text{\AA}$ ,  $\text{He I}\lambda 3891\text{\AA}$ ,  $\text{Ca K}$ ,  $[\text{Ne III}]\lambda 3968\text{\AA}$ ,  $\text{Ca H}$  line,  $[\text{S II}]\lambda 4070\text{\AA}$ ,  $\text{H}\delta$ ,  $\text{H}\gamma$ ,  $[\text{O III}]\lambda 4364\text{\AA}$ ,  $\text{He I}\lambda 5877\text{\AA}$  and  $[\text{O I}]\lambda 6300, 6363\text{\AA}$  doublet, and the area filled by purple lines around  $5000\text{\AA}$  shows the region masked out including the optical  $\text{Fe II}$  lines, broad and narrow  $\text{H}\beta$  and  $[\text{O III}]$  doublet, and the area filled by purple lines around  $6550\text{\AA}$  shows the region masked out including the broad and narrow  $\text{H}\alpha$ ,  $[\text{N II}]$  and  $[\text{S II}]$  doublets. In top left panel, solid blue line shows the determined host galaxy contributions, solid cyan line shows the determine AGN continuum emissions. Right panels show the best descriptions (solid red line) to the emission lines around  $\text{H}\alpha$  (solid dark green line), especially on the  $[\text{S II}]$  doublet, after subtractions of host galaxy contributions. In each right panel, solid blue line shows the determined narrow  $\text{H}\alpha$ , solid purple lines show the determine  $[\text{N II}]$  doublet, solid pink lines show the determined  $[\text{O I}]$  doublet, solid cyan lines show the determined  $[\text{S II}]$  doublet. In top right panel, solid green lines show the determined broad Gaussian components in the broad  $\text{H}\alpha$ , dashed blue line shows the determined power law continuum emissions underneath the emission lines. In each panel, the  $\chi^2$  (the summed squared residuals for the best-fitting results divided by the degree of freedom) is marked in red characters.

broad and narrow  $\text{H}\beta$ , two narrow and two broad Gaussian components are applied to describe the core and extended components of  $[\text{O III}]\lambda 4959, 5007\text{\AA}$  doublet (Shen et al. 2011; Greene & Ho 2005), one Gaussian component is applied to describe the  $\text{He II}$  line, broadened and scaled  $\text{Fe II}$  templates discussed in Kovacevic et al. (2010) are applied to describe optical  $\text{Fe II}$  lines, and a power law component is applied to describe the continuum emissions underneath the broad  $\text{H}\beta$ . The following restrictions are accepted to the model parameters, as the restrictions to the model parameters to describe the emission lines around  $\text{H}\alpha$ . First, the core (extended) components of  $[\text{O III}]$  doublet have the same redshift, the same line width and the flux ratio fixed to the theoretical value 3. Second, each emission component has intensity not smaller than zero. Third, the core components of  $[\text{O III}]$  doublet and the narrow  $\text{H}\beta$  have line widths (second moment) smaller than  $500\text{km/s}$ . Fourth, each broad Gaus-

sian component in broad  $\text{H}\beta$  has line width larger than the line width of narrow  $\text{H}\beta$ . Fifth, the extended components of  $[\text{O III}]$  doublet have line widths larger than the line widths of the core components. And when the fitting procedure is running, the starting values of the parameters are as follows. For each narrow emission lines, theoretical central wavelength,  $2\text{\AA}$  and 0 are accepted the starting values of central wavelength, second moment and line intensity. For the three broad Gaussian components in broad  $\text{H}\beta$ , the starting values of [central wavelength, second moment, intensity] are [4840, 20, 0], [4861, 25, 0] and [4880, 20, 0], respectively. Fig. 2 shows two examples on the best-fitting results to the emission lines around  $\text{H}\beta$  in one Type-1 AGN and one Type-2 AGN, through the Levenberg-Marquardt least-squares minimization technique.

#### 2.4. Final main data samples



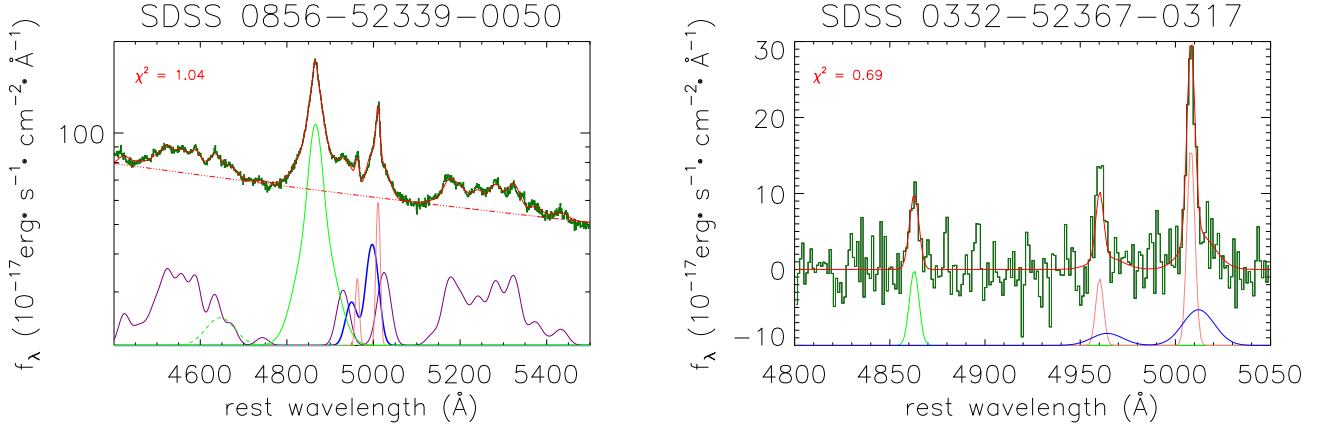


**Figure 2.** Left panel shows the best fitting results (solid red line) to emission lines around  $H\beta$  (solid dark green line) including apparent optical Fe II emission features in the Type-1 AGN 0856-52339-0050. Double-dot-dashed red line shows the determined power law continuum emissions, solid green line shows the determined broad  $H\beta$ , solid purple lines show the determined optical Fe II lines, dashed green line shows the determined broad He II line, solid pink lines show the determined core [O III] components, and thick blue solid lines show the determined blue-shifted extended [O III] components. Right panel shows the best fitting results (solid red line) to the emission lines around  $H\beta$  (solid dark green line) in the Type-2 AGN 0332-52367-0317, after subtractions of host galaxy contributions. Solid green line shows the determined narrow  $H\beta$ , solid lines in pink and in blue show the determined core and extended components of [O III] doublet. And the calculated  $\chi^2$  values are marked in the top-left corners in the panels. In order to show clearer emission features in the left panel, the Y-axis is in logarithmic coordinate.

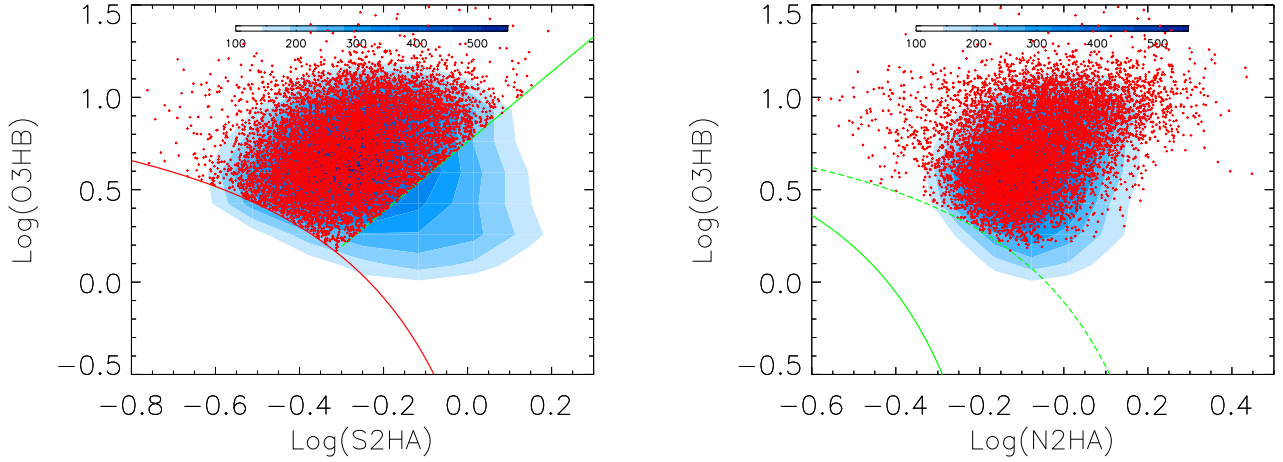


**Figure 3.** Properties of the collected 12999 Type-2 AGN shown in contours filled by bluish colors and the 8725 Type-2 AGN (excluding the Type-2 LINERs and the composite galaxies) shown as red pluses in the BPT diagrams of S2HA versus O3HB (left panel) and of N2HA versus O3HB (right panel). In left panel, solid red line and solid green line show the dividing lines as discussed in Kewley et al. (2006) between HII galaxies and AGN and between Seyfert 2 galaxies and Type-2 LINERs, leading Type-2 LINERs to lie into the region above the solid red line but below the solid green line. In right panel, solid and dashed green lines show the dividing lines between HII galaxies and composite galaxies and AGN, as discussed in Kauffmann et al. (2003).

Finally, starting with 12342 Type-1 AGN in the parent sample collected from SDSS pipeline classified quasars, and with 16269 Type-2 AGN in the parent sample collected from SDSS pipeline classified main galaxies, and 245590 HII galaxies in the parent sample collected from SDSS pipeline classified main galaxies, applying the following criteria,

- The measured line width and line flux of [S II] doublet described by Gaussian functions are at least 5 times larger than their corresponding uncertainties, indicating reliable [S II] doublet.
- For the Type-1 AGN, not only there are reliable [S II] doublet, but also there are reliable broad  $H\alpha$  emission lines with at least one broad Gaussian component with

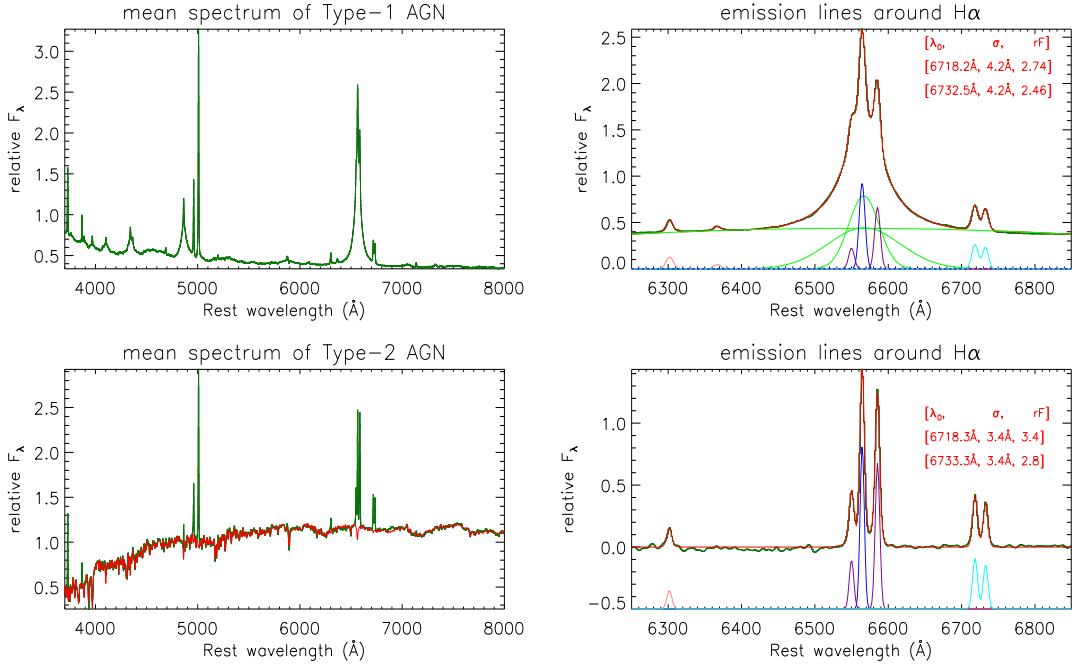


**Figure 4.** Left panels show properties of mean spectra (in dark green) of the 1251 Type-1 AGN (top-left panel) and the 1198 Type-2 AGN (bottom left panel) with high quality spectra in the main samples. In bottom left panel, solid red line shows the SSP method determined host galaxy contributions. Right panels show the best fitting results to the emission lines around H $\alpha$  in the mean spectrum of Type-1 AGN (top-right panel) and of Type-2 AGN after subtractions of the host galaxy contributions (bottom-right panel). In right panels, the symbols and line styles are the same as those in right panels of Fig. 1. In each right panel, top right corner lists the measured line parameters [central wavelength  $\lambda_0$ , second moment  $\sigma$ , relative flux  $rF$ ] of the [S II] doublet.

the measured line flux and line width at least 5 times larger than the corresponding uncertainties and second moment larger than  $600\text{km} \cdot \text{s}^{-1}$ .

- For the Type-2 AGN, not only there are reliable [S II] doublet, but also there are no broad H $\alpha$  emission lines with the determined three broad Gaussian components for broad H $\alpha$  with the measured line fluxes and line widths 2 times smaller than the corresponding uncertainties.
- For the HII galaxies, not only there are reliable [S II] doublet, but also there are no broad H $\alpha$  emission lines with the determined three broad Gaussian components for broad H $\alpha$  with the measured line fluxes and line widths 2 times smaller than the corresponding uncertainties.

leads main samples including 6039 Type-1 AGN with both apparent [S II] doublets and apparent broad H $\alpha$  emission lines, and 12999 Type-2 AGN with apparent [S II] doublets but no broad H $\alpha$  emission lines, and 199700 HII galaxies with apparent [S II] doublets but no broad H $\alpha$  emission lines. Here, the word "reliable" means the Gaussian function described emission component has its measured line parameters (central wavelength, second moment and line intensity) at least 5 times larger than the corresponding uncertainties.

Furthermore, as described in subsection 2.1, both Seyfert 2 galaxies and Type-2 LINERs (Low Ionization Nuclear Emission Line Regions) (LINERs without apparent broad emission lines) are collected into the main sample of Type-2 AGN. However, not similar as Seyfert 2 galaxies totally powered by central BH accreting process, there are different mechanisms applied to Type-2 LINERs, such as shock heating (Heckman 1980; Dopita & Sutherland 1996), photoionization by young stars (Terlevich & Melnick 1985; Filippenko & Terlevich 1992), photoionization by post-asymptotic giant branch (post-AGB) stars (Eracleous et al. 2010; Cid Fernandes et al. 2011), etc. More recent review on LINERs can be found in Marquez et al. (2017) which have shown that 60% to 90% of LINERs could be well considered as genuine AGN. Considering the controversial conclusion on physical nature of Type-2 LINERs (at least part of Type-2 AGN without AGN nature), Type-2 LINERs are not considered in the manuscript, in order to ignore effects of different physical natures of part of Type-2 LINERs on our final results. Not similar as Type-2 LINERs, Type-1 LINERs (LINERs with apparent broad emission lines) included in the parent sample of Type-1 AGN are well considered as AGN, due to their broad emission lines.

Based on the dividing lines between Seyfert 2 galaxies and Type-2 LINERs in the BPT diagram of O3HB (flux ratio of

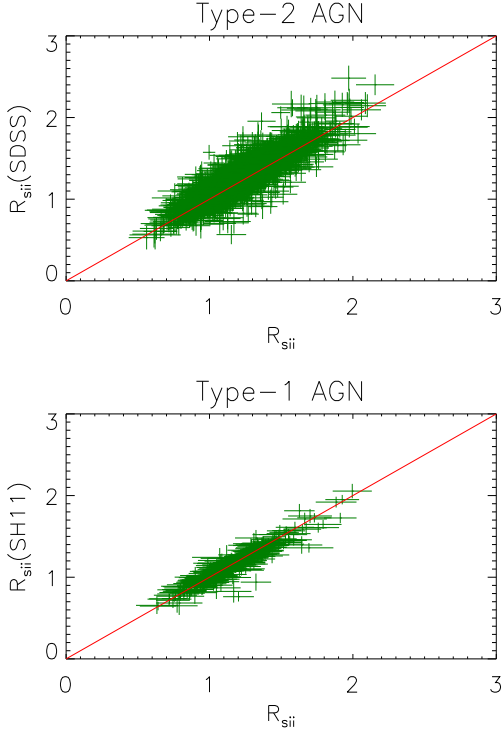


**Figure 5.** On the correlations between measured  $R_{sii}$  in the manuscript and  $R_{sii}(SDSS)$  determined from the SDSS pipeline determined line parameters of the Type-2 AGN (top panel), and between the measured  $R_{sii}$  in the manuscript and  $R_{sii}(SH11)$  determined from the reported line parameters of the Type-1 AGN in Shen et al. (2011) (bottom panel). In each panel, solid red line shows  $X = Y$ .

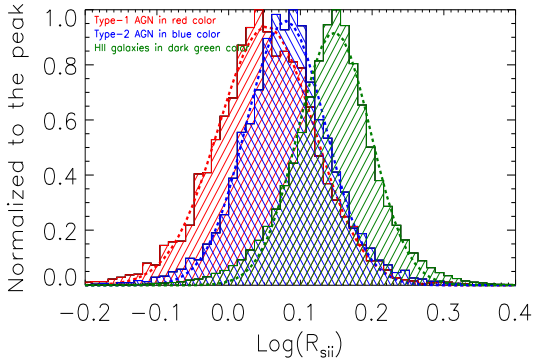


**Figure 6.** Distributions of  $\log(R_{sii})$  of the 6039 Type-1 AGN (histogram filled by red lines), the 8725 Type-2 AGN (histogram filled by blue lines), and the 199700 HII galaxies (histogram filled by dark green lines) in the final main samples, respectively. Thick dashed lines in red, in blue and in dark represent the corresponding best Gaussian profiles for the  $\log(R_{sii})$  distributions of the Type-1 AGN, the Type-2 AGN and the HII galaxies, respectively.

$[O\text{ III}]\lambda 5007\text{\AA}$  to narrow  $H\beta$ ) versus S2HA (flux ratio of total  $[S\text{ II}]\lambda 6716, 6731\text{\AA}$  to narrow  $H\alpha$ ) as shown in Kewley et al. (2006)

$$\log(O3HB) > \frac{0.72}{\log(S2HA) - 0.32} + 1.30 \quad (1)$$

$$\log(O3HB) > 1.89 \log(S2HA) + 0.76$$

there are 8793 Type-2 AGN, excluding the Type-2 LINERs and excluding the classified HII galaxies in the BPT diagrams of O3HB versus S2HA. Meanwhile, based on the dividing line between AGN and composite galaxies as discussed in Kauffmann et al. (2003) in the BPT diagram of O3HB versus N2HA (flux ratio of  $[N\text{ II}]\lambda 6583\text{\AA}$  to narrow  $H\alpha$ )

$$\log(O3HB) > \frac{0.61}{\log(N2HA) - 0.47} + 1.19 \quad (2)$$

among the 8793 Type-2 AGN, there are 68 classified composite galaxies excluded from the collected Type-2 AGN, in order to ignore probable strong effects of starforming. Therefore, there are 8725 (8793-68) Type-2 AGN included in the final main sample of Type-2 AGN. Fig. 3 shows properties of the collected Type-2 AGN in the BPT diagrams of S2HA versus O3HB (left panel) and of N2HA versus O3HB (right panel). The results in left panel of Fig. 3 show clear classifications of Type-2 LINERs. And the results in right panel of Fig. 3 show clear evidence to support that the collected Type-2 AGN, neither including Type-2 LINERs nor including composite galaxies, are reliable AGN with central AGN activities.

### 2.5. Spectroscopic properties of mean spectra of Type-1 AGN and Type-2 AGN

In the subsection, mean spectra are discussed in Type-1 AGN and Type-2 AGN, in order not only to provide further evidence to support that the emission line fitting procedure is appropriate and but also to provide further clues to answer the question whether asymmetric line profiles should be considered in  $[S\text{ II}]$  doublet.

The commonly accepted PCA (Principal Component Analysis) technique is applied to create mean spectra of Type-1 AGN and Type-2 AGN. PCA technique uses an orthogonal transformation to convert a set of observations of possibly correlated variables into a set of values of uncorrelated variables called principal components. Commonly, mean subtraction (or mean centering) is necessary for performing PCA to ensure that the first principal component describes the direction of maximum variance. However, if mean subtraction is not performed, the PCA technique determined first eigenvector represents the mean spectrum of input set of spectra. Here, we apply the convenient and public IDL PCA program `pca_solve.pro` written by D. Schlegel, which is included in SDSS software package of IDLSPEC2D (<http://spectro.princeton.edu/>).

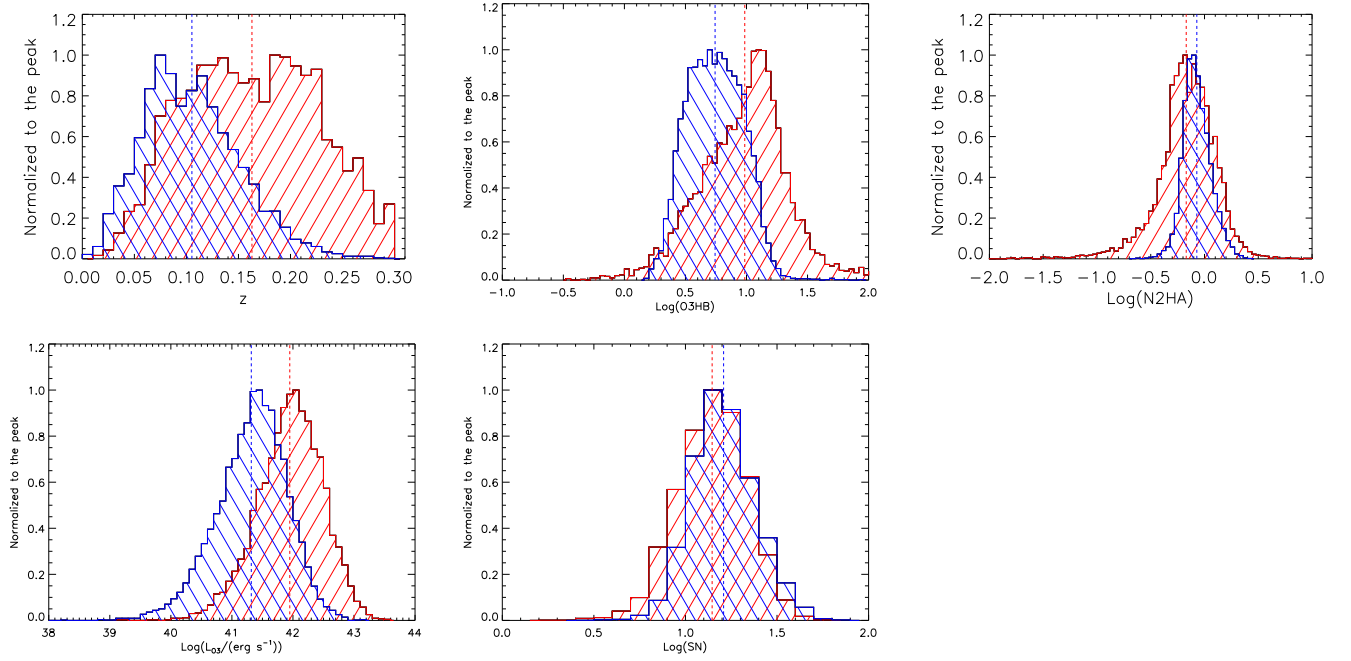


**Figure 7.** Distributions of redshift, O3HB, N2HA,  $L_{O3}$  and SN of the Type-1 AGN (histogram filled with red lines) and Type-2 AGN (histogram filled with blue lines) in the main samples. In each panel, vertical dashed line in red and in blue mark position of mean value of each distribution of Type-1 AGN and Type-2 AGN, respectively.

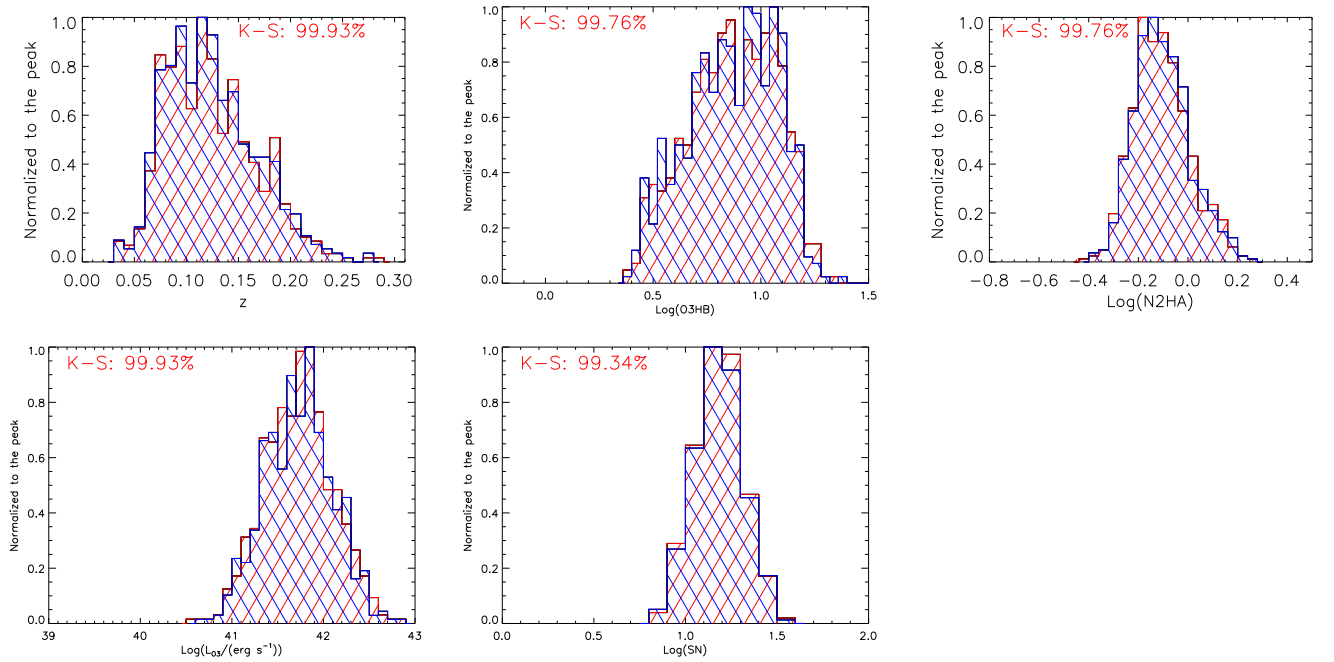


**Figure 8.** Distributions of redshift, O3HB, N2HA,  $L_{O3}$  and SN of the 548 Type-1 AGN (histogram filled with red lines) and the 548 Type-2 AGN (histogram filled with blue lines) in the subsamples. In each panel, the Kolmogorov-Smirnov statistic technique provided significance level is marked in red characters.



Here, in order to check probable asymmetric profiles of [S II] doublet, 1251 Type-1 AGN with spectral signal-to-noise larger than 20 and 1198 Type-2 AGN with spectral signal-to-noise larger than 25 are mainly considered. PCA technique determined mean spectra are shown in left panels of Fig. 4. The same SSP method is applied to determine host galaxy contributions in the mean spectrum of Type-2 AGN. Then, the same emission line fitting procedure discussed in subsection 2.2 is applied to measure the emission lines around  $H\alpha$  in the mean spectra of Type-1 AGN and of Type-2 AGN after subtractions of host galaxy contributions. The best fitting results are shown in right panels of Fig. 4 to the emission lines around  $H\alpha$ , with the determined line parameters of [S II] doublet marked in top right corner in each right panel.

It is clear that the two Gaussian components can be well applied to describe the [S II] doublet in the mean spectra of high quality Type-1 AGN and high quality Type-2 AGN, indicating there are few contributions of asymmetric kinematic components in [S II] doublets. Therefore, the results in Fig. 4 not only can be applied to support that the emission line fitting procedure can be well accepted, but also can be applied to support that there are few effects of asymmetric kinematic components in [S II] doublets on our final results.

### 3. MAIN RESULTS AND DISCUSSIONS

#### 3.1. To confirm the reliability of the measured line parameters of [S II] doublet

Comparing with line parameters from different methods/techniques can provide further and necessary information to confirm the reliability of the measured line parameters. For the [S II] doublet of which features with few effects from host galaxy absorption features in Type-2 AGN, it is necessary and interesting to confirm the reliability of our measured parameters of [S II] doublet, through comparing our measured values and the values calculated from SDSS pipeline provided parameters for the Type-2 AGN. Due to apparent effects of broad  $H\alpha$  on measured line parameters of [S II] doublet in Type-1 AGN, the parameters reported in Shen et al. (2011) rather than the parameters reported by the SDSS pipeline are considered for the Type-1 AGN.

In the subsection, properties of line flux ratio  $R_{sii}$  of [S II] $\lambda 6716\text{\AA}$  to [S II] $\lambda 6731\text{\AA}$  are well discussed, based on the SDSS pipeline produced line parameters of the Type-2 AGN, and based on the line parameters reported in Shen et al. (2011) of the Type-1 AGN in SDSS DR7 (Data Release 7).

For the 8725 Type-2 AGN in SDSS DR12 (excluding the Type-2 LINERs and composite galaxies), the SDSS pipeline measured line parameters of [S II] doublets are stored in

the database of 'galSpecLine'<sup>2</sup>. Top panel of Fig. 5 shows the correlation between the measured  $R_{sii}$  in the manuscript and  $R_{sii}(SDSS)$  determined from the SDSS reported line parameters. There is a strong positive linear correlation with Spearman Rank correlation coefficient about 0.935 with  $P_{null} < 10^{-20}$ . The linear correlation can be described by

$$\log(R_{sii}(SDSS)) = (-0.053 \pm 0.008) + (1.059 \pm 0.007) \log(R_{sii}) \quad (3)$$

after considering the uncertainties in both coordinates, through FITEXY code<sup>3</sup>. And the mean ratio of  $R_{sii}$  to  $R_{sii}(SDSS)$  is about  $0.981 \pm 0.001$ . The uncertainty 0.001 is determined by the commonly applied bootstrap method within 1000 loops. For each loop, more than half of the data points in the sample of ratio of  $R_{sii}$  to  $R_{sii}(SDSS)$  are randomly collected to create a new sample, leading to a re-measured mean value. After 1000 loops, based on distribution of the 1000 re-measured mean values, half width at half maximum is accepted as the uncertainty of the mean value. Therefore, the results in top panel of Fig. 5 can provide strong evidence to confirm the reliability of the measured line parameters of [S II] doublets of the Type-2 AGN in the main sample.

Meanwhile, bottom panel of Fig.5 shows the measured  $R_{sii}$  in the manuscript and  $R_{sii}(SH11)$  determined from the reported line parameters in Shen et al. (2011) for the Type-1 AGN in SDSS DR7. There is a strong positive linear correlation with Spearman Rank correlation coefficient about 0.96 with  $P_{null} < 10^{-20}$ . After considering the uncertainties in both coordinates, through the FITEXY code, the linear correlation can be described by

$$\log(R_{sii}(SH11)) = (-0.022 \pm 0.029) + (1.012 \pm 0.025) \log(R_{sii}) \quad (4)$$

And the mean ratio of  $R_{sii}$  to  $R_{sii}(SH11)$  is about  $1.007 \pm 0.006$ , with uncertainty determined by the bootstrap method within 1000 loops applied to data sample of the ratio of  $R_{sii}$  to  $R_{sii}(SH11)$ . Therefore, the results in bottom panel of Fig. 5 can provide strong evidence to confirm the reliability the measured line parameters of [S II] doublets of the Type-1 AGN in the main sample.

#### 3.2. Direct comparisons of $R_{sii}$

Based on the reliable measurements of [S II] doublets, distributions of  $R_{sii}$  (flux ratio of [S II] $\lambda 6716\text{\AA}$  to [S II] $\lambda 6731\text{\AA}$ ) are shown in Fig. 6 of the Type-1 AGN, the Type-2 AGN and the HII galaxies in the main samples. Mean values of  $\log(R_{sii})$  are about  $0.052 \pm 0.005$ ,  $0.081 \pm 0.003$  and

<sup>2</sup>Detailed information of 'galSpecLine' can be found in <http://skyserver.sdss.org/dr12/en/help/docs/tabledesc.aspx>

<sup>3</sup><https://idlastro.gsfc.nasa.gov/ftp/pro/math/fitexy.pro>

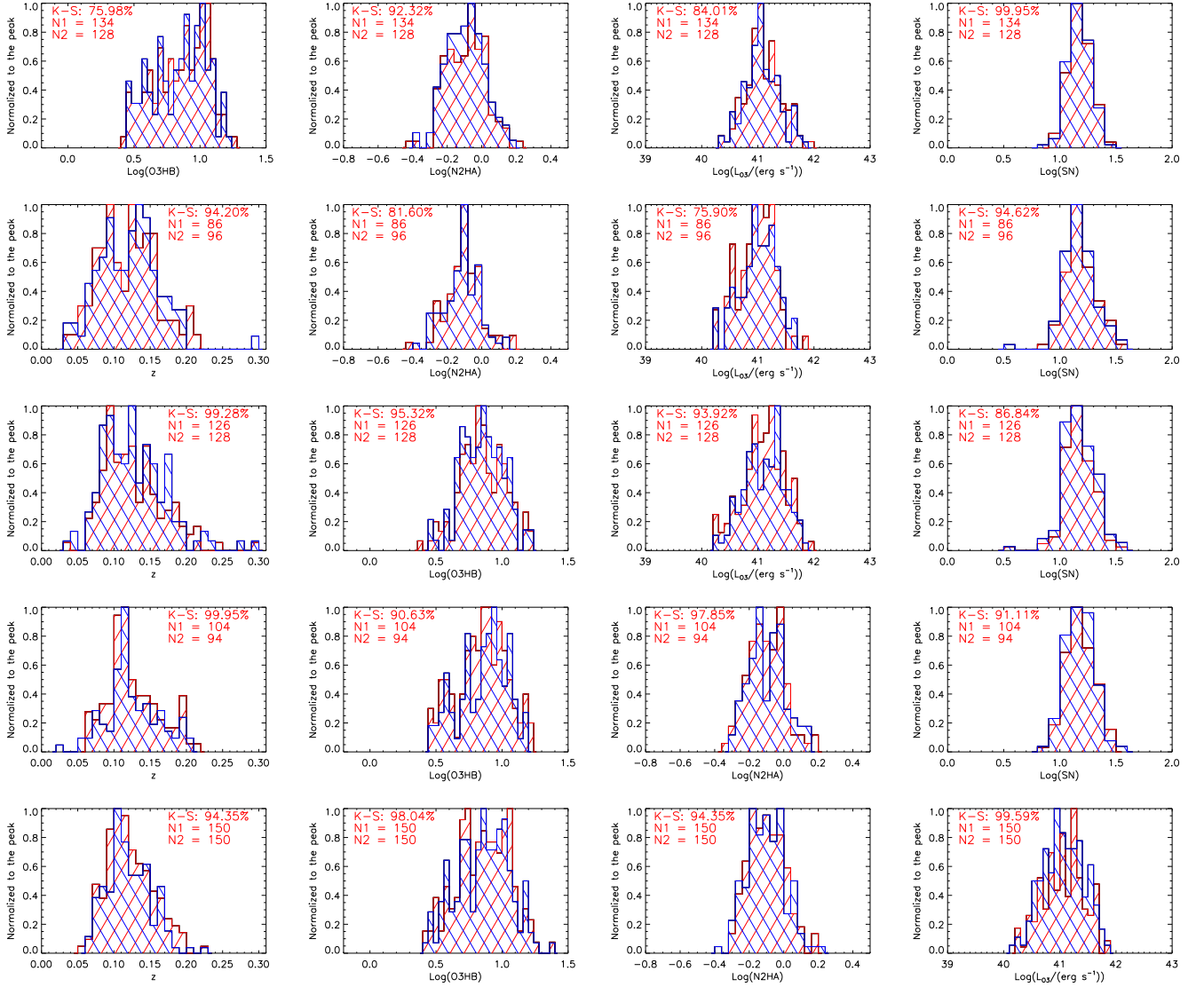


**Figure 9.** Within a narrow range of one parameter, distributions of the other four parameters of the collected Type-1 AGN and Type-2 AGN from the subsamples. Symbols and line styles have the same meanings as those in Fig. 8. And the numbers N1 and N2 of the collected Type-1 AGN and Type-2 AGN are marked in red characters in top region in each panel. From top to bottom, the Type-1 and Type-2 AGN are collected from the subsamples, through the criteria that  $|z - \bar{z}| < \sim 0.0134$ ,  $|\log(O3HB) - \log(\bar{O3HB})| < \sim 0.051$ ,  $|\log(N2HA) - \log(\bar{N2HA})| < \sim 0.036$ ,  $|\log(L_{O3}) - \log(\bar{L}_{O3})| < 0.092$ ,  $|\log(SN) - \log(\bar{SN})| < 0.05$ , where  $\bar{p}$  as mean value of parameter  $p$ .

$0.147 \pm 0.001$  of the Type-1 AGN, the Type-2 AGN (excluding the Type-2 LINERs and composite galaxies) and the HII galaxies, respectively. Uncertainty of each mean value is determined by the bootstrap method with 1000 loops applied. Meanwhile, based on the measured [S II] doublets in the mean spectra of high quality Type-1 AGN and high quality Type-2 AGN in Fig. 4,  $\log(R_{sii})$  are about 0.047 and 0.084 in high quality Type-1 AGN and in high quality Type-2 AGN, respectively, which are a bit different from the mean values in the AGN in the main samples, indicating a few effects of spectral signal-to-noise (SN) on our final results, besides to show the different  $\log(R_{sii})$  between high quality Type-2 AGN and high quality Type-1 AGN.

Based on the theoretical dependence of  $n_e$  on  $R_{sii}$  more recently discussed in Sanders et al. (2016); Kewley et al. (2019),

$$\frac{n_e}{\text{cm}^3} = \frac{627.1 \times R_{sii} - 909.17}{0.4315 - R_{sii}} \quad (5)$$

the mean electron densities  $n_e$  can be roughly estimated as  $291 \pm 18$ ,  $198 \pm 4$  and  $30 \pm 3$  in units of  $\text{cm}^{-3}$  of the 6039 Type-1 AGN, the 8725 Type-2 AGN and the HII galaxies, respectively, with uncertainties determined by accepted corresponding uncertainties of  $R_{sii}$ . Here, as discussed results in Sanders et al. (2016); Kewley et al. (2019), effects of electron temperature on  $n_e$  can lead to about 15% uncertainties of  $n_e$ , which cannot be applied to explain the apparent dif-

ference in  $n_e$  in the different kinds of emission line objects. And detailed discussions on effects of electron temperatures on estimating electron densities in NLRs can be found in the following subsection 3.6.

Moreover, as discussed in Kawasaki et al. (2017),  $R_{sii}$  should be effectively limited to the range from 0.4 to 1.5, when  $R_{sii}$  is applied to calculate electron density  $n_e$ . Then, with  $R_{sii}$  larger than 0.4 and smaller than 1.5, mean values of  $\log(R_{sii})$  are  $0.044\pm 0.003$ ,  $0.071\pm 0.003$  and  $0.116\pm 0.001$ , and the corresponding mean  $n_e$  in unit of  $\text{cm}^{-3}$  can be estimated as  $319\pm 11$ ,  $229\pm 4$  and  $102\pm 3$  of the 5467 Type-1 AGN, the 8389 Type-2 AGN and the 144210 HII galaxies among the objects in the main samples, respectively. The results can also roughly lead to apparently lower  $\log(R_{sii})$  (higher  $n_e$ ) in NLRs in Type-1 AGN, before considering necessary effects on the  $R_{sii}$  comparisons between the Type-1 AGN and the Type-2 AGN.

Considering the effective range of  $R_{sii}$  to estimate  $n_e$  in NLRs, the following discussed main samples of AGN include the 5467 Type-1 AGN with  $0.4 < R_{sii} < 1.5$  and the 8389 Type-2 AGN with  $0.4 < R_{sii} < 1.5$ .

### 3.3. Effects of different distributions of redshift, O3HB, N2HA or [O III] line luminosity?

In order to well explain the determined apparently higher  $n_e$  (only related to lower  $R_{sii}$ ) in NLRs in Type-1 AGN than in Type-2 AGN which are against the expected results by the Unified model of AGN, different effects are considered as follows, especially based on the different distributions of redshift, O3HB, N2HA and [O III] line luminosity  $L_{O3}$  between the 5467 Type-1 AGN and the 8389 Type-2 AGN in the main samples with  $0.4 < R_{sii} < 1.5$ . Distributions of the parameters of redshift, O3HB, N2HA,  $L_{O3}$  and SN are shown in Fig. 7. Here, redshift can be considered as evolutionary histories of AGN. And O3HB and N2HA can be well applied in BPT diagram (Baldwin et al. 1981; Kewley et al. 2001; Kauffmann et al. 2003; Kewley et al. 2006, 2019; Zhang et al. 2020) to identify AGN and to trace central AGN activities in AGN. Then, considering the mean value of each distribution shown in Fig. 7, properties of  $R_{sii}$  are checked in AGN with each parameter larger than and smaller than the mean value. Here, the shown  $L_{O3}$  are reddening corrected values through the measured Balmer decrements (flux ratio of narrow H $\alpha$  to narrow H $\beta$ ), after accepted the intrinsic Balmer decrement to be 3.1. And in the following subsections, there are no further discussions of reddening on our final results.

Considering distributions of redshift, the estimated mean values of  $\log(R_{sii})$  are about  $0.041\pm 0.003$  and  $0.048\pm 0.004$  in the 2752 low redshift Type-1 AGN with  $z < 0.16$  and in the 2715 high redshift Type-1 AGN with  $z > 0.16$  in the main sample of the 5467 Type-1 AGN with  $0.4 < R_{sii} < 1.5$ , respectively. Estimated mean values of  $\log(R_{sii})$  are about

$0.073\pm 0.003$  and  $0.068\pm 0.003$  in the 4434 low redshift Type-2 AGN with  $z < 0.105$  and in the 3955 high redshift Type-2 AGN with  $z > 0.105$  in the main sample of the 8389 Type-2 AGN with  $0.4 < R_{sii} < 1.5$ , respectively. Therefore, considering different mean  $\log(R_{sii})$  in different redshift ranges, there are accepted effects of different distributions of redshift on properties of distributions of calculated  $R_{sii}$  in Type-1 AGN and in Type-2 AGN.

Considering distributions of O3HB, the estimated mean values of  $\log(R_{sii})$  are about  $0.059\pm 0.003$  and  $0.032\pm 0.003$  in the 2544 Type-1 AGN with  $\log(O3HB)$  smaller than 0.98 and in the 2923 Type-1 AGN with  $\log(O3HB)$  larger than 0.98 in the main sample of the 5467 Type-1 AGN with  $0.4 < R_{sii} < 1.5$ , respectively. The estimated mean values of  $\log(R_{sii})$  are about  $0.079\pm 0.004$  and  $0.062\pm 0.003$  in the 4228 Type-2 AGN with  $\log(O3HB)$  smaller than 0.74 and in the 4161 Type-2 AGN with  $\log(O3HB)$  larger than 0.74 in the main sample of the 8389 Type-2 AGN with  $0.4 < R_{sii} < 1.5$ , respectively. Therefore, considering different mean  $\log(R_{sii})$  in different O3HB ranges, there are also accepted effects of different distributions of O3HB on properties of distributions of calculated  $R_{sii}$ .

Considering distribution of N2HA, the estimated mean values of  $\log(R_{sii})$  are about  $0.055\pm 0.003$  and  $0.035\pm 0.003$  in the 2584 Type-1 AGN with  $\log(N2HA)$  smaller than -0.17 and in the 2883 Type-1 AGN with  $\log(N2HA)$  larger than -0.17 in the main sample of the 5467 Type-1 AGN with  $0.4 < R_{sii} < 1.5$ , respectively. The estimated mean values of  $\log(R_{sii})$  are about  $0.079\pm 0.003$  and  $0.062\pm 0.003$  in the 4529 Type-2 AGN with  $\log(N2HA)$  smaller than -0.072 and in the 3860 Type-2 AGN with  $\log(N2HA)$  larger than -0.072 in the main sample of the 8389 Type-2 AGN with  $0.4 < R_{sii} < 1.5$ , respectively. Therefore, considering different mean  $\log(R_{sii})$  in different N2HA ranges, there are also accepted effects of different distributions of N2HA on properties of distributions of calculated  $R_{sii}$ .

Considering distribution of  $L_{O3}$  in unit of erg/s, the estimated mean values of  $\log(R_{sii})$  are about  $0.044\pm 0.003$  and  $0.046\pm 0.003$  in the 2604 Type-1 AGN with  $\log(L_{O3})$  smaller than 41.94 and in the 2863 Type-1 AGN with  $\log(L_{O3})$  larger than 41.94 in the main sample of the 5467 Type-1 AGN with  $0.4 < R_{sii} < 1.5$ , respectively. The estimated mean values of  $\log(R_{sii})$  are about  $0.076\pm 0.004$  and  $0.066\pm 0.003$  in the 3864 Type-2 AGN with  $\log(L_{O3})$  smaller than 41.32 and in the 4525 Type-2 AGN with  $\log(L_{O3})$  larger than 41.32 in the main sample of the 8389 Type-2 AGN with  $0.4 < R_{sii} < 1.5$ , respectively. Therefore, considering different mean  $\log(R_{sii})$  in different  $L_{O3}$  ranges, especially in Type-2 AGN, there are also accepted effects of different distributions of  $L_{O3}$  on properties of distributions of calculated  $R_{sii}$ .

Considering distribution of SN, the estimated mean values of  $\log(R_{sii})$  are about  $0.044 \pm 0.002$  and  $0.045 \pm 0.002$  in the 2650 Type-1 AGN with  $\log(SN)$  smaller than 1.15 and in the 2817 Type-1 AGN with  $\log(SN)$  larger than 1.15 in the main sample of the 5467 Type-1 AGN with  $0.4 < R_{sii} < 1.5$ , respectively. The estimated mean values of  $\log(R_{sii})$  are about  $0.069 \pm 0.003$  and  $0.073 \pm 0.003$  in the 4380 Type-2 AGN with  $\log(SN)$  smaller than 1.21 and in the 4009 Type-2 AGN with  $\log(SN)$  larger than 1.21 in the main sample of the 8389 Type-2 AGN with  $0.4 < R_{sii} < 1.5$ , respectively. Meanwhile, as the shown results in subsection above, the calculated mean  $R_{sii}$  in AGN in the main samples are different from the calculated  $R_{sii}$  through emission line properties in mean spectra of the collected high quality AGN. Therefore, considering different mean  $\log(R_{sii})$  in different SN ranges, there are also accepted effects of different distributions of SN on properties of distributions of calculated  $R_{sii}$ .

Before proceeding further, one point is noted. Not similar as the physical quantities of  $z$ , O3HB, N2HA and  $L_{O3}$ , SN is a parameter related to spectra quality. Why effects of different SN are considered? Actually, there is negative dependence of SN on redshift in AGN. The Spearman Rank correlation coefficients are about  $-0.57$  ( $P_{null} < 10^{-15}$ ) and  $-0.65$  ( $P_{null} < 10^{-15}$ ) for the collected 5467 Type-1 AGN with  $0.4 < R_{sii} < 1.5$  and for the 8389 Type-2 AGN with  $0.4 < R_{sii} < 1.5$ , respectively. Here, we do not show the dependence of SN on redshift in plots. However, considering the effects of different redshifts on  $R_{sii}$  comparisons between Type-1 AGN and Type-2 AGN, it is consequent to consider effects of different distributions of SN.

Due to discussions above, it is necessary and interesting to check effects of different distributions of redshift, O3HB, N2HA,  $L_{O3}$  and SN on the results in Fig 6. The convenient way is to create one subsample of Type-1 AGN which have the same distributions of redshift, O3HB, N2HA,  $L_{O3}$  and SN as those of a subsample of Type-2 AGN. Based on the distributions of  $z$ , O3HB, N2HA,  $L_{O3}$  and SN of the AGN in the main samples shown in Fig. 7 (5467 Type-1 AGN with  $0.4 < R_{sii} < 1.5$  and 8389 Type-2 AGN with  $0.4 < R_{sii} < 1.5$ ), it is easy to create a subsample of Type-2 AGN having the same distributions of  $z$ , O3HB, N2HA,  $L_{O3}$  and SN as those of the Type-1 AGN in the subsample, through finding minimum parameter distance  $D_p < D_{cri}$  calculated

as

$$\begin{aligned}
 D_{p,i} &= D_{z,i} + D_{O3HB,i} + D_{N2HA,i} + D_{L_{O3},i} + D_{SN,i} \\
 &= \left( \frac{z_{1,i} - z_2}{sca_z} \right)^2 + \left( \frac{\log(O3HB_{1,i}) - \log(O3HB_2)}{sca_{O3HB}} \right)^2 \\
 &\quad + \left( \frac{\log(N2HA_{1,i}) - \log(N2HA_2)}{sca_{N2HA}} \right)^2 \\
 &\quad + \left( \frac{\log(L_{O3,1,i}) - \log(L_{O3,2})}{sca_{L_{O3}}} \right)^2 \\
 &\quad + \left( \frac{\log(SN_{1,i}) - \log(SN_2)}{sca_{SN}} \right)^2 \quad for \ i = 1, \dots, N_1
 \end{aligned} \tag{6}$$

where  $z_{1,i}$ ,  $O3HB_{1,i}$ ,  $N2HA_{1,i}$ ,  $L_{O3,1,i}$  and  $SN_{1,i}$  mean parameters of the  $i$ th Type-1 AGN in the main sample with  $0.4 < R_{sii} < 1.5$  ( $N_1 = 5467$ ),  $z_2$ ,  $O3HB_2$ ,  $N2HA_2$ ,  $L_{O3,2}$  and  $SN_2$  mean parameters of  $N_2 = 8389$  ( $N_2 > N_1$ ) Type-2 AGN in the main sample with  $0.4 < R_{sii} < 1.5$ ,  $sca_z$ ,  $sca_{O3HB}$ ,  $sca_{N2HA}$ ,  $sca_{L_{O3}}$  and  $sca_{SN}$  are scale factors leading to  $D_z$ ,  $D_{O3HB}$ ,  $D_{N2HA}$  and  $D_{L_{O3}}$  not much different in quantity, and  $D_{cri}$  means a critical value to prevent high  $D_p$  leading to much different distributions of  $z$ , O3HB, N2HA,  $L_{O3}$  and SN between the created final two subsamples. Then, based on  $sca_z \sim 0.002$  and  $sca_{O3HB} \sim 0.01$ ,  $sca_{N2HA} \sim 0.007$  and  $sca_{L_{O3}} \sim 0.02$  and  $sca_{SN} \sim 0.0065$  and  $D_{cri} \sim 60$ , one subsample of 548 Type-1 AGN and one subsample of 548 Type-2 AGN are created, which have the same distributions of  $z$ , O3HB, N2HA,  $L_{O3}$  and SN with significance levels higher than 99% through the two-sided Kolmogorov-Smirnov statistic technique. Certainly, each object in the main samples is selected once into the two subsamples. The distributions of  $z$ , O3HB, N2HA,  $L_{O3}$  and SN for the AGN in the subsamples are shown in Fig. 8.

Simple descriptions are given as follows to determine the scale factors  $D_z$ ,  $D_{O3HB}$ ,  $D_{N2HA}$  and  $D_{L_{O3}}$  and the critical  $D_{cri}$  by three steps. First, starting values of the scale factors are set to be the differences between the mean redshift, between the mean  $\log(O3HB)$ , between the mean  $\log(N2HA)$ , between the mean  $\log(L_{O3})$  and between the mean  $\log(SN)$  of the 5467 Type-1 AGN and the 8389 Type-2 AGN in the main samples with  $0.4 < R_{sii} < 1.5$ :  $sca_z = 0.05$ ,  $sca_{O3HB} = 0.25$ ,  $sca_{N2HA} = 0.1$ ,  $sca_{L_{O3}} = 0.65$ ,  $sca_{SN} = 0.06$ . And the starting value of  $D_{cri} = 260$  is the mean value of  $D_{p,0}$  determined by the starting values of the scale factors. And then, based on the Equation (6), two subsamples are created. Second, for the created two subsamples, the two-sided Kolmogorov-Smirnov statistic technique is applied to check whether the two subsamples have the same distributions of  $z$ , O3HB, N2HA,  $L_{O3}$  and SN with significance levels higher than 99%. If the created two subsamples have different distributions of  $z$  and/or O3HB and/or N2HA and/or  $L_{O3}$  and/or SN (statistical significance level smaller than 99%), then smaller values should be re-assigned to the correspond-



ing scale factors and  $D_{cri}$ . Based on the re-given  $D_z$ ,  $D_{O3HB}$ ,  $D_{N2HA}$  and  $D_{LO3}$  and  $D_{cri}$ , two new subsamples are created, and then to check whether the two new subsamples have the same distributions of  $z$ , O3HB, N2HA,  $L_{O3}$  and  $SN$  with significance levels higher than 99%. Third, repeating the second step, until the created two subsamples have the same distributions of  $z$ , O3HB, N2HA,  $L_{O3}$  and  $SN$  with significance levels higher than 99%. The two subsamples of 548 Type-1 AGN and 548 Type-2 AGN in the manuscript are created after 15 attempts. And the basic parameters of redshift, O3HB, N2HA,  $SN$ ,  $L_{O3}$  and  $R_{sii}$  are listed in Table 1 and Table 2.

Moreover, in order to further confirm the two created subsamples having intrinsically same physical properties of  $z$ , O3HB, N2HA,  $L_{O3}$  and  $SN$  between Type-1 AGN and Type-2 AGN, it is necessary to check whether the collected Type-1 AGN and Type-2 AGN with one fixed parameter have the same distributions of the other four parameters. Here, Type-2 AGN and Type-1 AGN are collected with absolute value of one of the five parameters minus its mean value<sup>4</sup> smaller than 5%<sup>5</sup> of the total range of the parameter. Then, the two-sided Kolmogorov-Smirnov statistic technique is applied to check whether the collected Type-1 AGN and Type-2 AGN from the subsamples having the same distributions of the other four parameters. The results are shown in Fig. 9. It is apparent that the collected Type-1 AGN and Type-2 AGN with one given parameter have the same distributions of the other four parameters with significance level higher than 75% (actually most of the cases have the significance levels higher than 90%). Therefore, the collected 548 Type-1 AGN and 548 Type-2 AGN in the subsamples can be well and efficiently applied to check different  $R_{sii}$  (to simply trace properties of  $n_e$ ) properties between Type-1 AGN and Type-2 AGN, after considerations of necessary effects.

Based on the subsamples of the 548 Type-1 AGN and the 548 Type-2 AGN,  $R_{sii}$  distributions are shown in Fig. 10, with mean  $\log(R_{sii})$  about  $0.042 \pm 0.005$  and  $0.072 \pm 0.005$  of the Type-1 AGN and the Type-2 AGN, respectively, with uncertainties determined by the bootstrap method within 1000 loops. The new mean  $R_{sii}$  can lead the corresponding mean  $n_e$  in units of  $\text{cm}^{-3}$  to be estimated as  $326 \pm 7$  and  $225 \pm 8$  of the 548 Type-1 AGN and the 548 Type-2 AGN in the subsamples. Therefore, after considering the necessary effects of different distributions of redshift, O3HB, N2HA,  $L_{O3}$  and  $SN$ , Type-1 AGN have higher  $n_e$  in NLRs than Type-2 AGN.

Furthermore, the well-known Students T-statistic technique is applied to confirm that the mean values of  $\log(R_{sii})$  of the 548 Type-1 AGN and the 548 Type-2 AGN in the subsamples

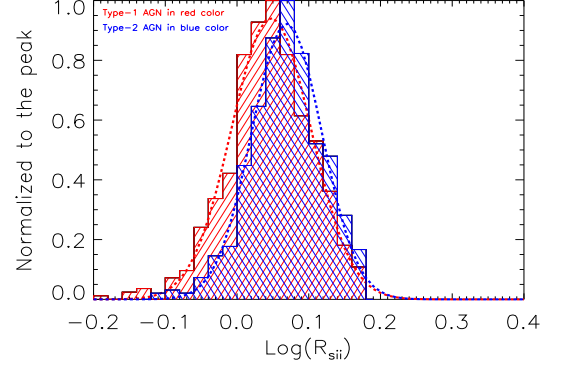


**Figure 10.** Similar as Fig. 6, but for the 548 Type-1 AGN and the 548 Type-2 AGN in the subsamples, which have the same distributions of redshift, O3HB, N2HA,  $L_{O3}$  and  $SN$ . The symbols and line styles have the same meanings as those in Fig. 6.

shown in Fig. 10 are significantly different with confidence level about  $2.4 \times 10^{-10}$  (higher than  $5\sigma$ ). And the two-sided Kolmogorov-Smirnov statistic technique indicates that the Type-1 AGN and the Type-2 AGN obey the same distributions of  $\log(R_{sii})$  with significance level about  $8.4 \times 10^{-11}$  (higher than  $5\sigma$ ). Therefore, before giving clear effects of electron temperature on measurements of electron densities (which will be well discussed in the subsection 3.6), Type-1 AGN have apparently higher electron densities  $n_e$  (only related to smaller  $R_{sii}$ ) in NLRs than the Type-2 AGN, with confidence level higher than  $5\sigma$ , against the expected results by the Unified model of AGN.

#### 3.4. Stronger AGN activities in Type-1 AGN?

Based on the higher  $n_e$  in NLRs in Type-2 AGN than in the HII galaxies as the shown results in Fig. 6, AGN activities can be well applied to explain the higher  $n_e$  in the Type-2 AGN than in HII galaxies, due to probable injecting electrons into NLRs through the galactic-scale outflows expected by the AGN feedback which plays key roles in galaxy evolution leading to tight connections between AGN and host galaxies as discussed in McNamara et al. (2007); Fabian (2012); Kormendy & Ho (2013); Heckman & Best (2014); King & Pounds (2015); Tombesi et al. (2015); Muller-Sanchez et al. (2018). If the AGN feedback expected outflows can lead to the higher  $n_e$  in Type-2 AGN than in HII galaxies, the stronger outflows could be also well applied to explain the higher  $n_e$  in NLRs in Type-1 AGN than in Type-2 AGN. More recently, Kakkad et al. (2018) have shown that there are statistical higher electron densities in NLRs in outflowing Seyfert galaxies than in non-outflowing Seyfert galaxies. Therefore, it is interesting to consider effects of outflows on our results.

As discussed in Ciccone et al. (2014); Fiore et al. (2017), the kinetic powers of outflows are tightly scaled with AGN

<sup>4</sup> To select different point from the mean value can lead to the same results

<sup>5</sup> The critical value 5% can lead about 100 Type-1 AGN and about 100 Type-2 AGN to be collected, leading to much clearer histogram distributions of the parameters.



bolometric luminosity, indicating stronger outflows in AGN with strong [O III] line luminosity. Similar results on the dependence of shifted velocities of [O III] lines on continuum luminosity can be found in Zhang (2021a). However, even the Type-2 AGN and the Type-1 AGN have the same properties of the [O III] line luminosity, the higher  $n_e$  can be also confirmed in Type-1 AGN as the results shown in Fig. 10. Meanwhile, considering the fitting results to the emission lines around H $\alpha$  in the mean spectra of high quality Type-1 AGN and high quality Type-2 AGN in Fig. 4, the [S II] doublets have symmetric line profiles in Type-1 AGN and in Type-2 AGN, because the [S II] doublets can be well described by two Gaussian components. If there were apparent effects of expected strong outflows on [S II] doublets, there should be double-peaked features and/or asymmetric line profiles as shown in Kakkad et al. (2018). Therefore, the symmetric line profiles of [S II] doublets support that there are no apparent different properties of outflows in current stages in the Type-1 AGN and in the Type-2 AGN, and it is not necessary to consider effects of asymmetric wings in [S II] doublets on our final results. Therefore, rather than the present injecting electrons into NLRs through galactic-scale outflows, longer durations of AGN activities triggering outflows in Type-1 AGN could be naturally applied to explain the higher  $n_e$  in NLRs in Type-1 AGN.

Either the higher  $n_e$  in NLRs in Type-1 AGN or the expected long durations of AGN activities triggering outflows in Type-1 AGN are against the expected results by the commonly and widely accepted Unified model of AGN.

### 3.5. Stronger star-forming contributions to NLRs in Type-2 AGN?

The main objective of the manuscript is to check the Unified Model of AGN through comparisons of electron densities in NLRs between Type-1 AGN and Type-2 AGN. Under the framework of the Unified Model of AGN, based on the same distributions of redshift between the 548 Type-1 AGN and the 548 Type-2 AGN in the subsamples, there are the same expected evolutionary histories between the Type-1 AGN and the Type-2 AGN in the subsamples, indicating the same host galaxy properties (including expected similar contributions of star-forming) between the 548 Type-1 AGN and the 548 Type-2 AGN in the subsamples.

However, if there were more contributions from HII regions in Type-2 AGN than in Type-1 AGN, lower electron densities in NLRs would be expected in Type-2 AGN, due to lower electron densities in HII regions, as the shown results for HII galaxies in Fig. 6. However, the assumption that more star-forming contributions in Type-2 AGN than in Type-1 AGN is against what have been expected by the Unified Model of AGN, to support our main final conclusion that the manuscript

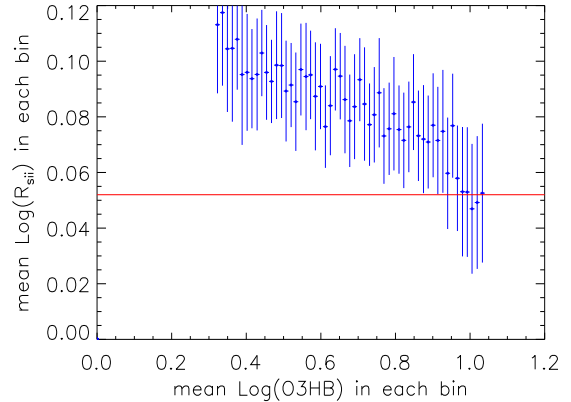


**Figure 11.** On the dependence of mean  $\log(R_{sii})$  on mean  $\log(O3HB)$  for the main sample of the 8725 Type-2 AGN (excluding the Type-2 LINERs and composite galaxies) divided into 55 bins (at least 50 objects included in each bin) with equal width of  $\log(O3HB)$ . Horizontal red line marks the position  $\log(R_{sii}) = 0.052$ .

provide interesting clues to challenge the Unified Model of AGN.

### 3.6. Further Discussions

In the discussed results above, effects of aperture sizes on the measured  $R_{sii}$  are not considered. Actually, Type-2 AGN with lower redshift than 0.1 should have their emission regions of [S II] doublet partly covered in the SDSS fiber spectra. However, if to consider the 140 Type-1 AGN and the 139 Type-2 AGN with redshift larger than 0.15 (corresponding fiber distance about 5200pc large enough to totally cover the NLRs of AGN with  $L_{O3} \sim 10^{41} \text{erg} \cdot \text{s}^{-1}$ ) in the subsamples, the mean  $\log(R_{sii})$  are about  $0.042 \pm 0.003$  and  $0.072 \pm 0.004$  in the Type-1 AGN and in the Type-2 AGN, also leading to higher  $n_e$  in NLRs of Type-1 AGN than Type-2 AGN. Here, the distances  $R_{NLRs}$  of NLRs to central BHs in AGN are simply determined by the empirical relation between  $R_{NLRs}$  and [O III] line luminosity, as well discussed in Liu et al. (2013); Hainline et al. (2013, 2014); Fischer et al. (2018); Dempsey & Zakamska (2018). Therefore, effects of aperture sizes have few effects on the final results.

Moreover, as described in Section 2, we can totally confirm that Type-1 AGN cannot be mis-collected into HII galaxy sample or into Type-2 AGN sample, because apparent broad H $\alpha$  in Type-1 AGN but no broad H $\alpha$  in HII galaxies nor in Type-2 AGN, however, we cannot give the totally confirmed conclusion that there are no Type-2 AGN mis-collected into the HII galaxy sample. Therefore, effects are simply discussed on our final results, if some Type-2 AGN were mis-collected into HII galaxies (or some HII galaxies mis-collected into Type-2 AGN). For the 8725 Type-2 AGN in the main sample, Fig. 11 shows the dependence of mean  $\log(R_{sii})$

on mean  $\log(O3HB)$  for the Type-2 AGN divided into 55 bins (at least 50 objects included in each bin) with equal width of  $\log(O3HB)$ . In Fig. 11, uncertainty of each mean  $\log(R_{sii})$  is calculated by the bootstrap method within 1000 loops. It is clear that in order to detect mean  $\log(R_{sii})$  to be about 0.042 (the mean  $\log(R_{sii})$  for the Type-1 AGN in the main sample) in Type-2 AGN, the Type-2 AGN with  $\log(O3HB)$  less than 1 should be the objects actually identified as HII galaxies, leading to the totally unreasonable results that about 95% Type-2 AGN in the main sample were HII galaxies. Therefore, mis-collected HII galaxies into Type-2 AGN sample can not be applied to explain the different  $n_e$  in NLRs between Type-1 AGN and Type-2 AGN. Meanwhile, considering the case that some Type-2 AGN were mis-collected into the HII galaxy sample, in order to detect mean  $\log(R_{sii})$  to be about 0.042 in Type-2 AGN, the HII galaxies with  $\log(R_{sii})$  smaller than 0.042 should be the objects actually identified as Type-2 AGN. Among the HII galaxies in the main sample, there are 1269 HII galaxies with  $\log(R_{sii})$  smaller than 0.052, even considering all the 1269 HII galaxies as Type-2 AGN, the mean  $\log(R_{sii})$  is about  $0.078 \pm 0.005$  in Type-2 AGN, re-confirming the higher electron density  $n_e$  in NLRs in Type-1 AGN than in Type-2 AGN.

Furthermore, as detailed discussions in Osterbrock (1989); Osterbrock & Ferland (2006); Kewley et al. (2019); Flury & Moran (2020), etc., there are apparent effects of electron temperature  $T_e$  on estimating electron density  $n_e$  by the parameter  $\log(R_{sii})$ , and the improved formula to estimate electron density can be described as (see Fig. 5.8 and corresponding discussions in Osterbrock & Ferland (2006)),

$$\frac{n_e}{\text{cm}^3} \times \left(\frac{10^4 K}{T_e}\right)^{0.5} \cong \frac{627.1 \times R_{sii} - 909.17}{0.4315 - R_{sii}} \quad (7)$$

after considering effects of electron temperature  $T_e$ . Therefore, it is necessary to consider effects of  $T_e$  on reported results on larger  $n_e$  (smaller  $\log(R_{sii})$ ) in Type-1 AGN. Electron temperatures  $T_e$  can be well traced by flux ratio  $O_{32}$  of the [O III] lines

$$O_{32} = \frac{f_{\lambda 4959} + f_{\lambda 5007}}{f_{\lambda 4364}} = \frac{7.9 \times \exp\left(\frac{3.29 \times 10^4 K}{T_e}\right)}{1 + 4.5 \times 10^{-4} n_e / T_e^{0.5}} \quad (8)$$

$$\sim 7.9 \times \exp\left(\frac{3.29 \times 10^4}{T_e}\right)$$

For the 548 Type-1 AGN and the 548 Type-2 AGN in the subsamples, emission lines around [O III] $\lambda 4364\text{\AA}$  within rest wavelength range from  $4250\text{\AA}$  to  $4450\text{\AA}$  are well measured by multiple-Gaussian functions, one narrow Gaussian function applied to describe narrow H $\gamma$ , one narrow Gaussian function applied to describe narrow [O III] $\lambda 4364\text{\AA}$ , two broad Gaussian functions applied to describe broad H $\gamma$  only in Type-1 AGN, after subtractions of host galaxy contributions (if

there are) which have been determined above through the SSP method. Fig. 12 shows one Type-1 AGN and one Type-2 AGN of which apparent [O III] $\lambda 4364\text{\AA}$  are best described by multiple Gaussian functions. Then, through the criterion that the measured flux and second moment of [O III] $\lambda 4364\text{\AA}$  at least 3 times larger than their corresponding uncertainties, there are 133 Type-1 AGN and 101 Type-2 AGN which have apparent [O III] $\lambda 4364\text{\AA}$ . The results indicate that only a small part of AGN have apparent [O III] $\lambda 4364\text{\AA}$ . That is the main reason why we do create our main samples (discussed in section 2) of AGN without considering properties of [O III] $\lambda 4364\text{\AA}$ . Not similar as [O III] $\lambda 4959, 5007\text{\AA}$  doublet which are commonly clear and strong in AGN, [O III] $\lambda 4364\text{\AA}$  emissions are commonly weak in AGN, leading to less number of AGN which have apparent [O III] $\lambda 4364\text{\AA}$  emission features. If not only apparent H $\alpha$ , H $\beta$ , [O III] $\lambda 4959, 5007\text{\AA}$ , [N II] and [S II] but also apparent [O III] $\lambda 4364\text{\AA}$  (line parameters are at least 5 times larger than their corresponding uncertainties) were considering to create new main samples, only about one seventh of the AGN in the main samples created in Section 2 were retained into new created main samples. Then, there should be only tens of AGN included in expected new subsamples which have the same distributions of  $z$ , O3HB, N2HA,  $L_{O3}$  and  $SN$ , leading to not reliable discussions on results through the new created subsamples.

Then, distributions of  $O_{32}$  and  $\log(R_{sii})$  are shown in top panels of Fig. 13, with mean values [ $O_{32}$ ,  $\log(R_{sii})$ ] of [ $61.49 \pm 6.42$ ,  $0.044 \pm 0.006$ ] in the 133 Type-1 AGN and of [ $92.27 \pm 4.12$ ,  $0.062 \pm 0.005$ ] in the 101 Type-2 AGN, respectively. Based on properties of  $O_{32}$ , bottom left panel of Fig. 13 shows distributions of  $T_e$  which are also listed in Table 1 and Table 2, with mean values of  $(1.95 \pm 0.14) \times 10^4 K$  in the 133 Type-1 AGN and of  $(1.41 \pm 0.07) \times 10^4 K$  in the 101 Type-2 AGN, respectively. Then, based on the calculated  $T_e$  and  $\log(R_{sii})$ , bottom right panel of Fig. 13 shows distributions of  $n_e/\text{cm}^3$  after corrections of effects of  $T_e$ . The improved mean electron densities  $n_e/\text{cm}^3$  are about  $394 \pm 36$  and  $283 \pm 23$  in the 133 Type-1 AGN and in the 101 Type-2 AGN, respectively, re-leading to apparently large  $n_e$  in NLRs in Type-1 AGN than in Type-2 AGN. Uncertainties of the mean values above are determined by the bootstrap method within 1000 loops. Furthermore, the two-sided Kolmogorov-Smirnov statistic technique is applied to determine that the 133 Type-1 AGN and the 101 Type-2 AGN obey the same distributions of  $\log(R_{sii})$  with significance level only about  $6 \times 10^{-5}$  (higher than  $4\sigma$ ). And the Students T-statistic technique is applied to confirm that the mean values of  $n_e$  of the 133 Type-1 AGN and the 101 Type-2 AGN in the subsamples are significantly different with confidence level about  $6.9 \times 10^{-7}$  (higher than  $5\sigma$ ). Moreover, as shown in bottom right panel of Fig. 13, it looks like there is a cut value  $\log(n_e) \sim 2.87$  for Type-2 AGN, it is also necessary to roughly check whether the cut value can lead to

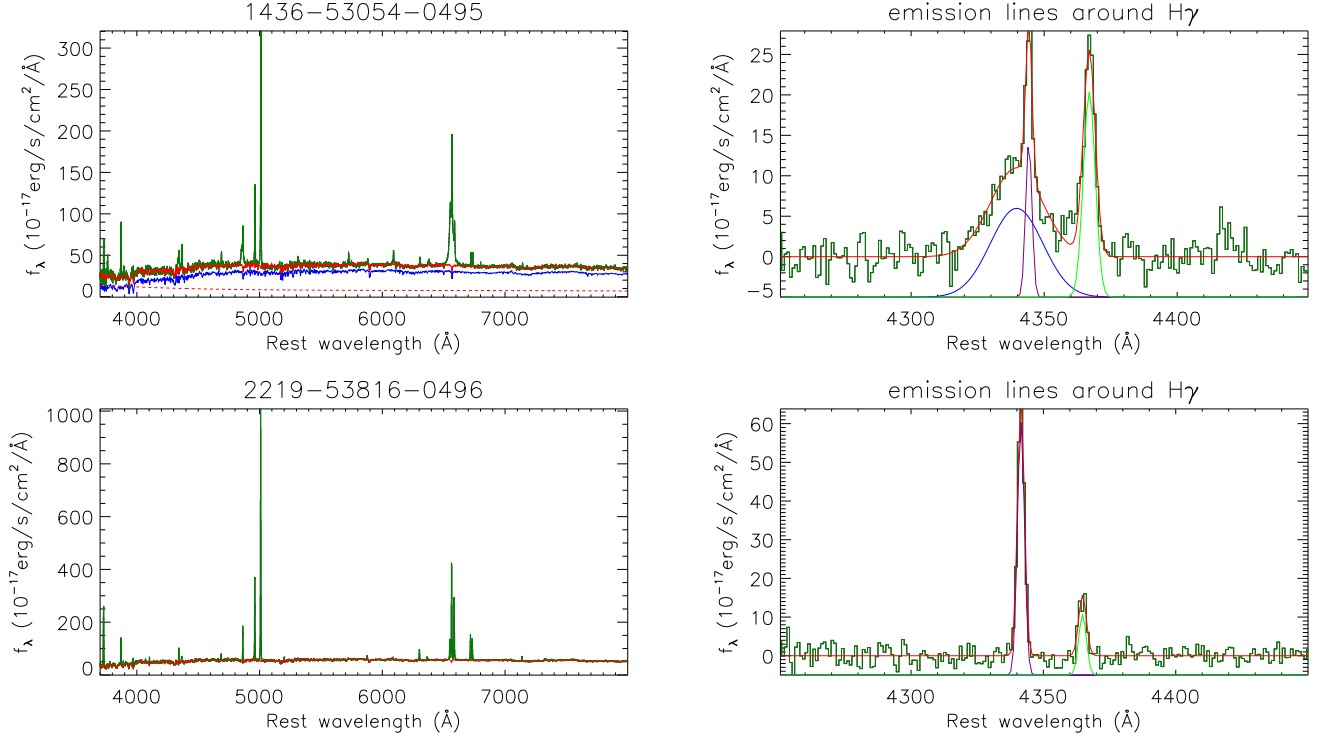


**Figure 12.** Left panels show the SDSS spectra (in dark green) of the Type-1 AGN 1436-53054-0495 (top panel) and the Type-2 AGN 2219-53816-0496 (bottom panel) in the subsamples, and the SSP method determined best descriptions (in red). In top left panel, solid blue line shows the determined host galaxy contributions and dashed red line shows the determined AGN continuum emissions. Right panels show the best descriptions (in red) to the emission lines around H $\gamma$  in the line spectrum (in dark green). In bottom region of each right panel, solid purple line and solid green line show the determined narrow H $\gamma$  and [O III] $\lambda$ 4364Å. And in bottom region of top right panel, solid blue line shows the determined broad H $\gamma$ . Title of each left panel marks the information of PLATE-MJD-FIBERID of the SDSS spectrum.

different results on  $n_e$ . Here, even accepted  $\log(n_e) \sim 2.87$  (the maximum value for Type-2 AGN) as a cut value, the mean values of  $\log(n_e)$  are  $2.51 \pm 0.03$  ( $323 \pm 21 \text{ cm}^3$ ) and  $2.45 \pm 0.02$  ( $282 \pm 14 \text{ cm}^3$ ) for the 107 Type-1 AGN with  $\log(n_e) < 2.87$  and the 101 Type-2 AGN with  $\log(n_e) < 2.87$ , leading to higher  $n_e$  in Type-1 AGN than in Type-2 AGN. Also, the two-sided Kolmogorov-Smirnov statistic technique can lead to probability only about  $1.9 \times 10^{-2}$  to support similar  $\log(n_e)$  distributions of the 107 Type-1 AGN with  $\log(n_e) < 2.87$  and the 101 Type-2 AGN with  $\log(n_e) < 2.87$ , and the Students T-statistic technique can lead to probability only about  $4.5 \times 10^{-3}$  to support similar mean values of  $n_e$  of the 107 Type-1 AGN with  $\log(n_e) < 2.87$  and the 101 Type-2 AGN with  $\log(n_e) < 2.87$ . Therefore, effects of electron temperatures can be applied to re-confirm the larger electron densities in NLRs of Type-1 AGN than in Type-2 AGN.

Moreover, based on  $T_e$  distributions shown in Fig. 13, effects of different  $T_e$  distributions can be checked by the following method, as what have been done in subsection 3.3. Through equation (6) with applications of only one parameter  $\log(T_e)$  of the 133 Type-1 AGN and the 101 Type-2 AGN shown in Fig. 13, one subsample of 62 Type-1 AGN and the other one subsample of 62 Type-2 AGN can be created with

the same  $\log(T_e)$  distributions. The two-sided Kolmogorov-Smirnov statistic technique can lead to probability 98.4% to support the same  $\log(T_e)$  distributions of AGN in the two subsamples. Left panel of Fig. 14 shows the  $\log(T_e)$  distributions of AGN in the two subsamples. Then, right panel of Fig. 14 shows the  $n_e$  distributions of AGN in the two subsamples. The mean values of  $\log(n_e)$  are about  $2.56 \pm 0.04$  ( $363 \pm 33 \text{ cm}^3$ ) and  $2.45 \pm 0.03$  ( $282 \pm 19 \text{ cm}^3$ ) for the 62 Type-1 AGN and the 62 Type-2 AGN in the subsamples having the same  $\log(T_e)$  distributions, leading to higher  $n_e$  in the 62 Type-1 AGN than in the Type-2 AGN in the new created subsamples. Uncertainties of the mean values above are determined by the bootstrap method within 1000 loops. Also, the two-sided Kolmogorov-Smirnov statistic technique can lead to probability only about  $2.6 \times 10^{-2}$  to support similar  $\log(n_e)$  distributions of the 62 Type-1 AGN and the 62 Type-2 AGN in the new created subsamples, and the Students T-statistic technique can lead to probability only about  $3.1 \times 10^{-2}$  to support similar mean values of  $\log(n_e)$  of the 62 Type-1 AGN and the 62 Type-2 AGN in the new created subsamples. Therefore, totally ignoring effects of different  $T_e$  distributions shown in Fig. 13, higher electron density in NLRs in Type-1 AGN can be well

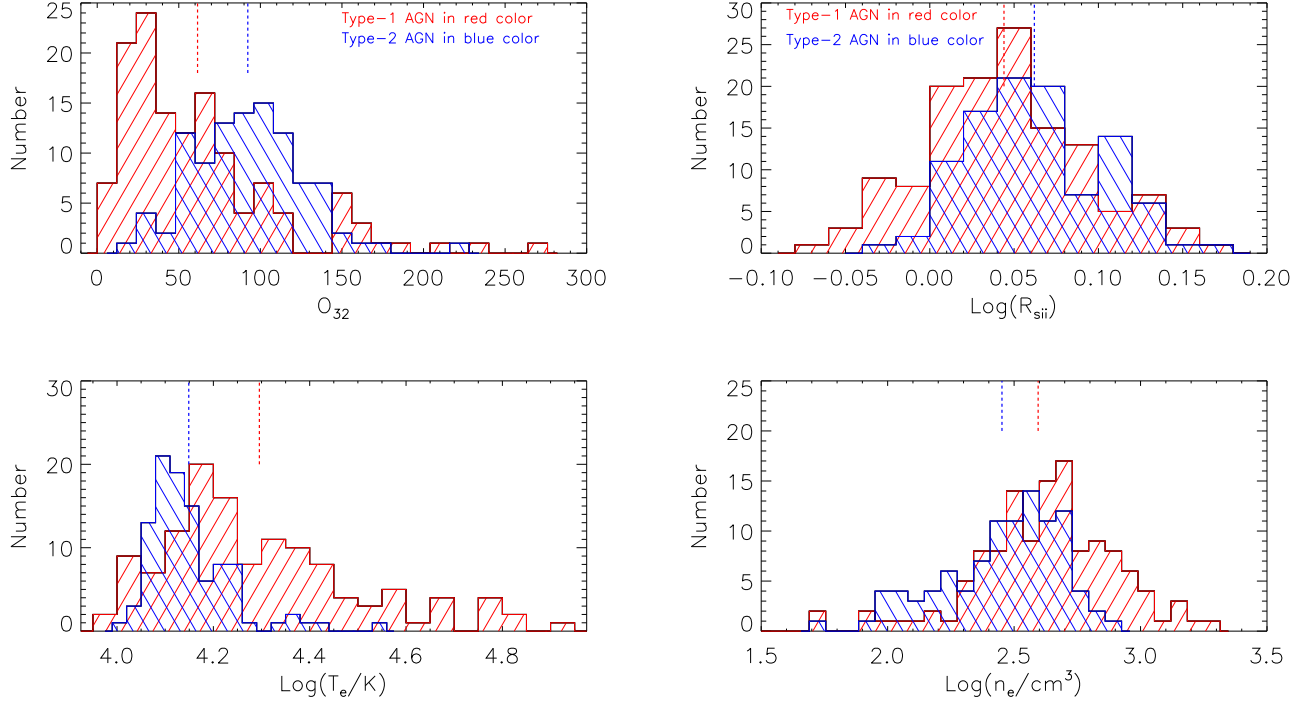


**Figure 13.** Distributions of  $O_{32}$  (top left panel),  $\log(R_{sii})$  (top right panel),  $\log(T_e/K)$  (bottom left panel) and improved electron density  $\log(n_e/cm^3)$  (bottom right panel) of the 133 Type-1 AGN (in red color) and the 101 Type-2 AGN (in blue color) which have apparent  $[O\ III]\lambda 4364\text{\AA}$ . In top region of each panel, vertical dashed lines in red and in blue mark the positions corresponding to the mean values of the Type-1 AGN and of the Type-2 AGN, respectively.

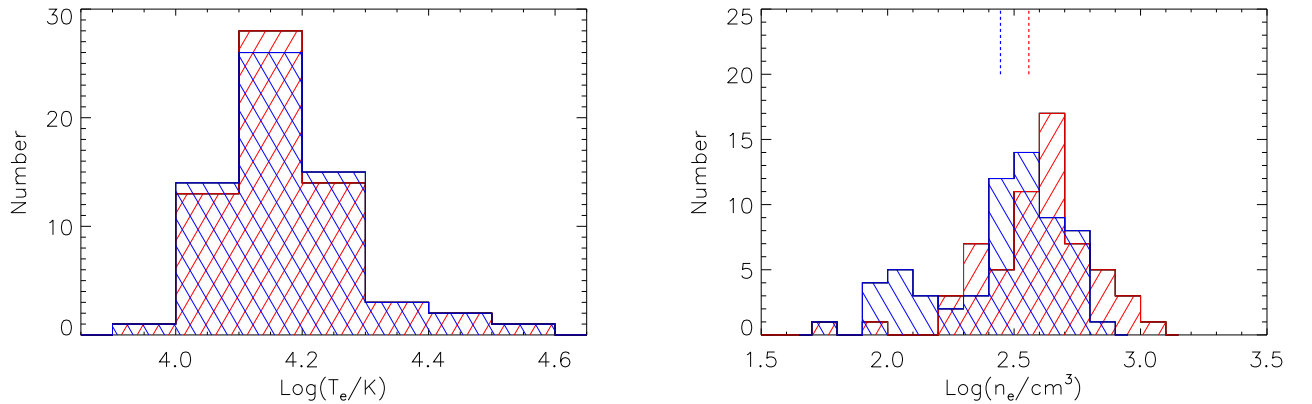


**Figure 14.** The same  $\log(T_e)$  distributions (left panel) and the  $\log(n_e)$  distributions (right panel) of the 62 Type-1 AGN and the 62 Type-2 AGN in the new created subsamples. In each panel, histogram filled by red lines shows the results for the 62 Type-1 AGN, and histogram filled by blue lines shows the results for the 62 Type-2 AGN. In right panel, vertical dashed red line and dashed blue line mark positions for mean values of  $\log(n_e)$  of the 62 Type-1 AGN and the 62 Type-2 AGN, respectively.

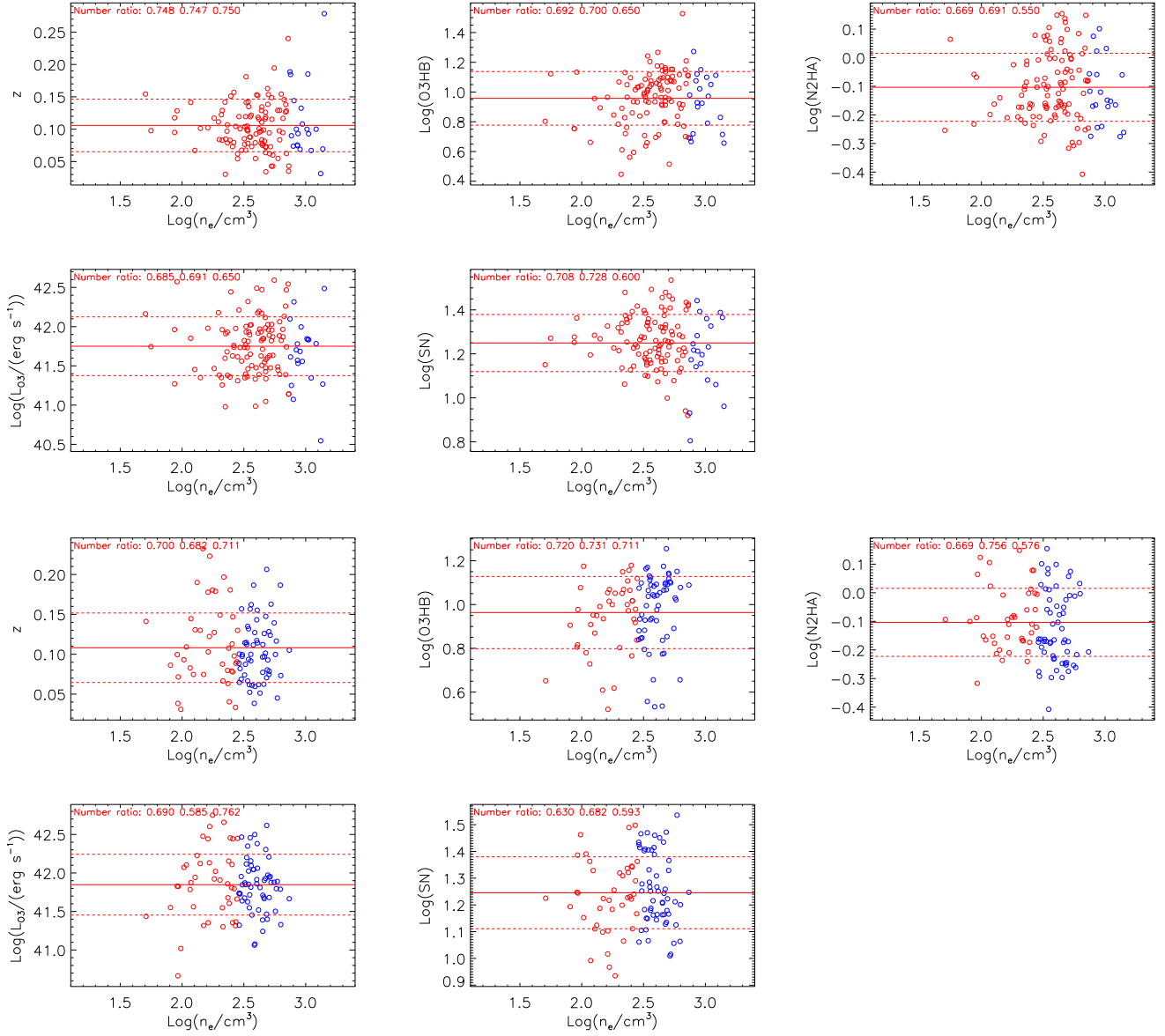


**Figure 15.** On the correlations between  $n_e$  and the parameters of  $z$ , O3HB, N2HA,  $L_{\text{O3}}$  and SN for the Type-1 AGN (panels in the first rows) and the Type-2 AGN (panels in the last rows) shown in bottom right panel of Fig 13. In each panel in the first two rows, open circles in red and in blue show the results for the Type-1 AGN with  $\text{log}(n_e) < 2.87$  and the Type-1 AGN with  $\text{log}(n_e) > 2.87$ , respectively. Horizontal solid red line and horizontal dashed red lines show the mean value of the parameter shown in Y-axis and corresponding 1RMS scatter bands for all the Type-1 AGN. In each panel in the last two rows, open circles in red and in blue show the results for the Type-2 AGN with  $\text{log}(n_e) < 2.45$  and the Type-2 AGN with  $\text{log}(n_e) > 2.45$ , respectively. Horizontal solid red line and horizontal dashed red lines show the mean value of the parameter shown in Y-axis and corresponding 1RMS scatter bands for all the Type-2 AGN. In top region of each panel of the Figure, the three number ratios are marked for the ratio of AGN outside of the 1RMS scatter bands to all the AGN, the ratio of AGN shown in blue outside of the 1RMS scatter bands to all the AGN shown in blue, and the ratio of AGN shown in red outside of the 1RMS scatter bands to all the AGN shown in red.



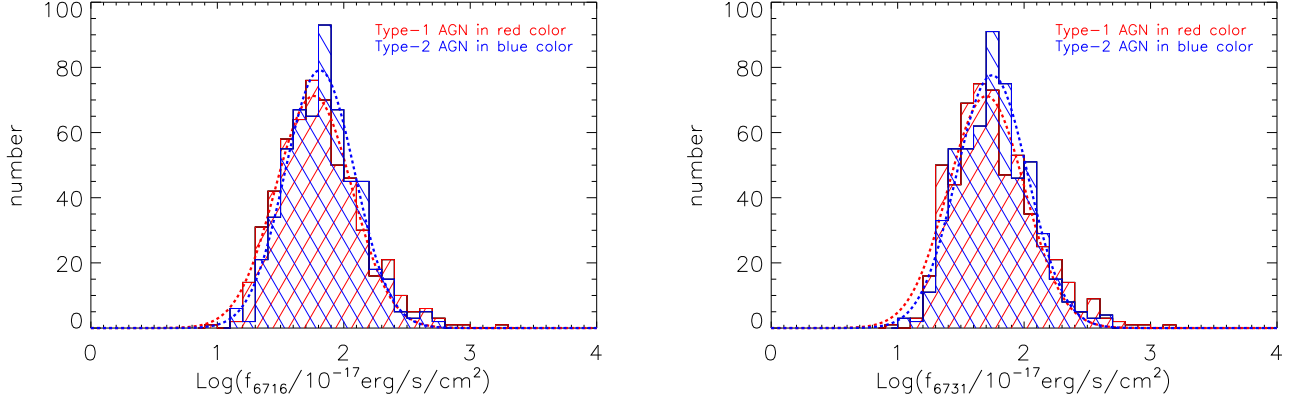


**Figure 16.** Distributions of  $f_{6716}$  (left panel) and  $f_{6731}$  (right panel) in the 548 Type-1 AGN (in red color) and in the 548 Type-2 AGN (in blue color) in the subsamples. Thick dashed lines in red and in blue represent the corresponding best Gaussian profiles for the distributions of the 548 Type-1 AGN and the 548 Type-2 AGN in the subsamples, respectively.

confirmed, even there are less numbers of AGN in the new created subsamples.

Furthermore, through the shown results in Fig. 13, it is interesting to consider whether the Type-1 AGN with higher electron densities  $\log(n_e) > 2.87$  have different physical properties from the other Type-1 AGN with  $\log(n_e) < 2.87$ . Then, panels in the first two rows of Fig. 15 shows correlations between  $n_e$  and the parameters of  $z$ , SN, O3HB, N2HA and  $L_{O3}$  of the Type-1 AGN shown in Fig. 13. The correlations have Spearman Rank correlation coefficients smaller than 0.2, thus rather than to determine linear fitting results (with determined parameters smaller than corresponding uncertainties by the FITEXY code), the mean values of  $z$ , SN, O3HB, N2HA and  $L_{O3}$  and corresponding 1RMS scatter bands are shown in each panel of Fig. 15. It is clear that there are the similar number ratios (marked in each panel) of Type-1 AGN outside of the 1RMS scatter bands to all Type-1 AGN, of the Type-1 AGN with  $\log(n_e) < 2.87$  outside of the 1RMS scatter bands to all the Type-1 AGN with  $\log(n_e) < 2.87$ , and of the Type-1 AGN with  $\log(n_e) > 2.87$  outside of the 1RMS scatter bands to all the Type-1 AGN with  $\log(n_e) > 2.87$ . The similar number ratios strongly indicate that the Type-1 AGN with  $\log(n_e) > 2.87$  are not outliers among the reported Type-1 AGN. Meanwhile, the panels in the last two rows shows similar results for the Type-2 AGN shown in Fig. 13 with accepted cut value  $\log(n_e) \sim 2.45$  (the mean value of  $\log(n_e)$  of the Type-2 AGN). Similar results can be found that there are similar number ratios (marked in each panel) of Type-2 AGN outside of the 1RMS scatter bands to all Type-2 AGN, of the Type-2 AGN with  $\log(n_e) < 2.45$  outside of the 1RMS scatter bands to all the Type-2 AGN with  $\log(n_e) < 2.45$ , and of the Type-2 AGN with  $\log(n_e) > 2.45$  outside of the 1RMS scatter bands to all the Type-2 AGN with  $\log(n_e) > 2.45$ . Therefore, the results in Fig. 15 strongly support that the se-

lected AGN with different  $n_e$  have similar physical properties as the other reported AGN in the manuscript.

Furthermore as well discussed in Filippenko & Halpern (1984) with two zones with different electron densities in NGC 7213, if there were higher electron density regions closer to central BHs could be visible in Type-1 AGN but probably seriously obscured in Type-2 AGN, higher electron densities (smaller  $R_{sii}$ ) could be well expected in Type-1 AGN. To put it simply, if the two-zone model was accepted, line fluxes ( $f_{6716}$ ,  $f_{6731}$ ) of each [S II] line include two components, one component ( $f_{6716,H}$ ,  $f_{6731,H}$ ) from higher electron density regions and the other one component ( $f_{6716,L}$  and  $f_{6731,L}$ ) from normal (or lower) electron density regions. Meanwhile, due to  $f_{6716,H}$ ,  $f_{6731,H}$  from higher electron density regions, we have

$$f_{6716,H}/f_{6731,H} < f_{6716,L}/f_{6731,L} \quad (9)$$

. Then, based on serious dependence of flux ratios of [S II] on electron densities, mean electron densities  $n_e$  can be simply determined by flux ratios of the two components as follows,

$$R_{sii} = \frac{f_{6716,H} + f_{6716,L}}{f_{6731,H} + f_{6731,L}} \quad (10)$$

$$n_e \times \left(\frac{10^4 K}{T_e}\right)^{0.5} \sim \frac{627.1 \times R_{sii} - 909.17}{0.4315 - R_{sii}}$$

. For type-1 AGN, due to no obscurations, all the parameters from observed line fluxes can be well accepted intrinsic values. However, for Type-2 AGN with orientation effects leading to higher electron density zones being seriously obscured, without contributions of  $f_{6716,H}$  and  $f_{6731,H}$ ,  $R_{sii}$  in Type-2 AGN should be  $R_{sii,T2} = \frac{f_{6716,L}}{f_{6731,L}}$ . Considering  $f_{6716,H}/f_{6731,H} < f_{6716,L}/f_{6731,L}$ , we will clearly have

$$R_{sii,T2} > R_{sii,T1} = \frac{f_{6716,H} + f_{6716,L}}{f_{6731,H} + f_{6731,L}} \quad (11)$$

with  $R_{sii,T1}$  as measurements of  $R_{sii}$  in Type-1 AGN. That is why two zone model can be applied to explain higher electron densities in Type-1 AGN based on flux ratio  $R_{sii}$  of [S II] emission lines. Meanwhile, after considering orientation effects expected obscurations on higher electron density regions, flux intensities of [S II] emission lines in Type-2 ( $f_{6716,L}$  and  $f_{6731,L}$ ) should be smaller than the flux intensities ( $f_{6716,L} + f_{6716,H}$  and  $f_{6731,L} + f_{6731,H}$ ) in Type-1 AGN. Therefore, it is interesting and necessary to check effects of the probable higher electron density regions closer to central BHs on our final results. However, the mean [S II] $\lambda 6716\text{\AA}$  ([S II] $\lambda 6731\text{\AA}$ ) line intensities  $\log(f_{6716}/10^{-17}\text{erg/s/cm}^2)$  ( $\log(f_{6731}/10^{-17}\text{erg/s/cm}^2)$ ) are about  $1.812\pm 0.013$  ( $1.767\pm 0.010$ ) and  $1.832\pm 0.013$  ( $1.765\pm 0.010$ ) in the 548 Type-1 AGN and the 548 Type-2 AGN in the subsamples respectively. The uncertainties are determined by the bootstrap method within 1000 loops. Distributions of  $f_{6716}$  and  $f_{6731}$  are shown in Fig. 16. Slightly higher [S II] $\lambda 6716\text{\AA}$  line intensities can be found in Type-2 AGN than in Type-1 AGN, and similar [S II] $\lambda 6731\text{\AA}$  line intensities can be found between Type-1 AGN and Type-2 AGN. Because the Type-1 AGN and the Type-2 AGN in the subsamples have the same redshift distributions, [S II] line luminosity distributions are not shown and discussed again. The results are against the expected higher [S II] line intensities in Type-1 AGN, therefore, higher electron density regions visible in Type-1 AGN (or higher electron density regions partly obscured in Type-2 AGN) can not be applied to well explain the higher electron densities in Type-1 AGN than in Type-2 AGN.

Finally, simple discussions are given on probable asymmetric components in [S II] doublet, although there are no clear clues to support apparent asymmetric components in [S II] doublet in the mean spectra of high quality AGN. As is known, asymmetric components in [S II] doublet could be tightly related to radial outflows. And galactic outflows could be tightly related to radio emissions, such as the more recent results in Jarvis et al. (2019). Therefore, among the AGN in the main samples, radio properties are checked through the FIRST (Faint Images of the Radio Sky at Twenty-Centimeters) database (Becker et al. 1995; Helfand et al. 2015), and to show whether are there quite different  $\log(R_{sii})$  between AGN without radio emissions and AGN with radio emissions. Among the 6039 Type-1 AGN collected from SDSS DR12, there are 4432 Type-1 AGN (no-radio Type-1 AGN) covered by FIRST but with radio emission intensity to be zero, and 1607 Type-1 AGN (radio Type-1 AGN) covered by FIRST with radio emission intensity larger than zero. Mean  $\log(R_{sii})$  are about  $0.052\pm 0.003$  for the 4432 no-radio Type-1 AGN and  $0.049\pm 0.003$  for the 1607 radio Type-1 AGN, respectively. Meanwhile, among the 12999 Type-2 AGN collected from SDSS DR12, there

are 10431 Type-2 AGN (no-radio Type-2 AGN) covered by FIRST but with radio emission intensity to be zero, and 2568 Type-2 AGN (radio Type-2 AGN) covered by FIRST with radio emission intensity larger than zero. Mean  $\log(R_{sii})$  are about  $0.088\pm 0.005$  for the 10431 no-radio Type-2 AGN and  $0.082\pm 0.005$  for the 2568 radio Type-2 AGN. Therefore, even considering effects of asymmetric components related to radio emissions, it can be re-confirmed that Type-1 AGN has higher  $n_e$  in NLRs than Type-2 AGN.

#### 4. FURTHER IMPLICATIONS

If the higher electron density  $n_e$  in NLRs in Type-1 AGN are intrinsically true, there could be some special type-1 AGN of which NLRs have electron densities high enough to be nearer to critical densities to forbidden emission lines, once strong injecting electrons can last long enough, leading to quite weak narrow forbidden emission lines. Therefore, in the near future, to detect so special Type-1 AGN without narrow forbidden emission lines is the main objective of one of our being prepared manuscripts.

#### 5. SUMMARY AND CONCLUSIONS

Finally, the main summary and conclusions are as follows.

- All the low redshift ( $z < 0.3$ ) Type-1 AGN and Type-2 AGN are collected from SDSS DR12. The [S II] $\lambda 6716, 6731\text{\AA}$  doublets are well measured. Based on the reliable [S II] $\lambda 6716, 6731\text{\AA}$  doublets, there are 6039 Type-1 AGN with reliable [S II] doublets and apparent broad H $\alpha$  emission lines, and 12999 Type-2 AGN with reliable [S II] doublets but no broad H $\alpha$  emission lines.
- After considering the controversial conclusion on physical nature of Type-2 LINERs (at least part of Type-2 AGN without AGN nature) and considering strong contributions from star-forming in composite galaxies, both Type-2 LINERs and composite galaxies are not considered in the final main sample of Type-2 AGN, lead the final main sample of Type-2 AGN including 8725 Type-2 AGN.
- Based on the reliable line flux ratio  $R_{sii}$  of [S II] $\lambda 6716\text{\AA}$  to [S II] $\lambda 6731\text{\AA}$ , higher electron densities  $n_e$  in NLRs can be found in Type-1 AGN than in Type-2 AGN, and in Type-2 AGN than in HII galaxies.
- After considering necessary effects of redshift and central AGN activities on the distributions of  $n_e$ , two subsamples of 548 Type-1 AGN and 548 Type-2 AGN are created to have the same distributions of  $z$ , O3HB, N2HA,  $L_{O3}$  and SN, still leading to higher  $n_e$  in NLRs of Type-1 AGN than Type-2 AGN, with confidence level higher than  $5\sigma$ .

- Comparing the  $n_e$  in NLRs between HII galaxies and Type-2 AGN, AGN activities related to central BH accreting power should play key roles in higher electron densities in NLRs due to injecting electrons by AGN feedback expected galactic-scale outflows.
- Unfortunately, even Type-1 AGN and Type-2 AGN have the same properties of O3HB, N2HA and  $L_{O3}$  at present times, the AGN in the subsamples, higher  $n_e$  in NLRs in Type-1 AGN can also be confirmed. Therefore, longer time durations of AGN activities in Type-1 AGN should be preferred.
- Considering lower electron densities in HII galaxies, stronger star-forming contributions to NLRs could be applied to explain the lower electron densities in NLRs in Type-2 AGN than in Type-1 AGN, if not considering the Unified Model expected similar host galaxy evolutionary histories for the AGN in the subsamples with the same distributions of redshift.
- After considering probable effects of asymmetric components in [S II] doublets related to radio emissions, it can be re-confirmed that Type-1 AGN without (with) radio emissions has higher  $n_e$  in NLRs than Type-2 AGN without (with) radio emissions.
- After considering effects of electron temperatures traced by flux ratio of [O III] $\lambda$ 4364, 4959, 5007Å emis-

sion lines on estimating electron densities in NLRs, more apparently large  $n_e$  in NLRs in Type-1 AGN than in Type-2 AGN.

- Either higher  $n_e$  in NLRs in Type-1 AGN than in Type-2 AGN or expected longer time durations of AGN activities triggering outflows in Type-1 AGN than in Type-2 AGN or stronger star-forming contributions in Type-1 AGN than in Type-2 AGN could provide interesting challenges to the currently accepted Unified model of AGN.

#### ACKNOWLEDGEMENTS

Zhang gratefully acknowledge the anonymous referee for giving us constructive and valuable comments and suggestions to greatly improve the paper. Zhang gratefully thanks the kind financial support from NSFC-12173020. This manuscript has made use of the data from the SDSS projects, <http://www.sdss3.org/>, managed by the Astrophysical Research Consortium for the Participating Institutions of the SDSS-III Collaborations. This manuscript has made use of the data from FIRST database <http://sundog.stsci.edu/>. This paper has made use of the MPFIT package <https://pages.physics.wisc.edu/~craigm/idl/cmpfit.html> and the FITEXY procedure <https://idlastro.gsfc.nasa.gov/ftp/pro/math/fitexy.p>

#### REFERENCES

- Aller, L. H.; Epps, H. W., 1976, ApJ, 204, 445  
 Alam, S., et al., 2015, ApJS, 219, 12  
 Antonucci, R., 1993, ARA&A, 31, 473  
 Baldwin, J. A.; Phillips, M. M.; Terlevich, R. 1981, PASP, 93, 5  
 Balokovic, M.; Brightman, M.; Harrison, F. A.; et al., 2018, ApJ, 854, 42  
 Becker, R. H., White, R. L., Helfand, D. J. 1995, ApJ, 450, 559  
 Bornancini, C.; Garcia Lambas, D., 2020, MNRAS, 494, 1189  
 Brown, A.; Nayyeri, H.; Cooray, A.; Ma, J.; Hickox, R. C.; Azadi, M., 2019, ApJ, 871, 87  
 Bruzual, G.; Charlot, S. 2003, MNRAS, 344, 1000  
 Cid Fernandes, R.; Stasinska, G.; Mateus, A.; et al., 2011, MNRAS, 413, 1687  
 Cappellari, M., 2017, MNRAS, 466, 798  
 Canto, J.; Meaburn, J.; Theokas, A. C.; Elliott, K. H., 1980, MNRAS, 193, 911  
 Cid Fernandes, R.; Mateus, A.; Sodre, L.; Stasinska, G.; Gomes, J. M., 2005, MNRAS, 358, 363  
 Cicone, C.; Maiolino, R.; Sturm, E.; et al., 2014, A&A, 562, 21  
 Dempsey, R.; Zakamska, N. L., 2018, MNRAS, 477, 4615  
 Dopita, M. A. & Sutherland, R. S., 1996, ApJS, 102, 161  
 Dors, O. L.; Cardaci, M. V.; Hagele, G. F.; Krabbe, A. C., 2014, MNRAS, 443, 1291  
 Dors, O. L.; Valerdi, M.; Freitas-Lemes, P.; et al., 2022, MNRAS, 514, 5506  
 Eracleous, M.; Hwang, J. A.; Flohic, H. M. L. G., 2010, ApJ, 711, 796  
 Fabian, A. C., 2012, ARA&A, 50, 455  
 Filippenko, A. V.; Halpern, J. P., 1984, ApJ, 285, 458  
 Filippenko, A. V. & Terlevich, R., 1992, ApJL, 397, 79  
 Fischer, T., Kraemer, S., Schmitt, H., et al., 2018, ApJ, 856, 102  
 Fiore, F.; Feruglio, C.; Shankar, F.; et al., 2017 A&A, 601, 143  
 Franceschini, A.; Braitto, V.; Fadda, D., 2002, MNRAS Letter, 335, 51  
 Flury, S. R.; Moran, E. C., 2020, MNRAS, 496, 2191  
 Greene, J. E.; Ho, L. C., 2005, ApJ, 627, 721  
 Hainline, K., Hickox, R., Greene, J., et al., 2013, ApJ, 774, 145  
 Hainline, K., Hickox, R., Greene, J., et al., 2014, ApJ, 787, 65  
 Heckman, T. M., 1980, A&A, 87, 152  
 Heckman, T. M.; Best, P. N., 2014, ARA&A, 52, 589  
 Heisler, C. A.; Lumsden, S. L.; Bailey, J. A., 1997, Nature, 385, 700  
 Helfand, D. J.; White, R. L.; Becker, R. H., 2015, ApJ, 801, 26

**Table 1.** Basic information of the 548 Type-1 AGN with reliable [S II] emissions in the subsample

(1)	(2)	(3)	(4)	(5)	(6)	(7)	(8)	(9)	(10)	(11)
0271-51883-0322	0.086	20.59	1.064	0.181	0.832	41.58	0.775	...	...	3.090
0273-51957-0460	0.096	13.19	1.189	0.005	0.780	41.78	1.210	...	...	2.284
0274-51913-0141	0.138	15.66	1.098	0.098	0.919	42.02	1.535	102.8	3.851	...
0279-51608-0392	0.072	17.36	0.932	-0.175	0.433	41.22	1.141	...	...	2.435
0288-52000-0088	0.118	11.83	1.266	-0.051	0.759	41.91	0.854	185.1	3.799	2.844
0289-51990-0056	0.114	15.73	0.612	-0.178	0.339	41.38	1.158	...	...	2.400
0291-51660-0451	0.089	17.19	0.882	-0.234	0.432	41.41	1.302	...	...	2.024
0291-51660-0470	0.142	11.35	1.021	0.104	1.245	41.65	1.234	...	...	2.226
0291-51928-0474	0.142	16.93	0.954	0.093	0.834	41.92	1.266	...	...	2.139
0295-51985-0255	0.086	13.41	0.740	-0.220	0.480	40.97	1.490	...	...	...
0297-51959-0439	0.103	12.75	0.521	-0.211	0.414	41.16	1.157	...	...	2.401
0308-51662-0007	0.119	12.92	0.942	-0.023	0.686	42.26	1.298	...	...	2.040
0308-51662-0008	0.119	15.80	1.034	-0.008	1.005	42.21	1.253	164.1	3.809	2.079
0309-51666-0116	0.132	14.31	1.150	-0.120	0.491	41.99	1.310	23.66	4.016	2.006
0326-52375-0259	0.096	15.44	0.692	-0.153	0.356	41.21	1.122	...	...	2.472
0326-52375-0580	0.119	13.18	1.209	0.030	1.157	42.03	0.774	...	...	3.092
0330-52370-0168	0.165	11.64	0.840	0.007	0.452	41.86	1.139	...	...	2.438
0336-51999-0611	0.086	18.09	0.812	-0.106	0.268	42.08	1.118	...	...	2.480
0339-51692-0544	0.159	14.10	0.817	-0.036	0.464	42.23	1.013	...	...	2.673
0341-51690-0131	0.085	24.22	0.808	-0.119	0.349	41.67	1.144	...	...	2.429
0349-51699-0624	0.176	13.91	1.012	-0.096	0.665	42.70	1.427	...	...	1.138
0350-51691-0169	0.228	10.07	0.773	-0.287	0.351	42.11	1.401	...	...	1.489
0350-51691-0520	0.078	21.99	0.965	-0.011	0.799	41.37	1.304	46.21	3.933	1.987
0354-51792-0617	0.068	24.71	1.021	0.101	0.639	41.68	1.421	59.88	3.905	1.212
0355-51788-0319	0.125	12.04	1.107	0.087	1.951	41.48	1.045	...	...	2.615
0366-52017-0299	0.159	18.58	0.998	-0.163	0.370	42.31	0.739	...	...	3.160
0371-52078-0215	0.110	15.14	1.013	-0.162	0.635	42.16	1.107	40.86	3.947	2.475
0371-52078-0457	0.224	8.549	1.003	-0.019	0.398	41.91	1.178	...	...	2.357
0372-52173-0446	0.217	11.28	0.739	-0.215	0.307	42.31	1.048	...	...	2.610
0381-51811-0403	0.198	9.365	0.787	-0.174	0.457	41.71	0.949	...	...	2.782
0385-51783-0251	0.166	10.93	1.069	-0.091	0.814	41.82	1.055	9.126	4.172	2.683
0385-51783-0547	0.097	17.50	1.026	-0.087	0.655	41.62	1.369	13.40	4.103	1.780
0385-51877-0550	0.097	18.68	0.983	-0.123	0.619	41.52	1.036	...	...	2.632
0388-51793-0408	0.113	14.78	1.185	-0.018	0.633	41.74	1.758	6.329	4.251	...
0390-51900-0327	0.063	24.88	0.749	-0.215	0.409	41.35	1.039	...	...	2.626
0400-51820-0047	0.098	21.69	1.058	0.023	0.599	42.03	1.047	...	...	2.611
0404-51812-0343	0.078	18.27	0.735	-0.160	0.708	41.02	1.078	...	...	2.555
0404-51877-0347	0.078	16.13	0.716	-0.188	0.657	41.00	0.928	...	...	2.818

NOTE— The first column shows the pmf information of plate-mjd-fiberid of each Type-1 AGN, the second column shows the redshift information of each Type-1 AGN, the third column shows the SN information of SDSS spectrum of each Type-1 AGN, the fourth column to the sixth column show  $\log(O3HB)$ ,  $\log(N2HA)$  and  $\log(S2HA)$  of each Type-1 AGN, the seventh column shows the logarithmic line luminosity (in units of erg/s) of  $[O\ III]\lambda 5007\text{\AA}$  of each Type-1 AGN, the eighth column shows the determined  $R_{sii}$  of each Type-1 AGN, the ninth column shows the determined  $O_{32}$  of each Type-1 AGN, the tenth column shows the determined logarithmic electron temperature  $\log(T_e)$  (in units of K) of the Type-1 AGN with reliable  $O_{32}$ , the final column shows the determined logarithmic  $n_e$  (in units of  $\text{cm}^{-3}$ ) of each Type-1 AGN.

In the last three columns, ... means no reliable value.

For the last column, if there is reliable  $T_e$ , the  $n_e$  is the value after correction of effects of  $T_e$ , if there is not reliable  $T_e$ , the  $n_e$  is the value determined through  $R_{sii}$ .

In the last column, ... means  $R_{sii}$  is so large that the equation 5 in the manuscript can not lead to a reliable value.

**Table 1.** –to be continued

(1)	(2)	(3)	(4)	(5)	(6)	(7)	(8)	(9)	(10)	(11)
0404-51877-0409	0.180	10.12	0.872	-0.132	0.651	42.24	1.080	...	...	2.551
0406-51876-0112	0.213	8.267	0.908	-0.075	0.370	42.17	0.839	...	...	2.972
0412-52258-0083	0.281	10.04	0.754	-0.122	0.466	42.84	1.263	...	...	2.148
0412-52258-0576	0.208	9.968	0.677	-0.182	0.315	41.67	1.538	...	...	...
0413-51821-0535	0.067	21.20	1.050	-0.152	0.345	41.34	1.147	24.77	4.010	2.427
0413-51929-0528	0.067	19.26	0.956	-0.162	0.432	41.45	1.061	29.91	3.985	2.580
0418-51817-0281	0.100	17.43	0.811	-0.198	0.361	41.73	1.228	...	...	2.240
0418-51817-0595	0.101	18.55	0.893	-0.140	0.498	41.34	1.183	18.20	4.054	2.374
0418-51884-0300	0.100	18.36	0.838	-0.206	0.360	41.73	0.961	68.87	3.890	2.706
0420-51871-0284	0.133	11.54	0.897	-0.042	0.556	41.84	1.359	...	...	1.786
0422-51811-0137	0.184	13.61	0.968	-0.007	0.340	42.24	0.727	...	...	3.184
0424-51893-0451	0.163	11.01	1.079	-0.089	0.718	41.88	1.023	...	...	2.654
0427-51900-0196	0.122	13.20	1.031	-0.077	0.382	41.80	1.202	...	...	2.303
0427-51900-0441	0.124	14.94	0.701	-0.126	0.448	41.08	1.285	...	...	2.081
0437-51869-0246	0.093	24.86	1.131	0.086	0.534	42.18	1.177	...	...	2.358
0441-51868-0450	0.128	14.75	0.837	-0.199	0.488	41.48	1.523	19.13	4.047	...
0442-51882-0431	0.111	13.58	0.575	-0.227	0.365	41.42	0.929	...	...	2.816
0447-51877-0526	0.111	20.82	0.783	-0.206	0.371	42.17	1.041	77.04	3.879	2.562
0460-51924-0348	0.196	10.30	1.043	0.125	1.105	42.22	1.394	...	...	1.552
0471-51924-0299	0.121	15.64	1.059	0.006	0.701	41.50	1.252	...	...	2.177
0472-51955-0469	0.225	9.657	1.096	-0.118	0.536	42.52	0.879	...	...	2.902
0473-51929-0612	0.083	16.60	1.152	-0.090	0.615	41.99	0.975	...	...	2.737
0481-51908-0077	0.097	16.51	1.026	0.084	0.859	41.88	1.037	86.29	3.868	2.563
0483-51902-0030	0.098	20.02	1.096	-0.110	0.580	41.84	1.138	69.22	3.890	2.385
0483-51924-0004	0.098	14.28	1.029	-0.104	0.674	41.53	1.205	...	...	2.296
0483-51924-0394	0.202	12.55	0.873	-0.155	0.336	42.50	1.007	...	...	2.683
0485-51909-0016	0.095	17.19	1.049	-0.151	0.686	41.96	1.223	68.80	3.890	2.199
0487-51943-0464	0.119	18.28	0.603	-0.256	0.333	41.54	1.058	...	...	2.593
0490-51929-0590	0.221	10.97	0.696	-0.164	0.482	41.85	1.066	...	...	2.577
0501-52235-0330	0.090	21.95	1.116	0.005	1.174	41.73	1.024	...	...	2.653
0503-51999-0085	0.078	30.38	0.879	-0.004	0.498	41.93	1.119	...	...	2.478
0509-52374-0287	0.097	18.67	1.122	0.064	0.904	41.74	0.976	56.18	3.912	2.691
0509-52374-0508	0.079	16.84	0.935	-0.205	0.286	41.76	0.917	11.78	4.125	2.899
0513-51989-0038	0.257	7.148	0.643	-0.160	0.461	41.76	1.045	...	...	2.616
0517-52024-0243	0.111	17.59	1.101	-0.040	0.726	41.76	1.955	...	...	...
0522-52024-0508	0.101	16.51	1.049	0.012	0.629	41.69	1.215	...	...	2.272
0524-52027-0131	0.185	12.04	0.790	-0.148	0.388	41.83	0.894	18.28	4.053	2.902
0528-52022-0585	0.116	17.93	0.860	-0.036	0.505	41.87	1.052	...	...	2.603
0529-52025-0142	0.074	16.49	0.745	-0.130	0.450	40.69	1.028	...	...	2.646
0531-52028-0502	0.195	10.63	0.440	-0.276	0.261	41.65	1.098	...	...	2.518
0533-51994-0050	0.138	10.65	0.812	-0.333	0.273	41.68	1.332	...	...	1.911
0533-51994-0352	0.159	11.28	0.793	-0.145	0.311	41.79	1.182	...	...	2.348
0543-52017-0206	0.072	14.68	0.911	-0.190	0.478	41.04	0.904	32.32	3.976	2.848
0543-52017-0547	0.179	12.93	1.064	-0.011	0.650	42.35	1.402	...	...	1.486
0545-52202-0073	0.098	14.44	0.859	-0.109	0.400	41.61	0.969	27.29	3.997	2.747
0553-51999-0112	0.096	20.41	0.948	-0.097	0.325	42.08	1.301	...	...	2.028
0561-52295-0046	0.085	24.94	0.981	-0.093	0.485	41.82	1.230	146.1	3.819	2.146
0561-52295-0081	0.093	14.01	0.486	-0.233	0.541	40.97	0.968	...	...	2.749



**Table 1.** –to be continued

(1)	(2)	(3)	(4)	(5)	(6)	(7)	(8)	(9)	(10)	(11)
0568-52254-0184	0.128	25.12	1.056	-0.079	0.346	42.46	0.995	27.09	3.998	2.702
0572-52289-0521	0.124	25.28	0.661	-0.178	0.191	42.00	1.248	...	...	2.187
0575-52319-0202	0.061	26.13	0.932	-0.076	0.405	41.61	1.190	32.82	3.974	2.317
0576-52325-0413	0.122	14.03	0.646	-0.226	0.397	41.19	1.301	2.968	4.480	2.269
0580-52368-0532	0.095	14.44	1.170	-0.122	0.691	42.08	1.004	...	...	2.688
0581-52356-0418	0.193	11.54	0.486	-0.187	0.313	42.12	0.996	...	...	2.702
0583-52055-0341	0.093	17.74	0.751	-0.145	0.343	42.00	1.150	...	...	2.417
0584-52049-0489	0.087	23.20	0.689	-0.138	0.349	42.12	1.059	...	...	2.590
0588-52045-0419	0.094	21.47	1.018	-0.096	0.475	41.66	1.070	...	...	2.570
0589-52055-0173	0.085	16.33	1.024	0.000	0.678	41.55	1.137	...	...	2.442
0590-52057-0202	0.095	15.14	0.555	-0.297	0.373	41.36	1.196	...	...	2.317
0591-52022-0519	0.097	18.85	1.175	0.113	0.625	42.04	1.057	...	...	2.593
0593-52026-0151	0.173	12.13	0.935	0.007	0.778	42.20	0.976	...	...	2.736
0601-52316-0343	0.102	15.22	0.985	-0.103	0.277	41.71	1.199	...	...	2.310
0601-52316-0465	0.206	8.330	0.658	-0.303	0.308	41.86	1.090	...	...	2.534
0605-52353-0571	0.076	19.72	1.211	0.006	1.086	42.06	0.990	...	...	2.712
0606-52365-0479	0.138	21.06	0.766	-0.061	0.371	41.40	0.910	...	...	2.849
0608-52081-0442	0.111	13.08	1.029	0.033	0.638	41.68	0.970	...	...	2.746
0616-52374-0479	0.110	9.000	0.790	-0.300	0.453	41.41	0.847	...	...	2.957
0617-52072-0130	0.172	10.52	0.938	-0.107	0.401	41.86	1.228	...	...	2.242
0617-52072-0283	0.147	13.37	0.697	-0.110	0.492	41.51	1.103	...	...	2.509
0620-52375-0391	0.168	11.36	0.956	-0.047	0.681	42.26	1.105	...	...	2.506
0621-52055-0237	0.107	17.82	0.945	-0.131	0.529	41.62	1.169	...	...	2.376
0628-52083-0589	0.160	12.25	0.860	-0.160	0.296	42.24	1.084	...	...	2.545
0630-52050-0363	0.144	10.71	0.923	0.057	0.556	41.64	1.109	...	...	2.497
0632-52071-0343	0.144	11.13	0.848	-0.020	0.549	41.59	0.877	...	...	2.904
0639-52146-0414	0.151	8.120	1.084	-0.017	0.852	41.57	1.254	...	...	2.172
0640-52200-0255	0.116	7.024	0.880	-0.271	0.276	41.35	1.001	...	...	2.692
0648-52559-0598	0.141	15.67	0.460	-0.234	0.325	41.76	1.053	...	...	2.601
0656-52148-0587	0.166	12.15	0.481	-0.182	0.347	41.68	1.152	...	...	2.412
0678-52884-0098	0.108	15.72	0.924	-0.240	0.359	41.55	0.998	16.45	4.069	2.732
0678-52884-0369	0.182	11.37	0.875	0.098	1.653	42.14	1.154	...	...	2.407
0716-52203-0386	0.121	15.84	1.126	0.145	0.760	41.90	1.033	...	...	2.636
0721-52228-0264	0.087	23.94	1.100	-0.025	0.691	41.95	1.131	...	...	2.455
0723-52201-0185	0.118	15.69	0.733	-0.124	0.204	41.90	0.823	...	...	3.000
0725-52258-0102	0.149	11.54	0.857	-0.089	0.388	41.66	0.810	...	...	3.024
0725-52258-0637	0.089	15.66	1.060	-0.025	0.657	41.81	1.253	...	...	2.175
0727-52207-0112	0.100	15.88	1.080	-0.125	0.492	42.19	0.992	54.73	3.914	2.666
0728-52520-0348	0.094	18.90	0.752	-0.058	0.760	41.27	1.069	46.14	3.933	2.539
0728-52520-0563	0.084	12.84	0.823	-0.109	0.463	41.10	1.255	...	...	2.168
0730-52466-0042	0.071	25.21	0.622	-0.211	0.368	41.26	1.251	...	...	2.180
0733-52207-0120	0.124	12.95	0.630	-0.137	0.492	41.32	1.467	...	...	...
0735-52519-0010	0.060	19.63	0.653	-0.112	0.375	41.13	1.041	...	...	2.623
0737-52518-0431	0.217	11.02	0.758	-0.114	0.365	42.47	1.004	...	...	2.687
0738-52521-0050	0.087	16.29	1.037	-0.003	0.674	41.64	1.138	28.54	3.991	2.437
0740-52263-0640	0.092	18.21	0.695	-0.208	0.487	41.47	0.782	66.75	3.893	3.024
0741-52261-0297	0.161	8.161	0.826	-0.172	0.463	41.83	1.013	...	...	2.672
0752-52251-0487	0.119	13.86	0.467	-0.272	0.322	41.03	0.992	...	...	2.708
0753-52233-0575	0.110	11.99	0.533	-0.039	0.529	41.43	1.007	...	...	2.683
0754-52232-0134	0.079	20.88	0.926	-0.185	0.475	41.60	1.211	...	...	2.283

**Table 1.** –to be continued

(1)	(2)	(3)	(4)	(5)	(6)	(7)	(8)	(9)	(10)	(11)
0755-52235-0384	0.118	13.86	0.452	-0.185	0.344	41.18	1.090	...	...	2.533
0755-52235-0597	0.150	17.57	0.460	-0.164	0.375	41.65	0.966	...	...	2.752
0756-52577-0376	0.151	10.98	0.954	-0.077	0.637	41.83	1.715	...	...	...
0756-52577-0504	0.112	17.75	0.571	-0.157	0.303	41.43	1.365	...	...	1.751
0759-52254-0070	0.079	17.66	0.730	-0.149	0.352	41.47	1.117	...	...	2.481
0762-52232-0009	0.126	15.17	0.480	-0.224	0.326	41.41	1.133	...	...	2.450
0765-52254-0518	0.141	14.98	0.523	-0.264	0.305	41.53	0.944	...	...	2.791
0772-52375-0170	0.116	15.58	0.914	-0.407	0.350	41.87	1.091	44.59	3.937	2.500
0780-52370-0043	0.148	17.93	0.936	-0.005	0.445	42.02	1.239	13.83	4.097	2.260
0781-52373-0248	0.181	8.614	1.112	0.085	0.704	42.33	1.276	...	...	2.110
0785-52339-0308	0.118	15.97	1.004	-0.147	0.383	41.99	0.755	...	...	3.128
0786-52319-0151	0.143	18.44	0.731	-0.100	0.307	41.71	1.289	...	...	2.070
0790-52441-0287	0.042	28.11	1.105	-0.070	0.458	41.87	1.211	80.74	3.874	2.220
0791-52435-0242	0.148	14.28	0.801	-0.164	0.375	42.12	1.344	...	...	1.860
0796-52401-0042	0.116	14.19	0.752	-0.080	0.453	41.85	0.910	...	...	2.848
0796-52401-0542	0.113	16.01	0.425	-0.182	0.311	41.40	1.099	...	...	2.517
0814-52370-0369	0.088	20.49	0.480	-0.047	0.707	41.25	1.025	...	...	2.650
0814-52443-0373	0.088	21.61	0.733	-0.050	0.742	41.54	1.045	...	...	2.615
0816-52379-0066	0.181	14.02	0.518	-0.178	0.171	41.87	1.376	...	...	1.688
0818-52395-0574	0.099	13.35	0.640	-0.079	0.432	41.51	1.499	...	...	...
0819-52409-0472	0.030	37.45	1.172	0.147	1.879	41.45	1.172	...	...	2.369
0827-52312-0211	0.139	16.69	1.025	-0.023	0.636	42.12	1.632	...	...	...
0828-52317-0073	0.120	12.94	0.917	-0.098	0.399	41.65	1.082	...	...	2.549
0831-52294-0289	0.137	15.33	0.894	-0.091	0.320	42.02	1.191	...	...	2.328
0833-52314-0336	0.155	11.53	0.579	-0.288	0.340	41.62	0.894	...	...	2.876
0835-52326-0058	0.074	19.17	0.928	-0.058	0.421	41.57	1.169	38.81	3.953	2.354
0835-52326-0327	0.184	6.379	0.689	-0.117	0.297	41.61	1.389	13.15	4.106	1.645
0835-52326-0335	0.097	14.94	0.727	-0.140	0.451	41.73	1.188	...	...	2.335
0836-52376-0453	0.101	18.71	0.965	-0.349	0.220	41.67	1.226	...	...	2.245
0837-52642-0329	0.115	15.36	0.953	-0.175	0.446	41.88	0.967	...	...	2.751
0846-52407-0618	0.093	14.40	0.571	-0.245	0.369	41.03	1.220	...	...	2.261
0850-52338-0613	0.163	16.15	0.795	-0.097	0.558	41.82	1.384	...	...	1.636
0856-52339-0493	0.085	19.24	0.495	-0.158	0.319	41.18	0.898	...	...	2.870
0858-52316-0432	0.154	14.14	0.803	-0.253	0.414	42.16	1.342	33.18	3.972	1.854
0870-52325-0486	0.132	10.77	0.916	-0.261	0.466	41.88	0.811	...	...	3.022
0874-52338-0513	0.042	34.31	1.152	-0.046	0.490	41.81	0.959	70.36	3.888	2.708
0874-52338-0627	0.119	14.84	1.204	0.057	1.119	42.02	0.945	208.9	3.789	2.684
0877-52353-0466	0.141	11.53	0.827	-0.110	0.524	41.59	0.901	18.60	4.051	2.889
0878-52353-0456	0.180	14.92	0.637	-0.168	0.295	42.00	0.935	38.67	3.954	2.783
0879-52365-0594	0.128	16.35	0.954	-0.144	0.410	42.16	1.100	...	...	2.515
0881-52368-0621	0.117	16.05	0.446	-0.258	0.396	41.29	1.157	...	...	2.402
0883-52430-0001	0.171	8.230	1.066	-0.178	0.422	42.22	1.179	...	...	2.355
0887-52376-0100	0.054	17.07	1.032	-0.103	0.561	41.31	0.918	72.44	3.885	2.778
0897-52605-0394	0.138	8.719	0.700	-0.252	0.320	41.38	0.949	30.44	3.983	2.773
0900-52637-0492	0.078	22.07	1.016	0.078	0.503	41.46	0.927	66.24	3.894	2.767
0903-52400-0475	0.145	16.82	0.770	-0.124	0.346	42.13	0.965	30.31	3.984	2.747
0906-52368-0014	0.104	14.25	0.687	-0.068	0.455	40.91	1.501	...	...	...
0911-52426-0307	0.070	25.09	1.078	0.169	0.836	41.80	1.393	...	...	1.567
0912-52427-0055	0.185	10.27	1.052	-0.063	0.332	42.43	1.170	...	...	2.374
0914-52721-0108	0.134	14.57	1.175	0.066	0.564	42.47	0.840	275.2	3.767	2.853

Table 1. –to be continued

(1)	(2)	(3)	(4)	(5)	(6)	(7)	(8)	(9)	(10)	(11)
0914-52721-0410	0.145	14.30	0.951	-0.010	0.689	41.76	1.133	...	...	2.451
0919-52409-0173	0.150	9.202	0.871	-0.137	0.397	41.57	1.071	...	...	2.569
0919-52409-0487	0.128	13.54	0.962	0.052	0.561	41.82	1.124	51.22	3.922	2.429
0919-52409-0619	0.138	16.22	0.603	-0.052	0.331	41.94	1.229	...	...	2.237
0920-52411-0329	0.138	14.38	0.615	-0.043	0.342	41.90	1.038	...	...	2.627
0921-52380-0244	0.085	10.71	0.665	-0.108	0.655	41.16	1.136	...	...	2.444
0923-52404-0586	0.119	18.08	0.777	-0.144	0.715	41.95	1.041	...	...	2.623
0925-52411-0489	0.083	19.31	0.920	-0.296	0.435	41.39	1.125	19.62	4.043	2.488
0928-52578-0121	0.246	12.24	0.732	-0.100	0.291	42.25	1.352	...	...	1.822
0929-52581-0570	0.128	23.06	1.133	-0.068	0.707	42.57	1.071	150.0	3.817	2.478
0931-52619-0582	0.102	18.78	0.633	-0.237	0.349	41.52	1.233	...	...	2.228
0935-52643-0002	0.075	18.68	0.698	-0.146	0.467	41.20	1.521	...	...	...
0937-52707-0039	0.141	10.29	0.826	-0.126	0.507	41.80	1.088	...	...	2.536
0940-52670-0020	0.121	12.92	0.969	-0.055	1.037	41.54	1.070	...	...	2.571
0947-52411-0302	0.125	15.45	1.032	0.039	0.647	41.79	1.148	5.975	4.264	2.552
0948-52428-0502	0.073	21.49	1.135	0.123	1.076	41.33	1.371	65.09	3.896	1.663
0950-52378-0619	0.197	11.61	0.540	-0.160	0.408	41.57	1.312	...	...	1.989
0958-52410-0128	0.071	21.82	1.099	-0.058	0.492	41.57	1.089	...	...	2.536
0960-52466-0532	0.069	23.20	0.714	-0.060	0.243	41.26	1.149	34.42	3.968	2.402
0961-52615-0538	0.175	15.19	0.813	-0.126	0.307	42.26	1.221	...	...	2.259
0963-52643-0557	0.072	25.63	1.078	0.010	0.571	41.47	0.781	26.83	4.000	3.079
0969-52442-0505	0.172	12.28	0.833	-0.124	0.457	41.95	1.089	...	...	2.536
0970-52413-0347	0.062	29.03	0.514	-0.162	0.307	41.63	0.869	59.72	3.905	2.872
0970-52413-0415	0.130	10.99	1.062	-0.059	0.573	41.98	1.088	...	...	2.536
0972-52428-0437	0.100	11.49	1.112	-0.165	0.490	41.78	1.136	33.89	3.970	2.430
0972-52428-0520	0.094	17.05	0.953	-0.316	0.321	41.88	1.346	21.28	4.031	1.866
0972-52435-0433	0.100	13.85	1.075	-0.165	0.502	41.70	1.249	52.26	3.919	2.146
0973-52426-0039	0.278	9.148	0.656	-0.261	0.356	42.48	1.031	13.68	4.099	2.690
0973-52426-0279	0.094	14.99	0.674	-0.182	0.835	41.26	1.393	...	...	1.562
0983-52443-0158	0.078	14.98	0.798	-0.265	0.352	41.49	0.987	...	...	2.717
0984-52442-0073	0.123	12.80	0.835	-0.197	0.457	41.90	1.168	...	...	2.378
0984-52442-0101	0.187	10.85	0.558	-0.218	0.373	41.86	1.222	...	...	2.254
0984-52442-0125	0.154	13.62	0.890	-0.213	0.553	41.82	0.939	12.98	4.108	2.853
0985-52431-0626	0.116	17.16	0.727	-0.086	0.394	41.91	1.338	...	...	1.886
0987-52523-0285	0.179	13.25	1.031	0.059	0.776	42.38	1.320	...	...	1.960
0990-52465-0238	0.136	13.88	0.878	-0.130	0.427	41.09	1.141	...	...	2.434
0991-52707-0036	0.126	18.23	0.964	0.136	0.805	41.98	1.276	118.9	3.837	2.028
0991-52707-0107	0.149	18.14	0.673	-0.267	0.545	42.24	1.007	...	...	2.683
0997-52734-0143	0.170	13.97	0.750	-0.053	0.127	42.07	1.246	...	...	2.195
0997-52734-0565	0.156	10.52	1.152	-0.092	0.782	42.02	1.286	...	...	2.076
1001-52670-0089	0.069	23.02	1.153	-0.118	0.484	41.70	1.232	...	...	2.229
1006-52708-0246	0.164	12.97	1.092	-0.160	0.611	42.43	1.297	...	...	2.041
1007-52706-0390	0.162	11.58	0.686	-0.127	0.449	41.47	0.930	...	...	2.814
1009-52644-0166	0.104	18.76	0.584	-0.124	0.509	41.46	1.142	...	...	2.432
1014-52707-0040	0.162	8.537	0.653	-0.199	0.392	41.36	1.314	...	...	1.982
1038-52673-0037	0.111	15.79	1.020	-0.042	0.598	42.06	0.805	...	...	3.034
1048-52736-0066	0.083	16.39	1.067	-0.172	0.638	41.38	1.333	61.96	3.901	1.857
1051-52468-0469	0.065	18.07	1.119	0.027	0.602	41.45	1.333	...	...	1.907
1056-52764-0534	0.173	13.86	0.908	-0.062	0.470	41.12	1.217	...	...	2.267
1057-52522-0219	0.164	12.54	0.735	-0.076	0.403	42.12	1.215	...	...	2.273

**Table 1.** –to be continued

(1)	(2)	(3)	(4)	(5)	(6)	(7)	(8)	(9)	(10)	(11)
1058-52520-0327	0.150	12.38	0.960	-0.073	0.571	41.91	1.163	...	...	2.389
1061-52641-0095	0.097	10.49	0.879	-0.090	0.461	41.39	1.016	...	...	2.666
1078-52643-0571	0.124	13.26	0.793	-0.229	0.557	41.44	1.238	...	...	2.214
1158-52668-0190	0.094	16.34	1.222	-0.238	0.358	41.79	1.004	...	...	2.688
1162-52668-0063	0.104	14.19	0.921	-0.368	0.392	41.46	1.306	...	...	2.012
1163-52669-0036	0.080	13.45	0.584	-0.250	0.315	41.38	1.290	...	...	2.067
1170-52756-0567	0.138	13.76	1.154	-0.064	0.606	42.13	1.247	...	...	2.191
1174-52782-0139	0.207	7.164	0.606	-0.194	0.498	41.29	1.163	...	...	2.389
1174-52782-0350	0.211	13.03	0.868	-0.180	0.320	42.40	0.791	...	...	3.059
1185-52642-0191	0.097	16.28	0.845	-0.001	0.561	41.50	1.263	...	...	2.147
1194-52703-0472	0.078	15.58	0.756	-0.128	0.423	41.22	0.900	...	...	2.866
1194-52703-0616	0.091	12.29	0.802	-0.137	0.419	41.31	1.187	...	...	2.336
1196-52733-0489	0.165	9.065	0.790	-0.189	0.383	41.79	0.974	...	...	2.739
1199-52703-0566	0.111	17.74	0.908	-0.044	0.256	42.03	1.147	...	...	2.422
1208-52672-0141	0.089	14.89	0.666	-0.274	0.309	41.25	0.958	24.58	4.011	2.772
1208-52672-0173	0.106	18.22	1.184	0.166	1.219	41.57	1.320	...	...	1.960
1223-52781-0560	0.074	14.61	0.875	-0.106	0.485	41.21	1.109	...	...	2.498
1223-52781-0584	0.119	11.46	0.960	-0.053	0.464	41.66	1.005	...	...	2.685
1226-52734-0434	0.125	17.87	0.614	-0.246	0.365	41.93	1.188	...	...	2.334
1233-52734-0522	0.118	12.05	0.465	-0.265	0.679	41.10	1.078	...	...	2.556
1235-52734-0275	0.108	13.19	0.904	-0.130	0.663	41.41	0.971	...	...	2.745
1235-52734-0340	0.209	7.080	0.825	-0.100	0.403	41.89	1.161	...	...	2.393
1236-52751-0509	0.162	9.147	1.077	-0.030	0.490	41.58	1.040	...	...	2.625
1269-52937-0306	0.076	27.55	0.729	-0.163	0.395	42.18	1.063	...	...	2.583
1278-52735-0247	0.101	10.81	0.856	-0.218	0.531	41.34	1.325	...	...	1.939
1282-52759-0271	0.131	9.564	0.830	-0.138	0.409	41.59	0.949	...	...	2.781
1299-52972-0294	0.125	13.76	1.018	0.018	0.744	41.71	1.196	...	...	2.317
1300-52973-0218	0.151	13.39	1.095	-0.160	0.593	42.44	1.053	173.3	3.804	2.504
1304-52993-0396	0.122	19.92	0.446	-0.216	0.290	41.35	1.050	30.07	3.985	2.600
1305-52757-0256	0.176	10.05	0.837	-0.210	0.205	41.85	1.230	...	...	2.236
1306-52996-0167	0.162	9.979	1.068	-0.040	0.882	41.60	0.938	60.16	3.904	2.753
1310-53033-0184	0.187	10.49	0.518	-0.159	0.426	41.43	1.225	...	...	2.248
1310-53033-0317	0.099	21.85	0.873	-0.029	0.374	41.72	1.173	...	...	2.369
1312-52781-0536	0.159	8.903	0.562	-0.207	0.358	41.67	0.897	...	...	2.871
1318-52781-0064	0.103	15.19	0.707	-0.272	0.354	41.34	1.085	36.98	3.959	2.522
1328-52786-0317	0.117	16.28	0.581	-0.111	0.323	41.88	1.103	...	...	2.509
1328-52786-0321	0.141	15.91	0.939	0.061	0.833	41.93	1.040	86.97	3.867	2.558
1329-52767-0311	0.145	12.22	1.053	-0.051	0.380	42.09	0.842	...	...	2.966
1330-52822-0637	0.167	16.24	1.055	-0.381	0.274	42.46	0.923	...	...	2.827
1331-52766-0097	0.169	7.997	1.053	-0.119	0.624	41.98	1.122	...	...	2.473
1332-52781-0196	0.168	12.77	0.652	-0.097	0.432	41.67	1.276	...	...	2.110
1333-52782-0477	0.219	11.97	0.785	-0.091	0.336	42.17	1.143	...	...	2.431
1336-52759-0201	0.186	13.79	0.557	-0.295	0.278	42.12	1.069	...	...	2.572
1336-52759-0430	0.151	14.02	0.817	0.143	2.298	41.70	1.114	...	...	2.488
1339-52767-0068	0.137	10.27	0.530	-0.255	0.272	41.56	0.997	...	...	2.700
1341-52786-0460	0.196	12.85	0.444	-0.129	0.335	41.81	0.918	...	...	2.834
1351-52790-0024	0.095	12.74	0.961	-0.072	1.312	41.42	1.078	...	...	2.556
1351-52790-0599	0.180	9.489	0.582	-0.239	0.324	41.83	1.039	...	...	2.626
1355-52823-0147	0.077	15.88	0.642	-0.210	0.453	41.10	1.144	...	...	2.428
1355-52823-0159	0.149	8.574	0.600	-0.201	0.473	41.92	1.299	...	...	2.034

Table 1. –to be continued

(1)	(2)	(3)	(4)	(5)	(6)	(7)	(8)	(9)	(10)	(11)
1358-52994-0218	0.085	16.90	1.169	-0.096	0.449	41.78	0.973	...	...	2.741
1363-53053-0274	0.074	27.55	0.872	-0.143	0.444	41.48	0.892	...	...	2.879
1367-53083-0379	0.115	24.99	0.797	-0.166	0.351	42.11	1.139	16.91	4.065	2.472
1368-53084-0071	0.087	20.48	1.117	0.105	0.986	41.89	1.162	116.9	3.839	2.311
1372-53062-0412	0.030	30.17	1.130	-0.100	1.104	40.97	1.098	46.24	3.933	2.485
1375-53084-0330	0.182	8.870	0.820	-0.189	0.515	41.81	1.127	...	...	2.463
1375-53084-0424	0.060	19.36	1.152	-0.296	0.332	41.63	1.111	98.39	3.855	2.421
1386-53116-0550	0.081	23.70	0.798	-0.173	0.355	41.54	0.906	161.7	3.810	2.760
1387-53118-0170	0.111	17.23	1.005	0.008	1.164	41.82	1.147	...	...	2.422
1394-53108-0576	0.093	13.05	0.975	-0.164	0.545	41.38	1.342	...	...	1.870
1396-53112-0329	0.141	15.68	0.661	-0.198	0.323	41.85	1.285	23.97	4.015	2.087
1398-53146-0207	0.145	13.43	1.191	-0.097	0.542	42.21	1.245	74.93	3.882	2.138
1398-53146-0470	0.094	18.94	1.527	0.013	0.699	41.96	1.370	80.13	3.875	1.659
1399-53172-0587	0.156	13.93	0.594	-0.236	0.296	41.73	1.172	34.59	3.967	2.353
1408-52822-0565	0.097	21.93	1.242	0.012	0.558	42.32	1.231	67.97	3.891	2.178
1418-53142-0206	0.088	22.71	0.964	-0.195	0.300	41.80	0.934	...	...	2.808
1419-53144-0221	0.097	14.71	1.183	-0.028	0.621	41.69	1.272	...	...	2.122
1419-53144-0313	0.091	21.94	0.546	-0.181	0.328	41.55	1.189	...	...	2.332
1420-53146-0262	0.153	13.34	1.059	-0.175	0.491	42.48	1.228	233.8	3.780	2.130
1428-52998-0351	0.104	14.10	0.999	-0.176	0.609	41.36	0.972	60.63	3.903	2.695
1429-52990-0072	0.125	10.97	1.032	0.134	0.718	41.53	1.092	...	...	2.529
1430-53002-0598	0.054	16.78	0.975	-0.001	1.174	40.98	0.965	59.43	3.906	2.707
1435-52996-0256	0.106	17.94	1.049	-0.024	1.035	41.93	1.224	58.14	3.908	2.205
1435-52996-0608	0.082	23.76	0.689	-0.204	0.477	41.10	1.157	...	...	2.401
1436-53054-0495	0.031	24.45	0.829	-0.275	0.264	40.54	1.143	15.70	4.077	2.469
1438-53054-0610	0.188	9.130	0.600	-0.182	0.551	41.76	1.140	...	...	2.437
1439-53003-0004	0.076	18.81	0.993	0.074	0.755	41.73	0.764	157.3	3.813	3.017
1439-53003-0116	0.078	25.18	0.970	-0.099	0.492	41.43	1.176	...	...	2.362
1442-53050-0620	0.209	12.40	0.607	-0.144	0.356	42.22	1.298	...	...	2.039
1458-53119-0339	0.146	12.92	0.544	-0.015	0.922	41.70	1.170	...	...	2.374
1461-53062-0199	0.098	19.87	0.633	-0.207	0.149	41.70	0.843	...	...	2.964
1465-53082-0534	0.086	25.93	0.848	-0.104	0.254	41.71	0.990	...	...	2.711
1569-53168-0325	0.196	9.853	0.695	-0.223	0.187	42.15	1.167	...	...	2.381
1575-53493-0437	0.136	11.45	0.487	-0.132	0.498	41.15	1.342	...	...	1.869
1576-53496-0044	0.146	9.759	0.955	0.060	0.701	41.27	0.987	...	...	2.717
1582-52939-0498	0.129	13.11	1.117	-0.043	0.766	42.06	1.433	103.3	3.850	0.945
1592-52990-0343	0.062	20.12	1.185	0.001	1.760	41.32	1.291	...	...	2.061
1601-53115-0427	0.054	21.14	0.783	-0.247	0.344	41.44	0.986	78.07	3.877	2.657
1603-53119-0229	0.127	20.44	0.746	-0.170	0.373	41.85	1.220	...	...	2.260
1606-53055-0573	0.135	19.34	1.348	0.262	1.280	42.32	1.036	...	...	2.632
1606-53055-0594	0.143	14.50	1.050	0.015	0.536	41.93	1.055	...	...	2.598
1614-53120-0300	0.093	16.31	0.899	-0.244	0.372	41.53	1.039	43.90	3.939	2.596
1619-53084-0613	0.115	16.58	0.712	-0.170	0.387	41.38	1.227	20.53	4.036	2.262
1623-53089-0475	0.165	11.96	1.303	0.202	0.562	42.41	0.959	...	...	2.764
1642-53115-0492	0.184	10.05	0.506	-0.138	0.348	41.50	1.070	...	...	2.570
1642-53115-0587	0.165	10.42	0.674	-0.206	0.346	41.79	1.054	...	...	2.599
1643-53143-0172	0.180	9.567	0.382	-0.280	0.311	41.39	1.260	...	...	2.154
1643-53143-0206	0.108	15.17	0.819	-0.192	0.287	41.36	1.030	...	...	2.642
1643-53143-0274	0.148	10.15	0.997	0.007	1.155	41.79	0.899	...	...	2.867
1645-53172-0108	0.127	11.93	0.703	-0.160	0.436	41.63	0.918	...	...	2.834



**Table 1.** –to be continued

(1)	(2)	(3)	(4)	(5)	(6)	(7)	(8)	(9)	(10)	(11)
1645-53172-0292	0.175	9.499	0.875	-0.148	0.459	41.97	0.983	...	...	2.724
1649-53149-0044	0.112	13.35	0.709	-0.271	0.387	41.31	1.190	...	...	2.331
1656-53533-0141	0.138	12.93	1.054	0.024	0.676	42.14	1.022	...	...	2.656
1658-53240-0627	0.183	8.698	0.837	-0.089	0.342	41.78	1.643	...	...	...
1666-52991-0575	0.051	30.37	0.898	-0.004	0.747	41.61	1.185	...	...	2.342
1668-53433-0309	0.063	17.57	1.097	-0.064	0.878	41.67	0.956	...	...	2.770
1672-53460-0144	0.072	25.04	0.471	-0.156	0.338	41.18	1.171	...	...	2.372
1673-53462-0054	0.109	14.77	0.566	-0.224	0.351	41.30	1.233	...	...	2.227
1673-53462-0138	0.073	31.14	1.051	0.028	0.652	41.50	1.049	36.12	3.962	2.589
1675-53466-0638	0.069	22.98	1.135	0.135	1.195	41.48	1.118	...	...	2.480
1692-53473-0476	0.119	12.65	1.086	-0.071	2.036	41.77	1.032	149.3	3.817	2.547
1693-53446-0113	0.067	24.24	0.967	-0.159	0.379	41.39	1.242	26.79	4.000	2.204
1696-53116-0505	0.179	10.08	1.039	-0.181	0.470	41.83	1.257	...	...	2.164
1697-53142-0207	0.118	12.89	0.938	-0.085	0.650	41.42	1.459	50.18	3.924	...
1700-53502-0418	0.085	14.61	0.900	-0.059	0.524	41.77	1.099	...	...	2.516
1706-53442-0028	0.157	10.05	0.941	-0.119	0.461	41.67	0.921	...	...	2.830
1708-53503-0545	0.128	13.66	0.890	-0.131	0.563	41.96	1.232	64.80	3.896	2.179
1720-53854-0068	0.161	11.40	0.586	-0.272	0.442	41.64	1.225	...	...	2.248
1724-53859-0007	0.085	16.13	1.187	0.110	0.755	41.79	1.049	...	...	2.609
1726-53137-0003	0.199	13.18	0.596	-0.320	0.343	42.03	0.943	...	...	2.792
1726-53137-0194	0.073	17.60	0.719	-0.169	0.536	41.07	1.158	15.24	4.082	2.441
1734-53034-0257	0.143	22.16	0.764	-0.080	0.414	41.95	1.312	...	...	1.991
1736-53052-0589	0.125	16.45	0.811	-0.077	0.330	41.53	1.009	...	...	2.679
1740-53050-0506	0.133	16.84	0.734	-0.223	0.281	41.73	0.974	...	...	2.739
1746-53062-0376	0.198	8.276	0.988	-0.185	0.597	42.35	1.051	...	...	2.605
1759-53081-0001	0.104	17.43	1.015	0.078	0.829	41.97	0.980	101.0	3.853	2.655
1759-53081-0203	0.114	18.84	0.984	-0.108	0.341	41.69	1.139	...	...	2.440
1763-53463-0223	0.095	15.88	1.113	0.114	1.096	41.91	1.532	...	...	...
1765-53466-0182	0.142	14.48	0.480	-0.087	0.462	41.26	1.009	...	...	2.679
1766-53468-0487	0.117	17.87	0.753	-0.232	0.346	41.96	1.376	31.05	3.981	1.679
1768-53442-0193	0.115	17.27	0.848	-0.096	0.431	41.51	1.070	...	...	2.571
1770-53171-0158	0.084	23.68	0.720	-0.229	0.610	41.90	1.040	77.53	3.878	2.564
1771-53498-0132	0.124	11.34	0.868	-0.030	0.566	42.01	1.190	...	...	2.331
1775-53847-0640	0.144	12.43	0.478	-0.202	0.286	41.41	1.245	...	...	2.196
1780-53090-0191	0.067	18.95	1.043	-0.292	0.502	41.56	1.031	98.27	3.855	2.568
1780-53090-0339	0.195	15.29	0.783	-0.021	0.359	42.14	0.911	...	...	2.847
1781-53297-0596	0.165	11.92	0.818	-0.051	0.474	41.96	1.281	...	...	2.093
1784-54425-0455	0.142	10.83	0.782	-0.216	0.497	41.63	1.118	...	...	2.481
1785-54439-0137	0.142	12.54	1.011	-0.132	0.478	41.81	1.023	60.75	3.903	2.606
1795-54507-0179	0.120	15.25	1.052	-0.117	0.631	41.68	1.136	4.926	4.314	2.602
1799-53556-0064	0.074	13.61	0.853	-0.198	0.807	41.15	1.030	...	...	2.641
1800-53884-0004	0.074	20.85	1.143	0.154	0.831	41.84	1.000	76.28	3.880	2.634
1800-53884-0223	0.119	16.45	0.601	-0.347	0.296	41.44	1.103	...	...	2.510
1801-54156-0180	0.126	16.18	1.001	-0.097	0.562	42.20	1.265	...	...	2.141
1803-54152-0334	0.084	19.91	0.991	-0.036	0.369	41.87	1.087	...	...	2.540
1814-54555-0087	0.161	14.04	1.017	0.033	0.707	42.01	1.214	...	...	2.275
1819-54540-0073	0.064	18.25	1.038	-0.032	0.614	41.89	1.178	...	...	2.358
1828-53504-0533	0.087	16.53	1.106	0.141	0.694	41.41	1.139	...	...	2.439
1842-53501-0610	0.058	26.26	1.090	-0.150	0.416	41.72	1.115	...	...	2.486
1844-54138-0016	0.058	32.80	0.830	-0.055	0.425	41.53	1.120	...	...	2.475

Table 1. –to be continued

(1)	(2)	(3)	(4)	(5)	(6)	(7)	(8)	(9)	(10)	(11)
1845-54144-0624	0.113	18.70	0.453	-0.276	0.282	41.19	1.214	...	...	2.274
1848-54180-0278	0.235	11.91	0.629	-0.223	0.268	42.37	0.813	...	...	3.019
1852-53534-0326	0.088	9.670	0.945	-0.082	0.433	41.15	1.194	...	...	2.321
1867-53317-0344	0.097	13.16	0.863	-0.186	0.415	41.36	0.657	...	...	3.342
1868-53318-0592	0.062	27.16	1.209	0.148	1.434	41.74	1.277	146.5	3.819	2.015
1877-54464-0252	0.078	16.41	1.039	-0.051	0.838	41.91	1.167	...	...	2.381
1877-54464-0322	0.140	10.02	0.819	-0.134	0.952	41.84	1.052	...	...	2.603
1922-53315-0096	0.155	9.757	0.700	-0.130	0.390	41.38	1.191	...	...	2.329
1924-53330-0160	0.107	15.89	0.709	-0.176	0.349	41.50	1.042	...	...	2.621
1924-53330-0264	0.121	14.40	1.075	-0.220	0.678	42.02	1.079	50.95	3.922	2.515
1929-53349-0432	0.084	20.62	0.655	-0.128	0.549	40.76	1.059	...	...	2.591
1931-53358-0315	0.043	26.64	0.693	-0.246	0.301	41.14	1.114	28.12	3.993	2.485
1937-53388-0442	0.240	8.310	1.113	-0.082	0.512	42.54	0.826	144.9	3.820	2.905
1942-53415-0579	0.169	9.983	1.167	-0.136	0.608	42.35	1.084	...	...	2.545
1945-53387-0152	0.139	15.61	0.892	-0.065	0.481	41.84	1.193	...	...	2.324
1949-53433-0331	0.158	12.77	0.764	-0.027	0.853	42.21	1.160	...	...	2.396
1951-53389-0109	0.121	22.03	0.731	-0.228	0.248	41.59	1.230	...	...	2.236
1953-53358-0222	0.117	16.84	0.845	-0.024	1.345	41.46	1.112	60.89	3.903	2.443
1954-53357-0120	0.144	16.47	1.272	0.074	0.769	42.31	1.187	103.1	3.851	2.262
1955-53442-0526	0.146	14.05	0.777	-0.121	0.411	41.61	0.947	...	...	2.784
1956-53437-0368	0.118	10.37	0.901	-0.073	0.426	41.79	1.626	...	...	...
1977-53475-0093	0.214	9.477	0.879	0.079	0.698	42.04	0.649	...	...	3.362
2000-53495-0178	0.187	10.32	0.496	-0.203	0.324	41.59	1.168	...	...	2.379
2014-53460-0510	0.067	17.77	1.068	-0.081	0.635	41.35	1.268	...	...	2.132
2025-53431-0640	0.079	21.15	0.806	-0.056	0.342	41.10	1.021	...	...	2.658
2026-53711-0333	0.126	18.41	0.984	0.077	0.824	42.31	1.048	...	...	2.610
2026-53711-0418	0.117	16.90	1.086	0.164	0.845	41.75	1.076	...	...	2.560
2029-53819-0140	0.188	8.528	0.979	-0.056	0.478	42.09	1.022	20.76	4.035	2.674
2032-53815-0335	0.149	11.43	0.984	-0.151	0.526	42.19	1.180	...	...	2.352
2034-53466-0632	0.170	8.750	1.018	-0.152	0.677	42.05	0.832	...	...	2.984
2035-53436-0385	0.125	11.07	1.071	0.004	0.463	41.80	1.150	...	...	2.416
2036-53446-0270	0.127	10.92	0.923	-0.209	0.478	41.41	1.111	...	...	2.494
2036-53446-0381	0.107	19.55	0.823	-0.006	0.184	41.95	1.077	...	...	2.557
2082-53358-0023	0.070	16.16	1.173	-0.036	1.215	41.32	1.259	...	...	2.157
2087-53415-0270	0.142	14.92	0.849	-0.001	0.363	40.88	1.228	...	...	2.241
2090-53463-0457	0.124	13.42	1.054	-0.179	0.469	41.81	1.051	...	...	2.604
2093-53818-0237	0.078	16.75	0.834	-0.145	0.637	40.84	1.205	...	...	2.297
2094-53851-0620	0.077	28.58	0.909	-0.009	1.114	41.71	1.207	59.34	3.906	2.244
2095-53474-0434	0.198	13.03	0.719	-0.183	0.351	42.01	1.217	...	...	2.266
2116-53854-0284	0.077	14.25	1.146	-0.180	0.587	41.48	1.203	...	...	2.302
2117-54115-0015	0.081	15.53	0.893	-0.115	0.317	41.38	1.049	...	...	2.609
2121-54180-0475	0.081	14.58	0.851	-0.088	0.396	41.03	1.120	...	...	2.477
2128-53800-0171	0.117	18.17	0.602	-0.199	0.359	41.71	0.887	...	...	2.887
2129-54252-0402	0.179	10.84	1.054	-0.254	0.460	42.32	1.232	...	...	2.230
2130-53881-0278	0.129	16.82	0.442	-0.225	0.328	41.69	0.948	...	...	2.783
2130-53881-0635	0.122	19.38	0.627	-0.241	0.327	41.78	0.941	...	...	2.795
2131-53819-0208	0.078	17.09	1.023	-0.024	0.772	41.50	1.462	...	...	...
2132-53493-0200	0.082	14.16	0.748	-0.100	0.354	41.37	1.290	...	...	2.066
2133-53917-0187	0.142	13.42	0.985	0.038	0.372	42.04	1.138	...	...	2.441
2137-54206-0533	0.199	14.99	1.257	0.038	0.651	42.60	0.964	...	...	2.757

**Table 1.** –to be continued

(1)	(2)	(3)	(4)	(5)	(6)	(7)	(8)	(9)	(10)	(11)
2143-54184-0070	0.151	17.92	1.072	-0.100	0.468	42.50	1.086	...	...	2.541
2143-54184-0605	0.184	7.931	0.928	-0.060	0.569	41.99	1.311	...	...	1.993
2144-53770-0183	0.105	18.09	0.897	0.029	0.401	41.64	1.053	...	...	2.601
2145-54212-0115	0.174	12.67	0.765	-0.186	0.332	41.83	0.996	...	...	2.701
2145-54212-0302	0.060	16.24	0.859	-0.111	0.589	41.33	0.779	...	...	3.082
2149-54509-0069	0.063	20.81	1.163	0.023	0.840	41.47	0.929	44.56	3.937	2.785
2150-54510-0283	0.083	25.88	0.917	-0.093	0.401	41.50	0.979	35.78	3.963	2.712
2150-54510-0491	0.099	22.93	1.099	0.032	0.581	41.84	1.295	27.43	3.997	2.047
2166-54232-0048	0.109	15.76	0.841	-0.184	0.458	41.70	1.038	...	...	2.627
2172-54230-0505	0.134	22.85	0.931	-0.101	0.367	41.93	1.015	78.97	3.876	2.607
2173-53874-0113	0.088	18.51	0.753	-0.070	0.420	41.34	1.368	...	...	1.736
2199-53556-0084	0.110	19.05	0.684	-0.123	0.683	41.92	1.094	...	...	2.526
2207-53558-0227	0.034	30.17	1.150	-0.050	0.900	41.57	0.823	108.6	3.846	2.924
2217-53794-0603	0.082	21.80	0.610	-0.173	0.390	41.25	1.250	34.92	3.966	2.166
2223-53793-0379	0.158	10.98	0.579	-0.130	0.533	41.46	0.997	...	...	2.699
2224-53815-0599	0.149	14.88	1.110	-0.029	0.844	42.15	0.960	...	...	2.762
2229-53823-0177	0.181	10.90	0.640	-0.189	0.324	41.84	1.091	...	...	2.531
2233-53845-0078	0.123	19.83	0.786	-0.233	0.334	41.73	1.261	...	...	2.154
2233-53845-0082	0.151	10.37	1.199	-0.040	0.517	42.16	1.503	...	...	...
2245-54208-0337	0.084	17.94	0.782	-0.184	0.394	41.76	1.181	...	...	2.351
2246-53767-0081	0.087	22.64	0.539	-0.260	0.383	41.54	1.060	...	...	2.589
2264-53682-0420	0.109	16.53	1.165	0.106	0.684	41.89	1.207	...	...	2.291
2270-53714-0367	0.096	22.73	0.761	-0.085	0.495	41.67	1.105	43.48	3.940	2.476
2272-53713-0489	0.194	11.97	1.069	-0.307	0.534	42.59	0.926	40.64	3.948	2.796
2273-53709-0152	0.107	14.04	1.030	-0.039	0.637	41.58	1.003	...	...	2.688
2275-53709-0468	0.153	18.01	1.010	-0.197	0.454	41.95	1.042	83.78	3.870	2.556
2283-53729-0079	0.092	19.48	0.514	-0.165	0.586	41.26	1.155	...	...	2.405
2290-53727-0088	0.133	13.80	1.142	0.041	0.824	41.93	1.202	...	...	2.304
2291-53714-0382	0.190	12.40	0.919	-0.011	0.506	42.62	1.315	...	...	1.977
2291-53714-0507	0.071	19.44	1.126	0.130	0.858	41.73	1.196	...	...	2.317
2293-53730-0106	0.152	13.40	1.030	0.039	0.380	42.17	1.050	...	...	2.607
2344-53740-0232	0.115	15.00	0.990	-0.088	0.422	42.30	1.018	...	...	2.663
2347-53757-0603	0.231	12.51	0.855	-0.020	0.430	42.36	1.300	...	...	2.034
2351-53786-0374	0.188	10.51	1.086	-0.015	0.636	41.89	0.923	...	...	2.825
2353-53794-0125	0.081	21.67	0.764	-0.043	0.519	41.76	1.170	...	...	2.375
2366-53741-0526	0.136	14.54	1.102	0.093	0.793	41.82	1.250	...	...	2.184
2368-53758-0550	0.051	20.15	0.807	-0.102	0.550	41.23	1.057	...	...	2.595
2372-53768-0580	0.151	19.58	0.701	-0.131	0.504	41.73	1.269	...	...	2.130
2428-53801-0173	0.095	16.24	0.710	-0.109	0.397	41.48	1.054	...	...	2.599
2430-53815-0447	0.103	12.82	1.187	-0.011	0.553	42.08	0.990	...	...	2.712
2433-53820-0249	0.126	16.11	0.637	-0.131	0.293	41.98	1.080	...	...	2.551
2439-53795-0406	0.148	15.13	0.816	-0.059	0.377	42.34	1.068	...	...	2.574
2440-53818-0033	0.180	9.227	0.726	-0.239	0.347	41.53	0.981	...	...	2.727
2440-53818-0110	0.139	10.55	0.841	-0.126	0.364	41.53	1.047	...	...	2.612
2440-53818-0610	0.099	21.28	0.659	-0.172	0.471	41.73	1.262	93.43	3.860	2.080
2477-54058-0031	0.140	13.05	0.790	-0.317	0.253	41.70	1.005	...	...	2.686
2489-53857-0043	0.220	8.799	0.787	-0.108	0.339	42.27	1.100	...	...	2.515
2489-53857-0581	0.097	16.14	0.854	-0.113	0.441	41.48	0.989	...	...	2.713
2490-54179-0124	0.088	16.25	1.068	-0.132	0.292	41.60	1.275	...	...	2.111
2493-54115-0212	0.115	20.05	1.072	-0.002	0.750	41.95	1.222	116.3	3.839	2.176

Table 1. –to be continued

(1)	(2)	(3)	(4)	(5)	(6)	(7)	(8)	(9)	(10)	(11)
2497-54154-0007	0.117	19.88	0.903	-0.241	0.389	42.26	1.063	...	...	2.583
2499-54176-0555	0.157	14.59	0.738	-0.197	0.470	41.82	0.975	...	...	2.737
2500-54178-0197	0.079	22.02	0.934	-0.200	0.398	41.33	1.030	40.19	3.949	2.617
2500-54178-0327	0.102	15.89	1.191	0.095	0.813	41.90	1.015	...	...	2.668
2507-53876-0416	0.035	26.24	1.108	-0.079	0.552	41.13	1.097	26.61	4.001	2.520
2507-53876-0424	0.209	9.439	0.558	-0.306	0.262	41.74	1.107	...	...	2.501
2509-54180-0303	0.095	16.49	0.544	-0.070	0.491	41.08	1.280	...	...	2.098
2524-54568-0442	0.125	16.57	0.726	-0.130	0.319	41.77	1.251	...	...	2.180
2524-54568-0589	0.072	20.42	0.605	-0.257	0.335	41.29	1.092	...	...	2.530
2528-54571-0602	0.132	19.09	0.501	-0.240	0.225	41.71	0.907	...	...	2.853
2529-54585-0423	0.147	16.82	0.642	-0.146	0.433	41.29	1.062	...	...	2.585
2530-53881-0569	0.152	15.40	1.175	0.148	1.171	42.17	1.198	148.7	3.818	2.222
2577-54086-0554	0.130	16.03	0.920	0.068	0.609	41.46	1.247	...	...	2.191
2578-54093-0172	0.094	17.51	0.724	-0.211	0.615	40.95	1.072	...	...	2.567
2581-54085-0088	0.075	10.82	1.254	0.089	0.788	41.56	0.904	...	...	2.858
2584-54153-0501	0.110	10.77	1.010	0.022	0.938	41.87	1.211	...	...	2.281
2587-54138-0057	0.075	25.67	0.759	-0.217	0.368	41.66	0.682	...	...	3.283
2591-54140-0510	0.106	16.46	0.791	-0.055	0.484	41.57	1.032	...	...	2.639
2593-54175-0016	0.122	9.707	1.256	-0.062	0.485	41.85	1.045	...	...	2.615
2593-54175-0422	0.181	10.81	0.949	-0.034	0.415	42.24	1.310	16.04	4.073	2.034
2595-54207-0203	0.144	12.95	0.831	-0.110	0.513	41.78	1.122	...	...	2.473
2595-54207-0589	0.145	19.54	1.097	-0.006	0.485	42.21	1.300	...	...	2.031
2596-54207-0640	0.181	10.45	0.876	-0.114	0.464	41.81	1.169	...	...	2.376
2597-54231-0555	0.171	11.31	0.397	-0.093	1.682	41.33	1.134	...	...	2.448
2602-54149-0235	0.113	14.91	0.973	-0.142	0.341	41.79	1.127	...	...	2.462
2605-54484-0077	0.150	9.429	0.937	-0.170	0.451	41.86	0.949	...	...	2.781
2606-54154-0158	0.183	12.23	0.959	-0.068	0.437	42.18	1.244	...	...	2.200
2613-54481-0638	0.204	12.02	0.637	-0.188	0.368	41.64	1.154	...	...	2.408
2616-54499-0367	0.075	27.67	1.121	0.023	0.542	41.78	0.730	63.03	3.899	3.128
2618-54506-0316	0.094	20.20	0.835	-0.152	0.573	41.22	1.116	...	...	2.484
2619-54506-0134	0.109	20.12	0.687	-0.279	0.237	41.66	0.904	...	...	2.859
2619-54506-0484	0.115	18.70	0.432	-0.285	0.190	40.99	1.064	...	...	2.581
2641-54230-0017	0.087	15.78	0.818	-0.293	0.357	41.38	1.172	...	...	2.370
2642-54232-0340	0.114	18.96	0.588	-0.124	0.432	40.91	1.109	8.961	4.176	2.585
2642-54232-0527	0.092	17.04	0.971	-0.170	0.268	41.83	1.135	13.88	4.097	2.495
2645-54477-0514	0.072	19.73	0.946	-0.038	0.498	41.70	1.149	...	...	2.418
2647-54495-0204	0.189	9.997	0.770	0.037	0.659	41.51	1.127	...	...	2.462
2651-54507-0589	0.182	11.11	0.723	0.110	1.217	41.73	1.271	...	...	2.122
2652-54508-0071	0.129	18.69	0.995	0.126	0.598	41.68	0.953	...	...	2.776
2652-54508-0350	0.055	28.63	0.534	-0.040	0.772	41.00	1.414	...	...	1.353
2655-54184-0562	0.102	21.21	0.965	-0.209	0.408	41.97	1.160	99.52	3.854	2.323
2664-54524-0270	0.078	20.99	1.093	-0.155	0.453	41.93	1.305	64.28	3.897	1.963
2745-54231-0119	0.134	19.48	1.010	-0.035	0.676	41.91	1.046	...	...	2.613
2746-54232-0236	0.126	13.63	0.420	-0.071	0.641	41.24	1.284	...	...	2.084
2753-54234-0086	0.126	16.17	1.148	0.033	0.502	42.26	1.186	31.27	3.980	2.329
2756-54508-0540	0.134	10.83	0.874	-0.177	0.594	41.70	1.014	...	...	2.670
2757-54509-0078	0.103	20.66	0.791	-0.091	0.295	42.14	1.115	...	...	2.487
2758-54523-0405	0.082	23.23	0.561	-0.176	0.435	41.35	0.961	53.43	3.917	2.720
2761-54534-0101	0.073	24.69	0.859	-0.164	0.401	41.62	0.816	86.99	3.867	2.947
2762-54533-0109	0.123	16.03	0.837	-0.075	0.579	41.83	1.072	...	...	2.567

**Table 1.** –to be continued

(1)	(2)	(3)	(4)	(5)	(6)	(7)	(8)	(9)	(10)	(11)
2767-54243-0077	0.149	14.95	1.074	-0.013	0.888	42.39	1.067	...	...	2.576
2767-54243-0278	0.142	13.22	1.131	0.165	0.967	42.27	1.517	...	...	...
2769-54527-0624	0.064	19.01	0.857	-0.254	0.359	41.15	1.120	...	...	2.476
2782-54592-0070	0.070	19.98	0.870	-0.144	0.413	41.47	1.119	...	...	2.478
2784-54529-0142	0.184	14.28	0.842	-0.072	0.454	41.90	1.311	...	...	1.995
2792-54556-0606	0.073	20.24	1.125	0.218	1.749	41.55	0.904	...	...	2.858
2881-54502-0432	0.111	15.69	1.207	0.090	0.530	42.18	1.022	...	...	2.656
2886-54498-0353	0.117	20.90	1.063	0.060	0.615	41.86	0.976	...	...	2.735
2947-54533-0076	0.134	15.20	0.681	-0.076	0.419	41.38	1.204	...	...	2.298
2952-54559-0406	0.124	21.73	0.963	-0.117	0.285	42.07	1.193	...	...	2.323
2973-54591-0085	0.040	28.63	0.916	-0.219	0.290	41.32	1.321	...	...	1.954
2973-54591-0101	0.089	15.24	1.095	-0.040	0.708	41.58	1.107	...	...	2.501

**Table 2.** Basic information of the 548 Type-2 AGN with reliable [S II] emissions in the subsample

(1)	(2)	(3)	(4)	(5)	(6)	(7)	(8)	(9)	(10)	(11)
0271-51883-0520	0.092	16.45	1.123	0.151	0.569	41.88	1.271	...	...	2.124
0272-51941-0429	0.167	8.227	0.804	-0.212	0.395	41.81	1.169	...	...	2.376
0272-51941-0529	0.177	12.20	1.107	-0.004	0.645	42.34	1.087	...	...	2.539
0274-51913-0115	0.095	17.53	0.688	-0.213	0.550	40.91	1.175	...	...	2.364
0275-51910-0115	0.127	14.54	0.459	-0.250	0.515	40.98	0.693	...	...	3.256
0276-51909-0147	0.108	17.80	0.452	-0.261	0.542	41.04	1.130	...	...	2.456
0277-51908-0189	0.068	16.78	0.950	-0.012	0.704	41.01	1.217	...	...	2.268
0280-51612-0187	0.100	18.86	0.999	-0.159	0.596	41.45	1.117	...	...	2.481
0281-51614-0214	0.077	15.67	0.685	-0.199	0.440	41.01	1.222	...	...	2.256
0282-51630-0380	0.086	15.94	0.979	-0.014	0.538	41.69	1.210	...	...	2.283
0282-51658-0597	0.105	15.59	1.172	-0.046	0.434	41.67	1.604	...	...	...
0283-51959-0385	0.106	12.85	0.935	-0.106	0.412	41.37	1.217	...	...	2.267
0284-51662-0077	0.109	10.42	1.051	-0.005	0.540	41.85	1.249	...	...	2.185
0287-52023-0559	0.100	17.65	0.804	-0.003	0.451	41.47	1.269	...	...	2.130
0288-52000-0173	0.050	30.08	0.918	-0.030	0.487	41.73	1.101	...	...	2.513
0294-51986-0399	0.185	11.98	0.744	-0.152	0.402	41.88	1.081	...	...	2.550
0296-51984-0322	0.138	13.93	0.502	-0.255	0.429	41.50	1.273	...	...	2.119
0300-51943-0026	0.083	19.00	0.733	-0.093	0.477	41.37	1.207	...	...	2.290
0301-51641-0080	0.082	13.29	0.783	-0.214	0.473	41.05	1.182	...	...	2.349
0301-51942-0608	0.166	10.21	0.640	-0.187	0.395	41.74	1.136	...	...	2.445
0305-51613-0047	0.135	10.89	0.478	-0.132	0.353	41.23	1.102	...	...	2.510
0306-51690-0150	0.137	13.05	0.803	-0.123	0.631	41.66	1.196	...	...	2.316
0306-51690-0449	0.144	12.60	0.541	0.007	0.394	41.73	1.308	...	...	2.005
0315-51663-0032	0.095	13.76	0.629	-0.084	0.359	41.48	1.210	...	...	2.284
0315-51663-0506	0.141	10.23	0.818	-0.358	0.498	41.78	1.371	...	...	1.717
0327-52294-0379	0.098	16.02	0.711	-0.181	0.385	41.40	1.060	...	...	2.588
0327-52294-0614	0.109	16.22	0.640	-0.323	0.466	41.47	1.101	...	...	2.513
0329-52056-0448	0.105	15.43	0.558	-0.105	0.370	41.86	1.225	...	...	2.248
0330-52370-0121	0.095	19.44	1.056	-0.082	0.639	41.85	1.295	...	...	2.048
0336-51999-0598	0.088	19.49	0.978	-0.311	0.473	41.36	1.233	101.1	3.852	2.154
0350-51691-0026	0.138	13.51	0.686	-0.099	0.313	41.53	1.513	...	...	...
0354-51792-0317	0.126	10.98	0.898	-0.001	0.587	41.96	1.434	...	...	...
0357-51813-0337	0.186	13.69	0.876	-0.072	0.574	41.87	1.125	...	...	2.466
0371-52078-0570	0.144	11.58	0.866	-0.106	0.563	41.74	1.123	...	...	2.470
0375-52140-0063	0.130	12.37	1.067	0.017	0.469	42.16	1.110	...	...	2.496
0379-51789-0112	0.053	18.30	1.016	-0.102	0.534	41.19	0.944	...	...	2.790
0383-51818-0306	0.122	16.89	0.852	-0.044	0.556	41.94	1.289	...	...	2.070
0389-51795-0520	0.127	14.95	0.684	-0.076	0.533	41.36	1.368	...	...	1.733
0390-51900-0214	0.107	17.76	0.551	-0.139	0.540	40.94	1.224	...	...	2.251
0397-51794-0401	0.200	11.10	0.995	0.134	0.634	42.25	1.445	...	...	...
0399-51817-0570	0.174	10.60	1.040	-0.150	0.504	41.91	0.804	...	...	3.035
0407-51820-0296	0.085	19.84	0.625	-0.131	0.538	40.87	1.301	...	...	2.029
0408-51821-0537	0.076	21.81	0.636	-0.189	0.359	41.31	1.121	...	...	2.473
0412-51931-0453	0.129	13.96	1.052	0.026	0.651	41.69	1.032	...	...	2.638
0412-52235-0444	0.129	12.79	1.093	0.029	0.606	41.90	0.993	...	...	2.706
0412-52250-0104	0.074	16.73	0.935	-0.169	0.607	41.31	1.331	85.12	3.869	1.849

NOTE—Column information are similar as those in Table 1, but for Type-2 AGN in the subsample.



Table 2. –to be continued

(1)	(2)	(3)	(4)	(5)	(6)	(7)	(8)	(9)	(10)	(11)
0412-52258-0104	0.074	21.29	0.952	-0.176	0.602	41.56	1.265	64.08	3.898	2.089
0414-51869-0027	0.149	12.06	1.056	0.130	0.826	41.66	1.438	...	...	...
0414-51869-0257	0.117	18.73	0.476	-0.250	0.418	41.22	1.533	...	...	...
0414-51901-0188	0.066	25.17	1.051	-0.007	0.916	41.54	0.970	...	...	2.745
0416-51885-0279	0.253	6.730	0.651	-0.130	0.259	41.69	0.829	...	...	2.990
0417-51821-0264	0.094	16.06	0.863	-0.227	0.440	41.49	1.271	...	...	2.124
0419-51868-0383	0.102	12.67	0.521	-0.040	0.471	41.35	1.281	49.38	3.926	2.058
0434-51885-0437	0.180	16.99	1.064	-0.380	0.364	42.45	1.292	117.0	3.839	1.978
0436-51883-0315	0.132	8.945	0.794	-0.160	0.328	41.64	1.173	...	...	2.367
0439-51877-0222	0.062	18.25	0.819	-0.229	0.442	41.25	1.304	...	...	2.019
0443-51873-0478	0.125	14.56	1.065	-0.095	0.398	41.66	1.122	82.69	3.872	2.408
0446-51899-0529	0.112	22.13	0.765	-0.215	0.321	42.10	1.172	62.64	3.900	2.320
0449-51900-0288	0.030	29.00	1.076	-0.069	0.726	41.01	1.205	121.2	3.836	2.214
0463-51908-0146	0.114	12.79	1.163	-0.001	0.575	42.11	1.462	94.28	3.859	...
0484-51907-0121	0.045	26.44	0.706	-0.212	0.304	41.10	1.336	...	...	1.895
0485-51909-0535	0.075	17.30	0.688	-0.176	0.676	41.09	1.517	...	...	...
0488-51914-0555	0.122	16.48	1.015	-0.078	0.381	42.13	1.755	77.65	3.878	...
0490-51929-0496	0.082	22.34	1.035	0.061	0.640	41.58	0.916	...	...	2.839
0492-51955-0329	0.207	13.37	0.572	-0.168	0.254	42.28	0.987	...	...	2.717
0494-51915-0049	0.126	15.53	0.420	-0.230	0.348	41.30	1.312	...	...	1.990
0494-51915-0219	0.133	13.89	0.631	-0.228	0.378	41.16	1.081	...	...	2.550
0507-52353-0391	0.189	8.868	0.558	-0.193	0.300	41.83	1.375	...	...	1.692
0513-51989-0424	0.103	14.74	1.013	-0.074	0.565	41.63	1.187	...	...	2.336
0514-51994-0485	0.128	14.64	1.142	0.018	0.600	42.20	1.103	78.04	3.877	2.449
0515-52051-0190	0.087	21.33	0.969	-0.211	0.449	41.77	1.109	...	...	2.498
0524-52027-0428	0.070	29.64	1.067	-0.006	0.375	41.46	0.834	69.83	3.889	2.926
0528-52022-0305	0.112	21.37	0.859	-0.034	0.447	41.69	1.158	...	...	2.399
0530-52026-0616	0.278	9.861	0.689	-0.104	0.370	42.81	1.911	...	...	...
0533-51994-0187	0.127	18.00	0.618	-0.268	0.351	41.92	1.182	50.74	3.923	2.311
0538-52029-0184	0.131	17.76	1.018	-0.020	0.641	42.05	1.299	...	...	2.034
0545-52202-0553	0.106	18.53	1.548	0.044	0.569	41.96	1.431	...	...	1.066
0546-52205-0608	0.078	23.23	1.136	-0.147	0.591	41.68	1.357	62.63	3.900	1.746
0549-51981-0011	0.105	17.66	1.088	-0.070	0.378	41.66	0.990	76.86	3.879	2.652
0550-51959-0309	0.245	13.31	0.761	-0.122	0.354	42.23	1.424	...	...	1.200
0550-51959-0366	0.118	14.11	0.565	-0.195	0.350	41.34	0.882	...	...	2.896
0558-52317-0364	0.171	12.08	0.868	-0.154	0.402	42.00	1.117	...	...	2.482
0558-52317-0531	0.125	18.63	1.004	-0.055	0.552	41.89	1.556	...	...	...
0560-52296-0136	0.113	16.33	0.626	-0.184	0.341	41.46	1.460	...	...	...
0565-52225-0164	0.125	9.947	1.199	-0.072	0.498	41.78	1.208	...	...	2.288
0576-52325-0222	0.115	13.40	1.008	-0.044	0.715	41.62	1.323	...	...	1.948
0579-52338-0454	0.156	9.846	1.070	-0.018	0.521	41.64	1.184	...	...	2.344
0579-52338-0460	0.155	14.68	0.758	-0.181	0.310	42.13	1.238	...	...	2.215
0581-52356-0400	0.091	25.18	0.929	-0.062	0.597	41.51	1.276	...	...	2.107
0582-52045-0105	0.181	10.32	1.054	-0.017	0.557	41.97	1.063	...	...	2.584
0583-52055-0005	0.135	15.64	0.485	-0.207	0.307	41.83	1.373	...	...	1.704
0583-52055-0184	0.144	10.12	0.812	-0.102	0.530	41.81	1.333	...	...	1.905
0585-52027-0525	0.199	12.12	0.629	-0.313	0.428	42.00	1.150	...	...	2.416
0587-52026-0611	0.082	14.33	0.575	-0.243	0.455	41.04	1.107	...	...	2.501
0588-52029-0563	0.128	10.66	0.826	-0.168	0.500	41.78	1.285	...	...	2.081
0590-52057-0284	0.112	18.01	0.911	-0.034	0.420	42.04	1.253	...	...	2.174

Table 2. –to be continued

(1)	(2)	(3)	(4)	(5)	(6)	(7)	(8)	(9)	(10)	(11)
0601-52316-0027	0.201	9.931	0.716	-0.174	0.403	41.59	0.975	...	...	2.737
0604-52079-0490	0.123	10.21	1.103	-0.059	0.529	41.95	1.172	93.84	3.859	2.299
0604-52079-0640	0.200	9.269	0.791	-0.166	0.594	41.57	1.132	...	...	2.453
0606-52365-0535	0.174	16.31	0.752	-0.109	0.435	41.83	1.166	...	...	2.383
0607-52368-0572	0.187	14.80	0.828	-0.007	0.579	42.08	1.128	...	...	2.460
0607-52368-0637	0.186	11.57	0.656	-0.191	0.291	41.78	1.615	31.83	3.978	...
0610-52056-0259	0.158	7.670	0.802	-0.174	0.531	41.76	0.866	...	...	2.924
0610-52056-0409	0.151	17.88	1.019	-0.168	0.348	42.07	1.413	...	...	1.359
0620-52375-0466	0.189	8.781	0.923	-0.037	0.423	42.05	1.309	...	...	2.000
0621-52055-0052	0.173	11.09	0.978	-0.036	0.597	42.15	1.338	...	...	1.887
0622-52054-0478	0.045	34.32	1.151	-0.054	0.432	41.88	1.361	171.9	3.805	1.680
0624-52377-0526	0.088	27.17	0.839	-0.132	0.409	41.73	1.204	135.1	3.826	2.212
0629-52051-0112	0.175	10.38	0.888	-0.095	0.732	41.89	1.086	...	...	2.540
0629-52051-0241	0.146	12.91	1.016	-0.155	0.490	42.44	0.982	137.9	3.824	2.637
0629-52051-0393	0.192	12.71	0.759	-0.181	0.463	42.07	1.113	...	...	2.489
0630-52050-0296	0.141	20.73	1.081	-0.003	0.469	42.16	1.526	...	...	...
0633-52079-0413	0.144	9.814	0.908	-0.179	0.689	41.87	1.442	83.30	3.871	...
0636-52176-0206	0.100	13.13	0.999	-0.095	0.480	41.58	1.002	...	...	2.691
0637-52174-0105	0.089	13.77	0.579	-0.233	0.540	41.34	0.999	...	...	2.696
0641-52199-0496	0.099	16.28	1.030	0.009	0.513	41.50	1.033	80.33	3.875	2.575
0645-52203-0513	0.082	23.06	0.728	-0.244	0.351	41.78	1.186	108.2	3.846	2.263
0657-52177-0017	0.162	11.57	0.657	-0.087	0.874	41.43	1.158	...	...	2.399
0657-52177-0357	0.144	11.02	0.948	0.063	0.978	41.60	1.072	...	...	2.567
0657-52177-0496	0.120	14.06	0.448	-0.192	0.361	41.31	1.226	...	...	2.247
0658-52146-0259	0.163	8.289	1.083	-0.124	0.688	41.93	1.026	...	...	2.650
0659-52199-0559	0.132	14.45	0.985	0.044	0.583	41.84	1.242	...	...	2.204
0663-52145-0143	0.112	19.63	0.757	-0.108	0.319	42.09	1.312	...	...	1.990
0664-52174-0214	0.173	10.30	1.046	-0.091	0.294	42.39	1.287	...	...	2.075
0677-52606-0465	0.108	14.22	0.993	-0.004	0.630	41.63	1.324	...	...	1.944
0681-52199-0259	0.095	19.61	0.535	-0.131	0.593	41.31	1.039	...	...	2.627
0683-52524-0360	0.117	6.530	0.829	-0.281	0.445	41.35	1.073	...	...	2.565
0705-52200-0120	0.187	10.23	0.817	-0.139	0.334	42.25	1.276	...	...	2.110
0718-52206-0038	0.180	15.24	0.999	-0.112	0.639	42.75	1.005	87.35	3.866	2.620
0721-52228-0359	0.082	25.93	0.933	-0.025	0.783	41.72	1.023	107.8	3.846	2.577
0723-52201-0523	0.183	9.701	0.526	-0.246	0.438	41.79	1.338	...	...	1.886
0725-52258-0009	0.099	13.48	0.826	-0.210	0.456	41.43	1.467	...	...	...
0725-52258-0383	0.107	8.821	0.759	-0.257	0.340	41.42	1.107	...	...	2.501
0725-52258-0530	0.175	13.85	0.554	-0.177	0.342	41.97	1.520	...	...	...
0732-52221-0612	0.125	12.47	1.198	0.059	0.701	41.95	1.110	...	...	2.495
0738-52521-0553	0.100	16.02	0.691	-0.159	0.575	41.15	1.170	...	...	2.375
0739-52520-0334	0.083	14.59	0.666	-0.269	0.426	41.13	0.770	...	...	3.099
0743-52262-0169	0.111	11.36	1.087	-0.141	0.636	41.84	1.148	...	...	2.420
0745-52258-0450	0.071	20.94	1.131	0.113	0.922	41.76	1.906	...	...	...
0745-52258-0520	0.038	25.97	1.083	-0.095	0.573	41.06	1.076	111.3	3.843	2.482
0750-52235-0052	0.137	13.82	1.135	0.202	0.988	42.20	1.069	...	...	2.573
0751-52251-0092	0.091	15.69	1.159	0.082	0.628	41.88	1.138	...	...	2.440
0752-52251-0014	0.143	17.51	0.443	-0.133	0.433	41.61	1.197	...	...	2.315
0752-52251-0380	0.099	15.12	1.123	-0.129	0.603	42.15	0.995	93.40	3.860	2.632
0757-52238-0604	0.091	22.03	0.553	-0.229	0.414	41.63	1.105	...	...	2.506
0766-52247-0390	0.183	7.602	0.973	-0.039	0.449	42.03	1.297	...	...	2.040

Table 2. –to be continued

(1)	(2)	(3)	(4)	(5)	(6)	(7)	(8)	(9)	(10)	(11)
0769-54530-0225	0.038	24.33	0.815	-0.295	0.556	40.66	1.146	97.36	3.856	2.353
0781-52373-0136	0.102	12.68	0.488	-0.190	0.307	41.13	1.079	...	...	2.553
0784-52327-0314	0.115	18.04	0.870	-0.057	0.440	41.58	1.381	...	...	1.656
0785-52339-0368	0.090	14.68	0.837	-0.134	0.527	41.66	1.268	53.17	3.918	2.092
0786-52319-0568	0.073	15.88	1.078	-0.187	0.428	41.32	1.112	62.11	3.901	2.442
0788-52338-0398	0.097	18.22	0.755	-0.194	0.589	41.45	1.163	...	...	2.388
0790-52433-0346	0.154	8.299	0.599	-0.203	0.413	42.02	1.176	...	...	2.361
0802-52289-0529	0.134	14.08	1.169	0.049	0.602	42.34	1.352	119.3	3.837	1.740
0816-52379-0362	0.061	21.45	0.772	-0.226	0.548	41.54	1.333	85.84	3.868	1.841
0817-52381-0025	0.096	20.72	1.132	0.069	0.636	41.93	1.230	...	...	2.235
0817-52381-0633	0.102	20.21	0.976	-0.100	0.423	41.65	1.233	...	...	2.228
0818-52395-0272	0.201	10.57	0.686	-0.207	0.390	42.23	1.162	...	...	2.391
0826-52295-0371	0.155	11.68	1.029	-0.125	0.504	42.13	1.099	...	...	2.516
0828-52317-0472	0.114	17.68	0.751	-0.180	0.354	41.96	1.169	...	...	2.376
0829-52296-0359	0.152	12.68	0.855	-0.190	0.403	42.29	1.470	...	...	...
0830-52293-0261	0.239	12.38	0.827	-0.044	0.607	42.34	1.018	...	...	2.663
0832-52312-0295	0.085	23.69	0.744	-0.170	0.474	41.53	1.159	...	...	2.397
0836-52376-0110	0.195	9.929	0.749	0.039	0.739	41.53	0.954	...	...	2.772
0840-52374-0277	0.040	30.86	1.156	-0.015	0.720	41.60	1.121	98.35	3.855	2.403
0847-52426-0500	0.139	11.39	0.890	-0.244	0.307	41.87	1.135	48.46	3.928	2.410
0848-52669-0606	0.135	18.58	0.952	0.056	0.786	42.25	1.005	...	...	2.686
0850-52338-0502	0.087	25.62	0.928	-0.116	0.387	41.84	1.381	48.93	3.927	1.616
0855-52375-0318	0.080	15.10	0.853	-0.292	0.393	41.39	1.229	75.80	3.880	2.179
0861-52318-0430	0.061	17.84	0.995	-0.290	0.405	41.51	1.511	112.1	3.843	...
0874-52338-0147	0.232	12.53	0.609	-0.235	0.290	42.47	1.031	70.02	3.888	2.584
0880-52367-0295	0.085	13.52	0.487	-0.200	0.365	40.92	1.184	...	...	2.344
0881-52368-0241	0.129	15.39	0.991	-0.165	0.516	42.12	1.428	148.2	3.818	1.030
0884-52374-0103	0.082	12.86	0.829	-0.086	0.568	41.13	1.060	...	...	2.589
0885-52379-0010	0.104	19.04	0.559	-0.084	0.247	41.48	1.003	...	...	2.690
0885-52379-0138	0.156	8.666	0.854	-0.115	0.329	41.65	0.930	...	...	2.814
0886-52381-0041	0.096	15.84	0.722	-0.101	0.595	41.73	1.066	...	...	2.577
0890-52583-0265	0.198	12.07	0.856	-0.136	0.446	42.40	1.283	...	...	2.087
0892-52378-0258	0.084	19.26	0.967	-0.056	0.461	41.65	1.278	...	...	2.102
0892-52378-0564	0.109	24.57	0.780	-0.150	0.572	42.10	1.238	141.0	3.822	2.125
0893-52589-0337	0.125	17.36	0.860	-0.028	0.801	41.39	1.351	...	...	1.826
0897-52605-0189	0.089	17.17	1.008	-0.069	0.507	41.66	1.160	...	...	2.395
0897-52605-0640	0.080	21.75	0.710	-0.187	0.518	41.14	1.049	...	...	2.608
0900-52637-0575	0.075	20.39	0.784	-0.063	0.523	41.21	1.084	...	...	2.544
0906-52368-0279	0.087	15.30	1.083	0.169	0.623	41.35	1.355	...	...	1.805
0909-52379-0491	0.073	11.46	1.211	0.088	0.794	41.64	1.340	...	...	1.875
0911-52426-0526	0.082	24.77	1.101	0.169	0.701	41.79	1.301	...	...	2.027
0914-52721-0163	0.114	18.36	0.936	0.022	0.713	41.56	1.202	...	...	2.303
0916-52378-0330	0.116	14.39	0.729	-0.077	0.657	41.87	1.286	...	...	2.077
0917-52400-0260	0.141	12.78	0.838	-0.147	0.547	41.69	1.086	...	...	2.541
0919-52409-0618	0.138	13.75	0.890	-0.088	0.345	42.05	1.345	...	...	1.854
0920-52411-0577	0.146	12.10	0.984	-0.107	0.604	41.91	1.050	...	...	2.606
0923-52404-0416	0.129	14.64	1.070	0.095	0.433	41.80	1.205	...	...	2.297
0926-52413-0121	0.116	11.96	1.067	-0.049	0.383	41.73	1.298	...	...	2.039
0926-52413-0494	0.149	16.83	1.227	0.062	0.772	42.26	0.796	...	...	3.050
0930-52618-0569	0.075	21.40	1.110	0.115	1.084	41.24	1.328	...	...	1.928

Table 2. –to be continued

(1)	(2)	(3)	(4)	(5)	(6)	(7)	(8)	(9)	(10)	(11)
0931-52619-0041	0.170	10.13	1.070	-0.076	0.445	41.81	1.320	...	...	1.959
0931-52619-0094	0.097	23.72	1.046	0.005	0.851	41.87	1.248	...	...	2.189
0931-52619-0613	0.109	15.08	0.952	-0.149	0.355	41.87	1.269	...	...	2.131
0933-52642-0116	0.084	17.71	0.701	-0.139	0.651	41.21	1.311	...	...	1.994
0936-52705-0183	0.104	13.96	1.056	-0.138	0.742	41.60	1.278	...	...	2.103
0940-52670-0043	0.103	16.22	1.051	0.080	0.646	41.92	1.206	...	...	2.293
0940-52670-0101	0.071	28.17	0.740	-0.125	0.367	42.19	1.315	...	...	1.978
0940-52670-0510	0.231	11.88	0.755	-0.096	0.438	42.21	0.891	...	...	2.882
0941-52709-0255	0.074	21.79	0.694	-0.140	0.393	42.09	0.982	...	...	2.726
0951-52398-0425	0.126	19.11	0.983	0.100	0.691	41.74	1.196	...	...	2.317
0954-52405-0515	0.062	22.63	1.110	-0.094	0.534	41.63	0.972	...	...	2.742
0958-52410-0229	0.121	13.45	0.469	-0.088	0.570	41.25	1.036	...	...	2.632
0960-52466-0388	0.119	14.92	0.957	-0.172	0.371	41.88	1.203	...	...	2.301
0964-52646-0130	0.213	11.80	0.726	-0.123	0.391	42.46	1.230	...	...	2.235
0964-52646-0191	0.132	16.30	0.842	-0.056	0.375	41.81	1.299	...	...	2.034
0964-52646-0479	0.209	12.55	0.902	-0.198	0.350	42.51	0.944	...	...	2.790
0965-52438-0048	0.127	18.57	1.362	0.255	0.464	42.24	1.009	...	...	2.678
0965-52438-0314	0.144	13.94	0.998	-0.007	0.530	41.89	1.101	...	...	2.513
0969-52442-0499	0.122	14.94	1.011	-0.158	0.619	42.00	1.200	...	...	2.307
0971-52644-0146	0.130	12.89	0.869	-0.199	0.430	41.94	1.267	129.3	3.830	2.052
0973-52426-0250	0.119	11.91	0.901	-0.097	0.728	41.38	1.408	...	...	1.421
0973-52426-0466	0.087	17.08	0.787	-0.182	0.426	41.63	1.349	...	...	1.837
0975-52411-0566	0.097	17.51	0.777	-0.111	0.450	41.90	1.458	105.7	3.848	...
0978-52431-0013	0.099	18.97	0.848	-0.197	0.315	41.84	1.087	55.18	3.913	2.496
0978-52441-0012	0.099	17.67	0.805	-0.205	0.307	41.82	1.497	60.13	3.904	...
0994-52725-0362	0.077	16.32	0.925	-0.092	0.513	41.33	0.984	...	...	2.722
0996-52641-0385	0.182	10.64	0.843	-0.176	0.742	41.88	1.090	...	...	2.534
0998-52750-0258	0.111	14.78	1.192	0.046	0.522	41.99	1.176	...	...	2.361
0998-52750-0475	0.169	10.76	0.574	-0.273	0.449	41.56	1.495	...	...	...
1006-52708-0040	0.068	16.16	0.856	-0.095	0.890	41.25	0.999	...	...	2.696
1007-52706-0403	0.114	17.67	0.557	-0.212	0.441	41.61	1.401	...	...	1.498
1007-52706-0404	0.126	15.17	1.040	-0.027	0.731	42.18	1.489	...	...	...
1010-52649-0258	0.120	24.73	0.638	-0.167	0.341	41.99	1.186	...	...	2.339
1012-52649-0167	0.111	15.39	0.754	-0.063	0.436	41.60	1.151	...	...	2.415
1013-52707-0276	0.107	20.95	0.971	-0.077	0.654	42.15	1.161	75.16	3.881	2.335
1021-52460-0492	0.215	7.136	0.573	-0.159	0.338	41.31	0.969	...	...	2.747
1031-53172-0257	0.122	18.63	0.462	-0.197	0.470	41.33	0.798	...	...	3.045
1041-52724-0338	0.032	35.41	1.197	0.173	0.695	41.41	1.198	...	...	2.312
1043-52465-0138	0.134	18.93	0.723	-0.122	0.605	41.74	0.902	...	...	2.862
1050-52721-0364	0.087	15.81	1.050	-0.109	0.589	41.54	0.973	84.65	3.869	2.676
1055-52761-0095	0.120	12.48	0.782	-0.189	0.379	41.47	1.170	...	...	2.374
1061-52641-0099	0.097	22.70	0.734	-0.077	0.775	41.53	1.294	...	...	2.052
1061-52641-0174	0.052	19.27	1.130	-0.305	0.452	41.71	1.385	120.5	3.836	1.542
1075-52933-0104	0.163	9.390	0.952	-0.131	0.577	41.76	1.100	...	...	2.515
1107-52968-0531	0.214	8.409	0.928	-0.039	0.698	42.09	1.245	...	...	2.196
1108-53227-0256	0.141	10.81	0.561	-0.258	0.336	41.59	0.707	...	...	3.227
1160-52674-0506	0.172	9.926	0.960	-0.088	0.527	41.85	0.974	...	...	2.739
1174-52782-0636	0.099	15.25	0.697	-0.099	0.404	41.44	1.210	...	...	2.283
1175-52791-0181	0.167	11.28	1.252	0.182	0.637	42.43	0.991	...	...	2.709
1176-52791-0453	0.136	10.71	0.871	-0.118	0.608	41.80	0.899	...	...	2.867

**Table 2.** –to be continued

(1)	(2)	(3)	(4)	(5)	(6)	(7)	(8)	(9)	(10)	(11)
1197-52668-0459	0.136	16.23	0.795	-0.066	0.461	41.56	1.293	...	...	2.057
1202-52672-0120	0.128	13.52	1.133	-0.084	0.328	42.00	1.601	46.19	3.933	...
1211-52964-0023	0.183	6.492	0.715	-0.128	0.304	41.64	1.142	...	...	2.432
1226-52734-0132	0.068	20.16	0.905	-0.074	0.498	41.69	1.192	...	...	2.327
1227-52733-0481	0.175	9.231	0.398	-0.268	0.363	41.51	1.087	...	...	2.538
1235-52734-0296	0.068	22.74	1.133	0.125	0.955	41.43	1.261	...	...	2.153
1240-52734-0597	0.077	23.04	0.885	-0.188	0.491	41.24	1.182	...	...	2.348
1264-52707-0102	0.091	13.73	0.951	-0.362	0.379	41.46	1.467	...	...	...
1268-52933-0223	0.141	16.32	1.173	0.132	0.550	42.20	1.051	...	...	2.604
1270-52991-0037	0.197	10.01	0.520	-0.216	0.331	41.62	1.074	...	...	2.563
1275-52996-0038	0.141	14.38	0.987	0.033	0.431	42.00	0.966	...	...	2.753
1276-53035-0575	0.123	12.91	0.895	-0.030	0.577	42.21	1.265	...	...	2.142
1282-52759-0191	0.141	20.27	0.698	-0.116	0.457	41.71	0.982	...	...	2.726
1292-52736-0497	0.064	25.85	0.965	-0.064	0.564	41.62	1.112	...	...	2.491
1311-52765-0483	0.102	15.95	0.875	-0.253	0.371	41.48	1.159	...	...	2.397
1319-52791-0180	0.099	15.17	0.696	-0.247	0.649	41.32	1.362	...	...	1.769
1330-52822-0207	0.078	16.66	1.178	-0.134	0.454	41.80	1.036	104.5	3.849	2.555
1333-52782-0113	0.129	15.35	0.631	-0.110	0.370	42.04	1.178	...	...	2.357
1334-52764-0511	0.196	11.60	1.068	-0.315	0.300	42.65	1.269	98.20	3.855	2.058
1338-52765-0184	0.097	17.38	0.933	-0.337	0.260	41.79	0.924	54.82	3.914	2.782
1339-52767-0492	0.098	22.86	0.798	-0.096	0.293	41.70	1.183	...	...	2.346
1348-53084-0340	0.086	15.60	0.905	-0.229	0.282	41.55	1.160	56.90	3.910	2.351
1353-53083-0248	0.144	16.20	0.795	-0.102	0.410	42.22	1.234	...	...	2.225
1358-52994-0476	0.073	25.24	0.794	-0.241	0.399	41.67	1.291	143.0	3.821	1.972
1360-53033-0309	0.106	17.92	0.888	-0.124	0.424	41.28	0.975	...	...	2.738
1362-53050-0167	0.078	25.00	1.012	0.063	0.543	41.64	1.181	...	...	2.351
1364-53061-0196	0.136	13.64	0.931	0.071	0.794	41.72	1.198	...	...	2.312
1369-53089-0290	0.073	24.04	0.812	-0.131	0.334	41.65	1.214	...	...	2.275
1380-53084-0057	0.120	13.31	0.742	-0.275	0.297	41.32	1.083	...	...	2.547
1387-53118-0203	0.114	15.23	0.882	-0.376	0.400	41.87	0.965	72.45	3.885	2.697
1387-53118-0360	0.080	22.86	0.786	-0.046	0.493	41.81	0.944	...	...	2.790
1388-53119-0542	0.115	19.28	0.683	-0.115	0.487	42.00	1.090	...	...	2.533
1399-53172-0457	0.116	14.04	0.839	-0.182	0.414	41.47	1.118	...	...	2.479
1403-53227-0129	0.126	15.55	0.747	-0.139	0.440	41.78	1.111	...	...	2.494
1407-52886-0236	0.126	10.75	0.911	-0.080	0.668	41.80	1.044	...	...	2.617
1418-53142-0461	0.091	17.84	0.930	-0.159	0.666	41.81	1.167	87.52	3.866	2.314
1424-52912-0581	0.139	9.820	0.947	0.049	0.787	41.22	1.082	...	...	2.549
1425-52913-0361	0.211	11.28	0.690	-0.209	0.335	42.39	0.890	...	...	2.882
1428-52998-0038	0.092	16.70	1.091	-0.083	0.484	41.97	1.343	110.6	3.844	1.786
1433-53035-0594	0.129	20.25	0.820	-0.217	0.363	41.75	1.190	...	...	2.329
1437-53046-0114	0.059	18.56	0.686	-0.096	0.489	41.05	1.269	...	...	2.130
1438-53054-0509	0.078	15.07	1.189	-0.034	0.447	41.31	1.144	...	...	2.429
1441-53083-0307	0.170	14.37	0.704	-0.031	0.512	42.10	1.107	...	...	2.502
1442-53050-0356	0.156	12.72	1.098	-0.170	0.515	42.46	1.082	132.9	3.827	2.462
1443-53055-0511	0.112	17.08	1.087	0.186	0.583	41.75	1.133	...	...	2.450
1444-53054-0163	0.113	17.85	0.819	-0.141	0.431	41.94	1.171	...	...	2.373
1446-53080-0268	0.073	19.40	1.077	0.110	0.596	41.72	0.925	...	...	2.822
1452-53112-0057	0.125	16.27	0.700	-0.212	0.333	41.81	1.344	...	...	1.857
1452-53112-0383	0.074	21.32	1.117	-0.163	0.533	41.94	1.339	116.7	3.839	1.802
1454-53090-0557	0.133	13.44	1.139	-0.086	0.564	42.15	1.181	...	...	2.350

Table 2. –to be continued

(1)	(2)	(3)	(4)	(5)	(6)	(7)	(8)	(9)	(10)	(11)
1459-53117-0040	0.193	11.89	0.437	-0.151	0.361	42.14	1.708	...	...	...
1462-53112-0395	0.199	7.570	0.823	-0.108	0.586	41.93	1.390	...	...	1.586
1465-53082-0345	0.123	16.39	0.461	-0.256	0.290	41.64	1.163	...	...	2.390
1495-52944-0248	0.130	14.42	0.481	-0.198	0.421	41.32	1.036	...	...	2.631
1501-53740-0460	0.173	9.414	0.700	-0.278	0.322	41.54	1.156	...	...	2.403
1541-53732-0123	0.154	10.25	1.030	-0.024	0.549	41.66	1.496	...	...	...
1542-53734-0101	0.166	12.00	0.441	-0.124	0.661	41.33	1.489	...	...	...
1551-53327-0391	0.094	10.29	0.866	-0.065	0.804	41.37	1.205	...	...	2.297
1551-53327-0576	0.178	10.70	0.554	-0.134	0.420	41.39	1.324	...	...	1.944
1556-53740-0469	0.077	13.69	0.816	-0.187	1.011	41.17	1.102	...	...	2.511
1572-53177-0278	0.152	10.67	1.178	-0.056	0.413	41.99	1.095	...	...	2.523
1574-53476-0615	0.088	18.49	1.092	0.083	0.800	41.82	1.119	...	...	2.478
1576-53496-0171	0.096	15.94	0.876	-0.109	0.407	41.51	1.167	...	...	2.380
1576-53496-0298	0.188	10.63	0.979	-0.014	0.572	42.20	1.135	...	...	2.446
1577-53495-0580	0.105	19.70	0.966	-0.126	0.482	41.75	1.600	...	...	...
1579-53473-0545	0.150	15.70	0.598	-0.051	0.343	41.97	1.381	...	...	1.652
1586-52945-0015	0.184	8.721	1.081	0.079	0.379	42.39	1.077	...	...	2.558
1586-52945-0356	0.093	18.00	0.786	-0.079	0.339	42.10	1.107	...	...	2.501
1595-52999-0307	0.100	11.51	0.880	-0.225	0.726	41.32	1.130	55.65	3.913	2.413
1605-53062-0287	0.175	11.30	0.735	0.121	0.739	41.68	1.314	...	...	1.981
1608-53138-0092	0.153	13.32	0.997	0.066	0.375	42.16	1.670	...	...	...
1610-53144-0101	0.164	8.747	0.627	-0.203	0.449	41.43	1.243	...	...	2.202
1610-53144-0511	0.117	10.65	0.978	-0.053	0.417	41.57	1.402	...	...	1.483
1614-53120-0166	0.090	18.79	0.743	-0.033	0.593	41.24	1.249	...	...	2.186
1618-53116-0143	0.092	22.36	0.508	-0.151	0.423	41.53	1.819	...	...	...
1620-53137-0105	0.094	18.94	1.142	0.145	0.508	42.01	1.234	...	...	2.224
1621-53383-0391	0.101	14.42	0.657	-0.066	0.493	40.99	1.143	...	...	2.431
1627-53473-0034	0.083	16.24	1.059	-0.043	0.572	41.91	1.583	...	...	...
1628-53474-0577	0.113	18.05	0.567	-0.247	0.324	41.59	1.458	...	...	...
1633-52998-0576	0.186	11.43	0.561	-0.208	0.286	41.82	1.169	...	...	2.376
1642-53115-0583	0.112	17.88	0.576	-0.129	0.354	41.40	1.170	...	...	2.374
1644-53144-0557	0.076	19.59	1.098	0.227	1.026	41.52	1.198	...	...	2.311
1648-53171-0604	0.077	16.19	0.774	-0.143	0.367	41.24	1.229	20.80	4.035	2.256
1649-53149-0404	0.081	13.98	0.870	-0.103	0.414	41.05	1.279	...	...	2.099
1650-53174-0115	0.150	9.055	0.558	-0.171	0.297	41.74	1.263	...	...	2.147
1651-53442-0162	0.117	15.92	0.679	-0.143	0.420	41.34	1.366	...	...	1.746
1653-53534-0371	0.063	14.63	0.890	-0.201	0.688	41.16	1.269	...	...	2.131
1655-53523-0604	0.093	25.44	1.064	-0.018	0.389	42.02	1.293	89.85	3.864	1.986
1659-53224-0203	0.118	15.83	1.098	0.181	0.846	41.90	1.393	...	...	1.564
1668-53433-0263	0.087	10.24	0.702	-0.129	0.472	41.07	1.298	...	...	2.040
1670-54553-0268	0.124	14.20	1.166	-0.001	0.478	41.68	1.463	...	...	...
1677-53148-0198	0.133	14.04	0.489	-0.077	0.505	41.27	1.053	...	...	2.602
1681-53172-0174	0.094	13.35	1.182	-0.035	0.569	41.78	1.050	...	...	2.606
1683-53436-0173	0.068	24.90	0.465	-0.160	0.424	41.23	1.144	...	...	2.429
1683-53436-0442	0.062	27.20	1.174	0.177	0.671	41.68	1.190	118.5	3.838	2.250
1684-53239-0372	0.094	16.41	1.052	-0.020	0.924	41.84	1.063	...	...	2.584
1686-53472-0229	0.097	12.60	0.928	-0.186	0.523	41.35	1.489	...	...	...
1692-53473-0552	0.123	13.95	0.878	-0.103	0.501	41.94	1.061	...	...	2.586
1695-53473-0549	0.138	15.55	0.648	-0.172	0.408	41.73	1.422	...	...	1.238
1706-53442-0315	0.059	28.86	0.533	-0.082	0.247	41.07	1.101	36.00	3.962	2.494



**Table 2.** –to be continued

(1)	(2)	(3)	(4)	(5)	(6)	(7)	(8)	(9)	(10)	(11)
1707-53885-0227	0.221	8.461	0.961	-0.028	0.639	42.01	0.932	...	...	2.811
1709-53533-0241	0.132	16.33	0.884	-0.070	0.548	41.85	1.344	...	...	1.859
1712-53531-0131	0.128	12.72	1.104	-0.018	0.448	41.95	1.170	...	...	2.374
1712-53531-0482	0.119	13.00	0.618	-0.114	0.471	41.33	1.380	...	...	1.662
1715-54212-0530	0.168	10.35	1.169	-0.126	0.562	42.21	1.296	...	...	2.045
1719-53876-0580	0.123	12.65	0.891	-0.092	0.395	41.72	1.629	...	...	...
1722-53852-0071	0.131	20.64	0.717	-0.071	0.616	41.36	1.361	...	...	1.775
1722-53852-0400	0.127	24.45	1.038	-0.115	0.576	42.49	1.444	126.7	3.832	...
1730-53498-0514	0.175	10.08	0.471	-0.148	0.546	41.47	1.222	...	...	2.256
1732-53501-0598	0.110	23.18	0.756	-0.228	0.584	41.54	1.338	...	...	1.887
1734-53034-0317	0.161	8.099	1.097	-0.191	0.335	42.25	1.166	...	...	2.382
1738-53051-0422	0.127	13.17	0.873	-0.131	0.461	41.19	1.251	...	...	2.181
1741-53052-0113	0.068	20.82	1.133	0.009	0.506	41.38	1.256	...	...	2.167
1742-53053-0360	0.140	17.40	0.924	-0.005	0.544	41.96	1.425	...	...	1.185
1742-53053-0584	0.168	13.24	0.761	-0.181	0.616	41.74	1.096	...	...	2.522
1745-53061-0385	0.222	9.272	1.068	-0.092	0.586	42.60	1.190	81.85	3.873	2.267
1747-53075-0216	0.142	11.53	0.900	-0.059	0.414	41.80	1.297	...	...	2.041
1748-53112-0543	0.134	10.62	1.009	0.112	0.860	41.45	1.163	...	...	2.389
1748-53112-0546	0.224	10.67	0.809	-0.261	0.356	42.05	1.249	...	...	2.186
1769-53502-0449	0.068	16.19	0.744	-0.138	0.537	40.75	1.212	...	...	2.279
1775-53847-0461	0.079	17.11	0.971	-0.023	0.581	41.42	1.254	...	...	2.172
1775-53847-0621	0.073	18.12	0.679	-0.193	0.596	40.97	1.244	...	...	2.200
1777-53857-0470	0.147	15.04	0.938	0.074	0.795	41.97	1.382	...	...	1.649
1783-53386-0124	0.072	16.66	1.098	0.012	0.623	41.45	1.262	...	...	2.150
1784-54425-0634	0.097	17.87	0.953	-0.334	0.423	41.63	1.190	142.3	3.821	2.242
1785-54439-0476	0.172	15.93	0.828	-0.089	0.450	42.22	1.196	...	...	2.316
1790-53876-0052	0.110	21.16	1.023	0.059	0.642	41.83	1.314	...	...	1.981
1798-53851-0023	0.105	16.57	1.209	-0.232	0.269	41.77	1.526	...	...	...
1798-53851-0132	0.101	18.15	1.092	-0.018	0.606	41.92	1.245	130.8	3.829	2.112
1806-53559-0389	0.063	16.87	1.107	-0.051	0.593	41.67	1.384	126.7	3.832	1.552
1808-54176-0354	0.080	21.50	0.629	-0.243	0.403	41.33	1.286	...	...	2.077
1811-53533-0034	0.127	17.80	0.694	-0.131	0.341	41.84	1.215	...	...	2.272
1819-54540-0421	0.070	17.08	0.654	-0.219	0.348	41.07	1.486	...	...	...
1819-54540-0438	0.068	28.72	1.110	0.042	0.800	41.76	1.785	...	...	...
1820-54208-0322	0.127	20.90	0.912	-0.086	0.550	41.92	1.322	...	...	1.951
1824-53491-0162	0.111	16.43	1.044	-0.047	0.529	42.04	1.002	117.6	3.838	2.610
1836-54567-0048	0.084	19.98	0.851	-0.132	0.468	41.21	1.189	...	...	2.332
1836-54567-0139	0.114	11.72	1.072	0.094	0.609	41.40	1.077	...	...	2.557
1843-53816-0329	0.115	14.87	0.667	-0.120	0.368	41.18	1.280	...	...	2.096
1872-53386-0620	0.121	11.74	1.253	-0.043	0.677	42.06	1.242	...	...	2.204
1875-54453-0620	0.089	19.34	0.628	-0.247	0.403	41.70	1.126	...	...	2.464
1877-54464-0461	0.070	23.31	0.742	-0.054	0.651	41.14	1.657	...	...	...
1921-53317-0294	0.189	8.700	0.843	-0.127	0.411	41.79	1.132	...	...	2.453
1924-53330-0369	0.093	12.33	0.791	-0.161	0.439	41.35	1.757	...	...	...
1925-53327-0058	0.144	15.18	0.888	-0.022	0.382	40.96	1.421	...	...	1.249
1930-53347-0483	0.051	31.36	0.787	-0.047	0.595	41.56	1.250	...	...	2.184
1933-53381-0082	0.149	8.641	1.034	0.003	0.833	41.55	1.410	...	...	1.402
1936-53330-0068	0.149	11.04	1.187	-0.059	0.654	42.22	1.564	...	...	...
1939-53389-0170	0.200	9.564	0.605	-0.289	0.292	41.77	1.322	...	...	1.951
1940-53383-0564	0.143	13.93	0.926	-0.200	0.500	41.86	1.012	115.5	3.840	2.593

Table 2. –to be continued

(1)	(2)	(3)	(4)	(5)	(6)	(7)	(8)	(9)	(10)	(11)
1945-53387-0487	0.133	12.92	0.797	-0.291	0.486	41.70	1.009	...	...	2.678
1945-53387-0506	0.079	25.07	0.682	-0.201	0.350	41.29	1.248	...	...	2.189
1946-53432-0368	0.137	11.87	0.835	-0.125	0.409	41.65	1.242	...	...	2.206
1948-53388-0376	0.144	10.01	0.870	-0.097	0.553	41.59	1.317	...	...	1.970
1959-53440-0152	0.141	10.19	0.750	-0.183	0.375	41.66	2.035	...	...	...
1959-53440-0206	0.137	14.88	0.607	-0.083	0.428	41.87	1.097	...	...	2.519
1972-53466-0525	0.179	12.78	0.931	-0.006	0.333	42.27	1.349	...	...	1.835
1983-53442-0595	0.150	11.47	0.785	-0.124	0.431	41.84	1.298	...	...	2.038
1986-53475-0599	0.132	20.24	0.521	-0.202	0.316	41.67	1.211	...	...	2.282
1993-53762-0326	0.198	8.071	0.941	-0.182	0.440	42.27	1.559	...	...	...
2000-53495-0074	0.106	19.46	0.857	-0.249	0.398	42.24	0.882	...	...	2.896
2001-53493-0059	0.073	15.85	1.192	0.104	0.788	41.85	1.164	...	...	2.387
2002-53471-0108	0.151	13.31	1.214	-0.097	0.483	42.29	1.557	...	...	...
2005-53472-0378	0.113	16.93	0.995	0.059	0.861	41.94	1.267	...	...	2.135
2011-53499-0244	0.068	14.59	1.102	-0.204	0.652	41.48	1.546	...	...	...
2011-53499-0382	0.165	11.13	0.796	0.037	0.546	41.84	1.262	...	...	2.150
2012-53493-0109	0.206	13.64	1.255	0.029	0.446	42.61	1.232	98.11	3.855	2.158
2015-53819-0550	0.140	16.59	0.965	0.093	0.792	42.01	1.266	...	...	2.140
2029-53819-0422	0.162	10.36	1.099	-0.060	0.606	41.87	2.023	50.19	3.924	...
2029-53819-0566	0.186	14.51	0.656	-0.159	0.243	42.04	1.196	51.25	3.922	2.277
2082-53358-0625	0.091	13.85	0.663	-0.197	0.477	41.26	1.236	...	...	2.220
2088-53493-0387	0.108	15.86	0.987	0.026	0.433	41.86	1.213	...	...	2.276
2088-53493-0639	0.071	17.55	0.977	-0.216	0.372	41.82	1.143	129.7	3.830	2.346
2090-53463-0566	0.094	21.81	0.624	-0.182	0.311	41.71	1.288	...	...	2.073
2097-53491-0604	0.061	25.41	0.937	-0.191	0.515	41.45	1.125	63.54	3.898	2.415
2101-53858-0513	0.196	10.40	0.470	-0.272	0.446	41.65	2.133	...	...	...
2105-53472-0350	0.078	19.53	0.979	-0.173	0.556	41.42	1.081	...	...	2.550
2105-53472-0446	0.083	15.01	0.927	-0.042	0.593	41.83	1.491	...	...	...
2108-53473-0295	0.197	12.13	0.934	-0.028	0.705	42.50	1.676	...	...	...
2112-53534-0582	0.141	16.79	0.651	-0.147	0.384	41.43	1.498	33.56	3.971	...
2124-53770-0435	0.093	21.43	1.100	0.036	0.515	41.62	1.296	...	...	2.044
2134-53876-0081	0.160	14.25	0.833	-0.289	0.423	42.11	1.157	...	...	2.401
2135-53827-0276	0.093	21.93	1.061	0.181	0.819	41.65	1.172	...	...	2.370
2138-53757-0334	0.116	11.38	0.702	-0.145	0.517	41.57	1.302	...	...	2.026
2138-53757-0544	0.108	19.84	0.629	-0.229	0.293	41.62	1.268	...	...	2.131
2140-53858-0319	0.073	14.11	0.830	-0.282	0.356	41.48	1.542	...	...	...
2142-54208-0375	0.105	21.51	1.289	0.010	0.618	42.26	1.315	...	...	1.978
2145-54212-0582	0.162	13.07	0.557	-0.239	0.300	41.73	1.380	...	...	1.659
2146-54230-0019	0.114	21.32	0.947	-0.194	0.206	41.94	1.097	...	...	2.520
2148-54526-0091	0.116	14.70	1.174	0.084	0.850	42.11	1.205	...	...	2.297
2149-54509-0545	0.112	14.33	1.021	-0.117	0.606	42.13	1.404	...	...	1.468
2156-54525-0221	0.078	24.77	0.927	-0.130	0.600	41.45	1.856	...	...	...
2160-53885-0611	0.087	22.31	0.555	-0.162	0.422	41.29	1.149	...	...	2.419
2161-53878-0639	0.159	9.918	0.733	-0.150	0.495	41.42	1.419	...	...	1.277
2168-53886-0154	0.152	15.46	1.091	-0.019	0.488	42.39	1.038	...	...	2.627
2169-53556-0106	0.123	13.39	1.015	-0.050	0.751	41.86	1.195	...	...	2.319
2173-53874-0418	0.117	18.05	0.956	-0.139	0.623	41.67	1.348	...	...	1.842
2201-53904-0632	0.162	13.16	1.032	0.010	0.433	42.03	1.247	...	...	2.192
2205-53793-0506	0.084	16.52	0.792	-0.133	0.438	40.87	1.165	...	...	2.386
2215-53793-0043	0.068	29.24	0.845	0.015	0.479	41.95	1.290	222.9	3.784	1.956

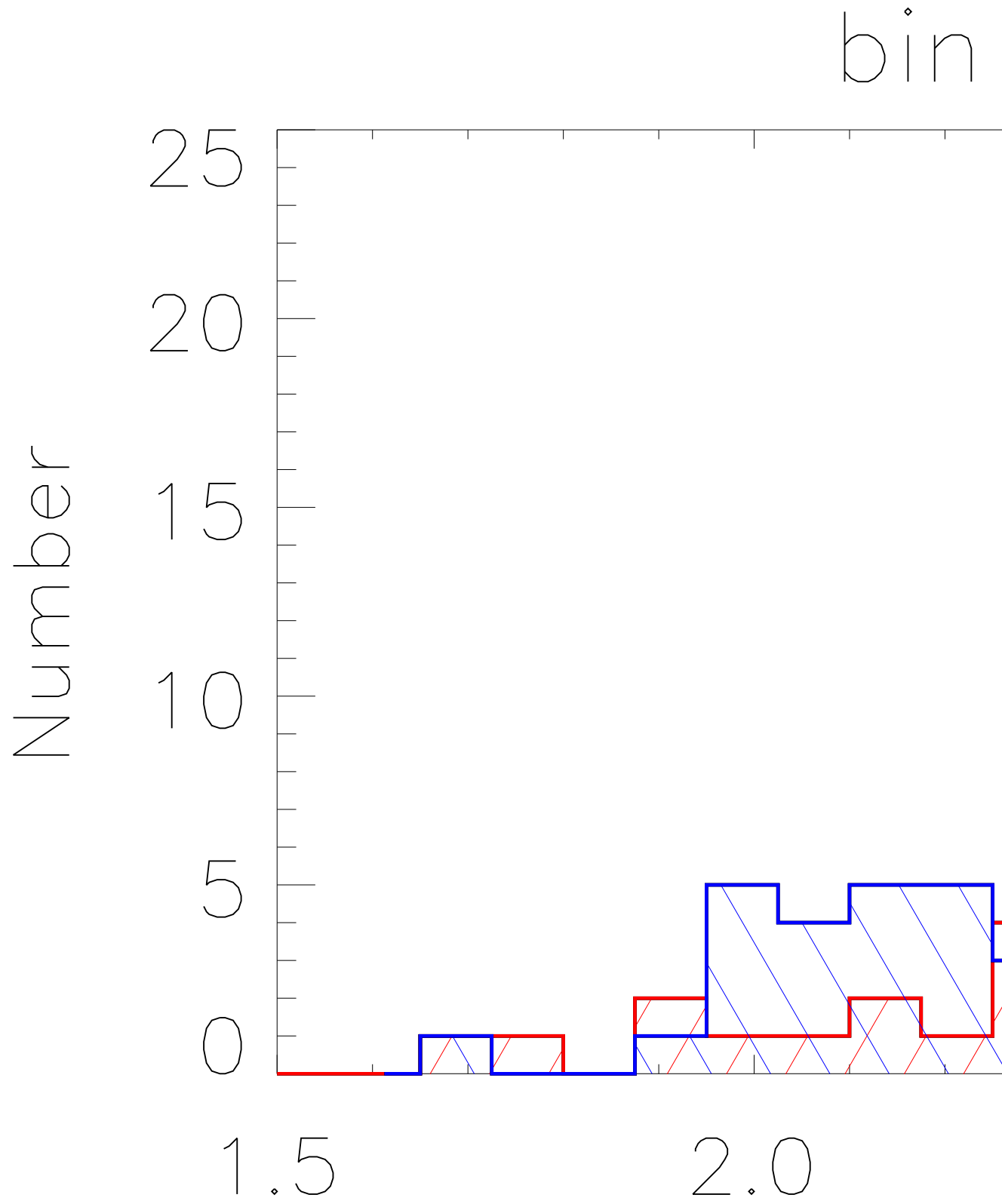
**Table 2.** –to be continued

(1)	(2)	(3)	(4)	(5)	(6)	(7)	(8)	(9)	(10)	(11)
2216-53795-0209	0.050	19.70	0.805	-0.060	0.600	41.23	1.148	...	...	2.421
2217-53794-0566	0.146	13.73	0.850	0.124	0.774	41.70	1.366	...	...	1.747
2219-53816-0090	0.132	8.967	0.660	-0.247	0.322	41.48	1.528	...	...	...
2219-53816-0496	0.033	31.45	0.917	-0.203	0.474	41.31	1.170	110.4	3.844	2.296
2220-53795-0124	0.172	13.83	1.090	0.070	0.557	42.40	1.104	...	...	2.507
2226-53819-0247	0.156	15.53	0.853	-0.065	0.544	42.28	1.342	...	...	1.867
2230-53799-0498	0.106	18.17	1.196	0.128	1.277	41.61	1.342	...	...	1.869
2232-53827-0282	0.101	25.15	1.148	0.053	0.568	42.21	1.210	...	...	2.284
2271-53726-0279	0.081	23.94	0.811	-0.123	0.573	41.69	1.440	...	...	...
2274-53726-0019	0.128	15.74	1.017	-0.032	0.638	41.49	1.267	...	...	2.134
2275-53709-0005	0.074	14.77	0.936	-0.126	0.598	41.19	1.181	...	...	2.350
2279-53708-0431	0.096	15.86	1.079	-0.033	0.532	41.47	1.045	...	...	2.616
2285-53700-0366	0.086	19.54	0.440	-0.058	0.474	41.22	1.182	...	...	2.349
2289-53708-0028	0.177	10.38	1.053	-0.279	0.334	42.44	1.228	102.2	3.851	2.167
2342-53742-0092	0.051	28.25	1.054	-0.054	0.636	41.81	0.914	142.8	3.821	2.753
2344-53740-0489	0.161	13.45	0.741	-0.093	0.446	42.04	1.227	...	...	2.243
2355-53792-0351	0.103	13.65	1.020	-0.203	0.526	41.37	1.338	...	...	1.887
2357-53793-0063	0.079	18.52	0.969	0.076	0.655	41.68	1.160	...	...	2.396
2358-53797-0181	0.107	19.12	0.849	-0.021	0.628	41.84	1.271	...	...	2.124
2359-53826-0053	0.117	12.90	1.004	0.055	0.816	41.69	1.531	...	...	...
2366-53741-0016	0.110	11.95	0.490	-0.239	0.354	41.09	1.175	...	...	2.363
2366-53741-0438	0.110	16.55	1.046	0.022	0.667	41.64	1.091	...	...	2.532
2374-53765-0174	0.064	26.59	1.074	-0.138	0.494	41.73	1.966	104.2	3.850	...
2420-54086-0318	0.132	10.52	0.908	-0.211	0.624	41.40	0.986	...	...	2.718
2421-54153-0587	0.225	10.77	0.671	-0.161	0.381	41.86	1.060	...	...	2.589
2424-54448-0231	0.156	15.78	0.721	-0.223	0.346	41.90	1.032	...	...	2.639
2424-54448-0402	0.092	12.65	0.923	-0.076	0.753	41.40	1.643	...	...	...
2425-54139-0032	0.168	11.50	0.812	-0.059	0.458	42.01	1.051	...	...	2.604
2425-54139-0288	0.171	11.64	0.439	-0.182	0.560	41.73	1.539	...	...	...
2430-53815-0461	0.093	14.20	1.174	-0.153	0.601	42.07	1.212	111.8	3.843	2.201
2431-53818-0320	0.145	11.22	0.602	-0.265	0.314	41.58	1.288	...	...	2.071
2431-53818-0352	0.202	11.43	0.488	-0.135	0.447	41.52	1.114	...	...	2.488
2431-53818-0510	0.118	17.06	0.421	-0.219	0.534	41.38	1.352	...	...	1.821
2436-54054-0507	0.149	12.27	0.929	-0.098	0.670	41.87	1.263	...	...	2.147
2479-54174-0278	0.138	16.34	0.934	0.039	0.781	41.42	1.420	...	...	1.262
2481-54086-0514	0.155	18.49	0.975	-0.194	0.395	42.38	1.134	74.06	3.883	2.389
2488-54149-0548	0.147	13.43	1.098	-0.143	0.406	42.30	1.219	89.49	3.864	2.195
2490-54179-0036	0.151	12.46	0.414	-0.200	0.359	41.46	0.883	...	...	2.896
2491-53855-0039	0.169	13.38	0.649	-0.090	0.468	41.62	1.256	...	...	2.166
2494-54174-0596	0.279	9.636	0.624	-0.269	0.399	42.38	1.397	...	...	1.528
2497-54154-0470	0.162	15.39	1.088	-0.022	0.671	42.09	1.230	28.06	3.994	2.233
2504-54179-0356	0.179	9.698	0.802	-0.148	0.286	41.96	1.371	...	...	1.718
2505-53856-0509	0.156	18.47	1.112	-0.073	0.364	42.45	1.201	80.04	3.875	2.243
2507-53876-0181	0.163	13.22	0.774	0.012	0.407	42.14	1.075	...	...	2.561
2508-53875-0349	0.183	13.41	0.575	-0.292	0.464	42.23	1.225	...	...	2.247
2510-53877-0559	0.102	20.07	0.730	-0.266	0.349	41.58	1.270	...	...	2.126
2515-54180-0355	0.096	14.55	0.536	-0.251	0.689	41.38	1.132	28.47	3.992	2.448
2516-54241-0130	0.086	9.755	0.927	-0.059	0.706	41.09	1.201	...	...	2.305
2520-54584-0401	0.149	20.87	0.802	-0.101	0.654	41.90	1.178	95.34	3.858	2.286
2525-54569-0400	0.213	8.963	0.883	0.080	0.746	42.16	1.406	...	...	1.449

Table 2. –to be continued

(1)	(2)	(3)	(4)	(5)	(6)	(7)	(8)	(9)	(10)	(11)
2529-54585-0125	0.216	8.508	0.786	-0.102	0.350	42.35	1.182	...	...	2.348
2529-54585-0479	0.152	12.21	1.085	-0.027	0.418	42.01	1.311	...	...	1.994
2530-53881-0463	0.204	11.56	0.660	-0.154	0.398	41.57	1.339	...	...	1.880
2578-54093-0047	0.157	10.60	0.567	-0.119	0.396	41.48	1.264	...	...	2.144
2579-54068-0015	0.174	11.86	0.901	0.074	0.791	42.10	1.171	...	...	2.373
2579-54068-0461	0.208	7.977	0.680	-0.273	0.294	41.86	1.221	...	...	2.257
2580-54092-0315	0.165	13.21	0.857	-0.072	0.836	41.15	1.373	...	...	1.704
2580-54092-0518	0.178	8.608	1.051	-0.137	0.476	42.02	1.242	71.92	3.886	2.148
2581-54085-0540	0.161	13.17	0.758	-0.041	0.335	42.21	1.219	...	...	2.263
2583-54095-0184	0.142	15.04	1.085	0.107	0.669	41.95	1.419	...	...	1.279
2593-54175-0294	0.115	18.77	0.970	0.119	0.541	41.94	0.835	...	...	2.978
2596-54207-0211	0.079	21.71	0.999	-0.009	0.616	41.85	1.050	152.8	3.815	2.515
2599-54234-0617	0.088	14.68	0.695	-0.114	0.317	41.38	1.201	...	...	2.304
2604-54484-0470	0.071	26.11	0.864	-0.166	0.434	41.42	1.348	...	...	1.840
2609-54476-0074	0.152	11.79	0.943	-0.044	0.489	41.88	1.455	...	...	...
2613-54481-0085	0.112	16.09	0.836	-0.187	0.427	41.71	1.581	84.38	3.870	...
2615-54483-0453	0.131	11.64	1.037	0.002	0.712	41.85	1.283	96.39	3.857	2.018
2617-54502-0353	0.194	13.15	0.476	-0.163	0.522	41.79	1.273	...	...	2.119
2641-54230-0012	0.110	13.63	0.536	-0.218	0.485	41.24	0.987	...	...	2.716
2642-54232-0239	0.116	13.33	1.021	-0.176	0.366	41.79	1.380	59.53	3.905	1.610
2647-54495-0225	0.071	23.69	0.738	-0.189	0.381	41.32	1.229	...	...	2.238
2649-54212-0348	0.093	21.14	1.067	0.016	0.711	42.04	1.297	...	...	2.041
2657-54502-0388	0.117	20.34	1.092	-0.048	0.456	41.91	1.296	105.3	3.849	1.971
2658-54502-0073	0.152	17.62	0.609	-0.251	0.302	42.19	1.230	...	...	2.234
2661-54505-0213	0.246	7.926	1.122	-0.111	0.465	42.49	1.113	...	...	2.490
2662-54505-0499	0.073	20.96	1.004	0.012	0.832	41.41	1.187	...	...	2.336
2742-54233-0186	0.090	18.63	0.451	-0.137	0.369	41.22	1.748	...	...	...
2747-54233-0459	0.114	14.59	1.042	-0.204	0.418	42.06	1.741	99.23	3.854	...
2748-54234-0289	0.097	15.02	0.824	-0.168	0.455	41.42	1.017	...	...	2.665
2758-54523-0589	0.189	9.174	0.798	-0.198	0.586	41.88	1.230	...	...	2.236
2758-54523-0590	0.112	17.38	1.137	0.133	0.515	41.85	1.308	...	...	2.005
2764-54535-0183	0.117	20.67	0.956	-0.096	0.190	42.16	1.232	...	...	2.231
2764-54535-0640	0.185	12.92	0.962	-0.038	0.486	42.11	1.308	...	...	2.005
2765-54535-0151	0.143	10.19	0.984	-0.012	0.676	41.80	1.230	...	...	2.236
2769-54527-0504	0.120	17.61	0.734	-0.055	0.453	41.93	1.322	...	...	1.953
2769-54527-0609	0.189	13.30	0.949	-0.018	0.683	42.22	1.315	99.62	3.854	1.907
2769-54527-0639	0.077	21.96	1.017	-0.151	0.454	41.35	1.222	73.61	3.883	2.197
2771-54527-0146	0.126	19.91	0.577	-0.231	0.377	41.75	1.164	...	...	2.388
2784-54529-0374	0.061	17.83	1.075	-0.044	0.716	41.32	1.227	...	...	2.243
2786-54540-0254	0.112	14.13	0.994	-0.089	0.398	42.20	1.326	161.6	3.810	1.843
2787-54552-0572	0.129	23.04	1.119	-0.078	0.539	42.44	1.386	101.6	3.852	1.543
2789-54555-0363	0.084	19.37	0.703	-0.157	0.574	41.46	1.168	...	...	2.379
2792-54556-0347	0.066	29.49	0.557	-0.179	0.316	41.62	1.103	94.31	3.859	2.439
2881-54502-0055	0.066	20.36	1.149	0.030	0.547	41.30	1.425	87.39	3.866	1.125
2883-54525-0338	0.092	16.52	0.521	-0.042	0.554	41.04	1.082	...	...	2.548
2884-54526-0615	0.127	20.72	0.784	-0.165	0.453	41.98	1.318	...	...	1.967
2885-54497-0095	0.140	14.07	0.973	-0.000	0.662	41.88	1.466	...	...	...
2950-54559-0024	0.068	16.65	1.029	-0.054	0.544	41.95	1.216	...	...	2.270
2950-54559-0608	0.142	10.73	0.863	-0.037	0.470	41.65	1.187	...	...	2.337
2954-54561-0102	0.080	20.73	0.872	-0.149	0.569	41.41	1.253	...	...	2.175
2970-54589-0049	0.080	18.78	1.167	-0.002	0.692	41.99	1.358	...	...	1.791
2974-54592-0260	0.095	18.10	1.041	-0.162	0.611	41.93	1.134	...	...	2.448

- Hiner, K. D., et al., 2009, *ApJ*, 706, 508
- Jarvis, M. E., Harrison, C. M., Thomson, A. P.; et al., 2019, *MNRAS*, 485, 2710
- Kakkad, D.; Groves, B.; Dopita, M.; et al., 2018, *A&A*, 618, 6
- Kauffmann, G., et al. 2003, *MNRAS*, 346, 1055
- Kewley, L. J.; Dopita, M. A.; Sutherland, R. S.; Heisler, C. A.; Trevena, J. 2001, *ApJ*, 556, 121
- Kewley, L. J.; Groves, B.; Kauffmann, G.; Heckman, T., 2006, *MNRAS*, 372, 961
- Kewley, L. J.; Nicholls, D. C.; Sutherland, R. S., 2019, *ARA&A*, 57, 511
- Kewley, L. J.; Nicholls, D. C.; Sutherland, R.; et al., 2019, *ApJ*, 880, 16
- Kawasaki, K., Nagao, T., Toba, Y., Terao, K., Matsuoka, K., 2017, *ApJ*, 842, 44
- Kazuma, J., Nagao, T., Wada, K., Koki Terao, K., Takuji, Y., 2021, *PASJ*, 73, 1152
- King, A.; Pounds, K., 2015, *ARA&A*, 53, 115
- Kormendy, J.; Ho, L. C., 2013, *ARA&A*, 51, 511
- Kovacevic, J.; Popovic, L. C.; Dimitrijevic, M. S., 2010, *ApJS*, 189, 15
- Kuraszkiewicz, J.; Wilkes, B. J.; Atanas, A.; et al., 2021, *ApJ*, 913, 134
- Liu G., Zakamska, N., Greene, J., et al., 2013, *MNRAS*, 430, 2327
- Lyke, B. W.; Higley, A. N.; McLane, J. N.; et al., 2020, *ApJS*, 250, 8
- Marquez I., Masegosa J., Gonzalez-Martin O., et al., 2017, *Frontiers in Astronomy and Space Sciences*, 4, 34
- Marinucci, A.; Bianchi, S.; Nicastro, F.; Matt, G.; Goulding, A. D., 2012, *ApJ*, 748, 130
- Mateos, S., et al., 2016, *ApJ*, 819, 166
- McNamara, B. R.; Nulsen, P. E. J., 2007, *ARA&A*, 45, 117
- Miller, J. S.; Goodrich, R. W., 1990, *ApJ*, 355, 456
- Moran, E. C.; Barth, A. J.; Kay, L. E.; Filippenko, A. V., 2020, *ApJL*, 540, 73
- Muller-Sanchez, F.; Nevin, R.; Comerford, J. M.; et al., 2018, *Natur*, 556, 345
- Nagao, T., et al., 2004, *AJ*, 128, 109
- Netzer, H., 2015, *ARA&A*, 53, 365
- Oh, K., et al., 2015, *ApJS*, 219, 1
- Onori, F.; Ricci, F.; La Franca, F.; et al., 2017, *MNRAS Letter*, 468, 97
- Osterbrock, D. E., 1955, *AJ*, 60, 175
- Osterbrock, D. E., 1955a, *ApJ*, 122, 235
- Osterbrock, D. E.; Flather, E., 1959, *ApJ*, 129, 26
- Osterbrock, D. E., 1960, *ApJ*, 131, 541
- Osterbrock, D. E., 1989, *Astrophysics of Gaseous Nebulae and Active Galactic Nuclei*, Published by University Science Books, ISBN 0-935702-22-9
- Osterbrock, D. E.; Ferland, G. J., 2006, *Astrophysics of gaseous nebulae and active galactic nuclei*, 2nd. ed., CA: University Science Books
- Peters, C. M.; Richards, G. T.; Myers, A. D.; et al., 2015, *ApJ*, 811, 95
- Proxauf, B.; Ottl, S.; Kimeswenger, S., 2014, *A&A*, 561, 10
- Riffel R. A.; Dors, O. L.; Armah, M.; et al., 2021, *MNRAS*, 501, L54
- Rakshit, S.; Stalin, C. S.; Chand, H.; Zhang, X. G., 2017, *ApJS*, 229, 39
- Richards, G. T., et al., 2002, *AJ*, 123, 2945
- Ross, N. P.; et al., 2012, *ApJS*, 199, 3
- Sanders, R. L., Shapley, A. E., Kriek, M., et al. 2016, *ApJ*, 816, 23
- Savic, D.; Goosmann, R.; Popovic, L. C.; Marin, F.; Afanasiev, V. L., 2018, *A&A*, 614, 120
- Shen, Y.; Richards, G. T.; Strauss, M. A., et al., 2011, *ApJS*, 194, 45
- Siebenmorgen, R.; Haas, M.; Krugel, E.; Schulz, B., 2005, *A&A*, 436, 5
- Stanghellinir, L., Kale, J. B., 1989, *ApJ*, 343, 811
- Seaton, M. J., 1954, *MNRAS*, 114, 154
- Saraph, H. E.; Seaton, M. J., 1970, *MNRAS*, 148, 367
- Terlevich, R.; Melnick, J., 1985, *MNRAS*, 213, 841
- Tran, H. D., 2003, *ApJ*, 583, 632
- Tombesi, F.; Melendez, M.; Veilleux, S.; Reeves, J. N.; et al., 2015, *Natur*, 519, 436
- Villarroel, B.; Korn, A. J., 2014, *Nature Physics*, 10, 417
- Zhang, Z. T.; Liang, Y. C.; Hammer, F., 2013, *MNRAS*, 430, 2605
- Zhang, X. G., 2014, *MNRAS*, 438, 557
- Zhang, X. G.; Feng, L., 2016, *MNRAS*, 457, 3878
- Zhang, X. G.; Feng, L., 2017, *MNRAS*, 468, 620
- Zhang, X. G.; Bao M.; Yuan, Q., 2019, *MNRAS Letter*, 490, 81
- Zhang, X. G.; Feng Y.; Chen, H.; Yuan, Q., 2020, *ApJ*, 905, 97
- Zhang, X. G., 2021, *MNRAS*, 502, 2508
- Zhang, X. G., 2021a, *ApJ*, 909, 16, ArXiv:2101.02465
- Zhang, X. G., 2021b, *ApJ*, 919, 13, ArXiv:2107.09214
- Zhang, X. G., 2021c, *MNRAS*, 507, 5205, ArXiv:2108.09714
- Zhang, X. G., 2022a, *ApJS*, 260, 31, ArXiv:2203.12810
- Zhang, X. G., 2022b, *ApJS*, 261, 23, ArXiv:2205.00194
- Zhang, X. G., 2023, *MNRAS*, 519, 4461, arXiv:2301.01957
- Zou, F.; Yang, G.; Brandt, W. N.; Xue, Y., 2019, *ApJ*, 878, 11





Log(SN)

1.6  
1.4  
1.2  
1.0  
0.8  
0.6  
0.4

